Modulation of the HGF/c-Met/Akt and p38 cell signaling pathways by 3,3'-diindolylmethane in MDA-MB-231 breast cancer cells

By

Holly Lynn Nicastro

A dissertation submitted in partial satisfaction of the

requirements for the degree of

Doctor of Philosophy

in

Molecular and Biochemical Nutrition

in the

Graduate Division

of the

University of California, Berkeley

Committee in Charge:

Professor Leonard Bjeldanes, Chair

Professor Jen-Chywan Wang

Professor Gary Firestone

Fall 2010

Abstract

Modulation of the HGF/c-Met/Akt and p38 cell signaling pathways by 3,3'-diindolylmethane in MDA-MB-231 breast cancer cells

by

Holly Lynn Nicastro

Doctor of Philosophy in Molecular and Biochemical Nutrition

University of California, Berkeley

Professor Leonard Bjeldanes, Chair

Cancer is a leading cause of death worldwide, with cancer deaths expected to continue to rise, necessitating new prevention and treatment strategies. Bioactive food components like *Brassica*-derived 3,3'-diindolylmethane (DIM) are a promising area of study for cancer prevention and treatment. Due to its efficacy, availability, low cost, and low toxicity, DIM is currently in use as a treatment for recurrent respiratory papillomatosis and is in clinical trials for the prevention and treatment of prostate and cervical cancers.

DIM's anticancer activities include induction of cell cycle arrest and apoptosis, inhibition of angiogenesis, and immune activation. Though some mechanisms for these activities in various cancer cells have been uncovered, it is clear that DIM works through multiple pathways. More research is necessary to determine the full extent of DIM's effects and to identify specific cellular targets of DIM. This dissertation focuses on DIM's effects on the signaling pathways of two specific pathways, HGF/c-Met/Akt and p38 MAPK.

Akt signaling is frequently dysregulated in breast cancer. Although it has been reported that DIM inhibits Akt signaling in breast cancer cells, the mechanism(s) for this action, as well as the kinetics and effects of lower, physiologically relevant concentrations of DIM, have remained unknown. In chapter 2 we demonstrate that physiologically relevant concentrations of DIM inhibit short- and long-term activation of Akt in the highly invasive MDA-MB-231 breast cancer cells. DIM also selectively inhibits HGF-induced Akt activation, which is one novel mechanism by which DIM inhibits Akt. In addition, DIM inhibits cell cycle progression and *in vitro* metastasis and induced apoptosis, which are all consistent with Akt inhibition.

The roles of specific upstream activators of the Akt pathway, including c-Met, in this activity have not been investigated. In chapter 3, we demonstrate that DIM inhibits motility and proliferation of MDA-MB-231 breast cancer cells downstream of HGF, and that DIM promotes ligand-dependent degradation of c-Met and inhibits c-Met activation.

Even with its strong inhibition by DIM, the Akt pathway is just one of several signaling pathways modified by DIM. DIM also exerts some of its anti-cancer effects by activating the p38 pathway. DIM activates p38 in various cancer cells, including breast cancer cells, and that p38 activation as well as regulation of expression of various genes have been shown to play a role in DIM's effects in breast cancer cells. However, the connection between these two effects has not been reported. In chapter 4 we demonstrate through gene expression profiling that 25 μM DIM for 4 hours regulates the expression of over 400 genes in MDA-MB-231 cells. We also show that DIM activates p38 under physiologically relevant conditions and this activation is partly responsible for DIM-induced up regulation of several genes and for DIM's induction of apoptosis.

Future experiments should focus on determining a specific mechanism by which DIM inhibits c-Met and should establish the relationship between c-Met inhibition and Akt inhibition, as well as between c-Met/Akt inhibition and cell cycle progression, proliferation, apoptosis, and motility in MDA-MB-231 breast cancer cells. The results of the gene expression profiling study also provide many opportunities for follow up experiments.

In summary, DIM is a promising anti-breast cancer compound that exerts its effects in part by inhibiting the HGF/c-Met/Akt pathway and by activating the p38 pathway.

TABLE OF CONTENTS

LIST OF FIGURES AND TABLES

LIST OF ABBREVIATIONS

4E-BP1	Eukaryotic translation initiation factor 4E-binding protein 1
4OHT	4-hydroxytamoxifen
AR	Androgen receptor
BHA	N-(tert-Butyl) hydroxylamine HCL
CsA	Cyclosporin A
DIM	3,3'-diindolylmethane
DMSO	Dimethylsulfoxide
EGF	Epidermal growth factor
EGFR	Epidermal growth factor receptor
EGFRvIII	Epidermal growth factor receptor, variant III
eIF	Eukaryotic translation initiation factor
ER	Estrogen receptor
ERK	Extracellular signal-regulated kinase
FBS	Fetal bovine serum
GO	Gene ontology
GSK	Glycogen synthase kinase
HER2	Human epidermal growth factor receptor 2
HGF	Hepatocyte growth factor
Hrs	Hepatocyte growth factor-regulated tyrosine kinase substrate
HUVEC	Human umbilical vein endothelial cells
I3C	Indole-3-carbinol
iAkt	4-hydroxytamoxifen-inducible Akt
IGF-1	Insulin-like growth factor-1
IκB	Nuclear factor-κB inhibitor
IKK	IκB kinase
IL-24, *IL24*	Interleukin-24 (protein), interleukin-24 (gene)
JNK	c-Jun N-terminal kinase
Lact	Lactacystin
LY	LY294002
MAPK	Mitogen-activated protein kinase
MAP2K	Mitogen-activated protein kinase kinase
MAP3K	Mitogen-activated protein kinase kinase kinase
mTOR	Mammalian target of rapamycin

mTORC2	Mammalian target of rapamycin complex 2
NF-κB	Nuclear factor-κB
NSCLC	Non-small cell lung cancer
PAO	Phenylarsine oxide
PARP	Poly ADP ribose polymerase
PBS	Phosphate buffered saline
PDGF	Platelet-derived growth factor
PDGFR	Platelet-derived growth factor receptor
PDK-1	Phosphatidylinositol-dependent kinase-1
PI	Propidium iodide
PI3K	Phosphatidylinositol-3 kinase
PIP_2	Phosphatidylinositol-4,5-bisphosphate
PIP_3	Phosphatidylinositol-3,4,5-trisphosphate
PP2A	Protein phosphatase 2A
PS	Phosphatidylserine
PTP	Protein tyrosine phosphatase
QPCR	Quantitative polymerase chain reaction
ROS	Reactive oxygen species
RTK	Receptor tyrosine kinase
S6K	Ribosomal S6 kinase
SB	SB202190
SH2	Src homology 2
SOV	Sodium orthovanadate
VEGF	Vascular endothelial growth factor

CHAPTER 1

Literature Review

Inhibition of kinase signaling pathways in cancer cells by 3,3'-diindolylmethane

Introduction

Cancer is a leading cause of death worldwide, accounting for 13% of all deaths. The World Health Organization projects that cancer deaths will continue to rise, with 12 million estimated cancer deaths in 2030. Approximately 35%, with a range of 10-70%, of all cancer occurrences can be attributed to diet [1,2]. The observation that consumption of fruits and vegetables is inversely correlated with cancer risk suggests that bioactive food components are a promising area of study for cancer prevention and treatment [3-6]

Of particular interest are vegetables of the *Brassica* genus like broccoli, cabbage, or kale, which contain numerous bioactive compounds, including glucosinolates like glucobracissin [7-9]. Glucobracissin is located in a separate subcellular compartment from its degradation enzyme, myrosinase. When the vegetables are chewed or cut, myrosinase can catalyze the breakdown of glucobracissin to indole-3-carbinol (I3C), which itself has anticancer activity in a variety of cancers [10-15]. Upon consumption, I3C is exposed to the acidic environment of the stomach, and is rapidly converted into condensation products; the major product is 3,3'-diindolylmethane (DIM) [16]. Figure 1-1 depicts the structures of I3C and DIM. DIM also has anticancer activity in several cancer cells and in rodent cancer models [17-20]. Both DIM and I3C are current treatments for recurrent respiratory papillomatosis, a disease manifesting as benign laryngeal tumors, and are the subjects of clinical trials for the prevention and treatment of prostate, breast, and cervical cancers [21-24].

DIM is a promising compound for cancer treatment and prevention because it is effective in cell culture and rodent models, it is naturally-occurring in common vegetables and therefore widely available, it has very low toxicity, and it is bioavailable. Pharmacokinetic studies using rodents show that concentrations of 32-200 μM DIM can be achieved in tissues, with the highest levels in the liver, followed by the kidney, lung, heart, and brain [25]. Based on the maximal DIM levels achievable in rodents and on maximum tolerated doses of pure DIM in humans, Howells and colleagues estimate that concentrations of up to 50 μM DIM can be considered physiologically relevant [26].

DIM's anticancer activities include induction of cell cycle arrest and apoptosis, inhibition of angiogenesis, and immune activation [18-20,27-29]. Though some mechanisms for these activities in various cancer cells have been uncovered, it is clear that DIM works through multiple pathways, and more research is necessary to determine the full extent of DIM's effects and to identify specific cellular targets of DIM. Much research by our lab and others has been dedicated to determining the specific molecular mechanisms of DIM's action on cancer cells. Many of these studies show that DIM affects cell signaling pathways, particularly kinase activation and signaling. This dissertation focuses on DIM's effects on the signaling pathways of three specific kinases, p38 MAPK, Akt, and c-Met, a receptor tyrosine kinase with autophosphorylation activity.

Kinases are enzymes that transfer a phosphate group from ATP to tyrosine, serine, or threonine residues on a protein. Humans have 518 kinases, and documented mutations in 150 kinases are associated with diseases including various cancers [30]. Kinases show great potential as cancer drug targets, as aberrant kinase signaling can play a role in cancer initiation, promotion, or progression [31]. Over a dozen kinase inhibitors have FDA approval for cancer treatments, and over 100 more inhibitors are in clinical trials. Because of the side effects associated with these inhibitors, it is worthwhile to study inhibition of kinase signaling pathways by naturally-occurring compounds like DIM that have lower toxicity. Furthermore, studying the

inhibition of kinase pathways by DIM is crucial for determining the ultimate upstream targets of DIM.

In this review, I will summarize the literature on DIM's effects on activation and signaling of kinase pathways in cancer cells, including MAP kinases, Akt, and growth factor receptor tyrosine kinases, and discuss potential and known mechanisms for these responses.

MAPKs

Mitogen-activated protein kinase (MAPK) signaling cascades consist of the MAPKs themselves, MAP kinase kinases (MAP2Ks), MAP kinase kinase kinases (MAP3Ks), and their regulators. MAP3Ks phosphorylate MAP2Ks, and MAP2Ks phosphorylate MAPKs. MAPKs then phosphorylate, and therefore regulate, numerous transcription factors, kinases, and other enzymes on serine and threonine residues (Figure 1-2)[32]. These pathways can be activated by growth factors, cytokines, or various cellular stresses [33]. MAP2Ks are dual kinases that recognize unique secondary structures on one specific MAPK and phosphorylate both a tyrosine and a threonine residue, allowing for specificity in signaling. In contrast, MAP3Ks can phosphorylate multiple MAP2Ks. Further regulation of MAPK signaling is provided by scaffolding proteins and by phosphatases. Twelve MAPKs, seven MAP2Ks, and fourteen MAP3Ks have been described to date [34].

The MAPKs can be divided in to four groups: extracellular signal-regulated kinases (ERKs), p38s, c-Jun N-terminal kinases (JNKs), and ERK5. Figure 1-3 depicts mammalian MAPK cascades. DIM's effects on ERK, p38, and JNK kinases have been examined.

p38 and JNK

The p38 family consists of four known members: p38α, p38β, p38γ, and p38δ. p38α and β are ubiquitously expressed, whereas the other p38 proteins are tissue-specific. It is believed that p38α is responsible for the majority of p38 signaling, especially in cancer cells, since p38β is expressed in very low levels [35]. This review will therefore focus on DIM's effects on p38α, which will be referred to as "p38" in this dissertation. The p38 cascade is activated by cellular stresses or cytokines. Substrates of p38 include the transcription factors p53, ATF2, MEF2, and C/EBPβ [36,37].

The JNK family consists of three proteins, including JNK1, JNK2, and JNK3, which can be alternatively spliced to produce at least ten isoforms. JNK1/2 is found in all cells and JNK3 is brain-specific [38]. JNK proteins are activated by cellular stresses, growth factors, or differentiation factors. Substrates of JNK include c-JUN, which when phosphorylated forms a heterodimer with c-FOS to form the transcription factor AP1 [39].

The net results of activation of p38 in cells are apoptosis, cytokine production, inhibition of cell cycle progression, or differentiation, while activation of JNK could result in growth, differentiation, survival, or apoptosis, depending on the stimulus or cell type for either MAPK [35]. Figure 1-4 shows activation of p38 and JNK and highlights their phosphorylation substrates. Because both MAPKs are activated by cellular stresses, and DIM induces oxidative stress and ER stress in cells, the effects of DIM on the two MAPKs are often studied together [27,40].

Activation of p38 and JNK by DIM has been demonstrated in breast, prostate, cervical, glioma, and non-small cell lung cancer cells. In MCF-7 breast cancer cells, our lab demonstrated that 50 μM DIM induced p38 and JNK activation after 30 minutes and up to 4 hours, with peak activation after 1-2 hours [28]. Blocking p38/JNK activation by pharmacological inhibitors of the MAPKs or by transfection with dominant negative forms of p38 or JNK blocked DIM-induced interferon-gamma (IFNγ) promoter activation and gene expression. Pre-treatment of cells with BAPTA, a calcium chelator, or cyclosporin A, a calcineurin inhibitor, also prevented DIM-induced IFNγ promoter activation. Because p38 and JNK directly phosphorylate transcription factors known to bind to the IFNγ promoter, the authors concluded that calcium signaling is the ultimate upstream regulator of DIM's IFNγ-inducing activity. However, a direct link between calcium signaling and p38/JNK activation was not demonstrated in this study.

Later, in the same cell line, our lab demonstrated that DIM activates p38 and JNK by inducing formation of reactive oxygen species (ROS) [27]. By non-competitively inhibiting mitochondrial H^+-ATP synthase, DIM stimulated mitochondrial production of ROS. DIM (50 μM) activated p38 and JNK after 40 min and through 5 hours. Activation, determined by phosphorylation, of p38 and JNK was reversed by pre-treatment of MCF-7 cells with the antioxidants ascorbic acid and α-tocopherol. This study also demonstrated that activation of p38 and JNK activate the transcription factor Sp1, leading to increased transcription of the cyclin dependent kinase inhibitor $p21^{cip1/waf1}$.

Conversely, in LNCaP and DU145 prostate cancer cells, activation of p38 by DIM resulted in increased gene expression of the cyclin dependent kinase inhibitor $p27^{kip1}$, but not $p21^{cip1/waf1}$ [41]. This induction was also mediated by Sp1, and was blocked by transfection of cells with a dominant negative form of p38 or by pre-treatment of cells with a pharmacological inhibitor of p38. In this study, the same concentrations of DIM (50 μM) that activated p38 in breast cancer cells activated p38 in prostate cancer cells, but activation was measured only after 24 hours. The differences in response in breast versus prostate cancer cells suggest that DIM activates p38 signaling differently between the two tissue types. DIM did not activate JNK after 24 hours in either cell line examined in this study.

Khwaja et al. [42] also examined p38 activation in prostate cancer cells. They found activation of p38 as soon as 1 minute after treatment with 500 μM DIM in PC-3 cells, and this activation increased through 8 hours, the latest time point measured. This very high and insoluble concentration of DIM resulted in 0% cell survival after 48 hours. The authors found that knockdown of p38 by siRNA blocked DIM's induction of the pro-apoptotic protein $p75^{NTR}$. However, since lower, less toxic, concentrations of DIM (50 -100 μM) also induced $p75^{NTR}$ protein levels in PC-3 and DU145 cells, examination of p38 activation by these concentrations of DIM would have been more relevant.

Rahimi et al. measured p38 activation by 20-50 μM DIM in breast cancer, glioma, and non-small cell lung cancer cells and observed activation of p38 with no changes in total p38 in all cell lines after 48 hours [43].

In C33A cervical cancer cells, DIM resulted in activation of IRE1α, determined by detection of the alternatively spliced version of XBP-1 that is associated with IRE1α-catalyzed splicing [40]. IRE1α can stimulate phosphorylation of JNK as a result of endoplasmic retiuculum (ER) stress through interaction with TRAF2/ASK1 at the ER membrane [44,45]. IRE1α activation was biphasic and peaked at 3 and 18 hours after treatment with 75 μM DIM. JNK phosphorylation was detected after 3 hours, the earliest time point used, and lasted for 18 hours. At 24 h, no phosphorylated JNK was detected. This study found that DIM was more

effective at killing cancer cells that were undergoing stress, including nutrient limitation, hypoxia, or ER stress, and that activation of JNK, possibly by IRE1α, may be responsible for this effect. While IRE1α can result in activation of both JNK and p38, the authors did not report any effects on p38 by DIM in C33A cells.

All studies reporting activation of p38 or JNK1/2 by DIM either did not report any changes in p38 or JNK1/2 protein expression or showed that expression of these proteins does not change [27,28,40-42]. However, gene expression profiling studies indicate that DIM also affects levels of MAP2K and MAP3K transcripts. Carter et al. reported that 100 μM DIM results in a 2-fold increase in *MAP2K4* in C33A cervical cancer cells after 6 hours [46]. Li et al found changes of -2 to -3.9-fold in *MAP3K14*, *MAP2K3*, *MAP2K4*, and *MAP4K3* in PC3 prostate cancer cells treated with 40 μM DIM for 24 and 48 hours [47]. The same group later showed decreased *MAP3K14* by 1.7-fold after 24 hours and 1.6-fold after 48 h, and decreased *MAP3K12* gene expression by 1.8-fold after 48 hours in MDA-MB-231 breast cancer cells treated with 40 μM DIM [48]. However, these gene expression studies did not test protein levels or the relationship between decreased MAP2K and MAP3K expression and increased p38 and JNK activation.

Overall, reports are fairly consistent that DIM activates p38 and JNK in cancer cells, with more support for p38 activation. However, the kinetics and the concentrations necessary to see these effects vary according to cell line. The mechanisms for p38 and JNK activation are varied and include reactive oxygen species, calcium signaling, ER stress, or possibly changes in expression of upstream activators.

ERK

There are four ERK family proteins, named ERK1 – ERK4, although ERK1 and ERK2 are the most extensively studied, and the only two studied in relation to DIM. In this review, "ERK" will refer to ERK1/2 unless stated otherwise.

The ERK signaling pathway consists of RAF kinases, the MAP3Ks; MEK1/2, the MAP2Ks; and ERK (Figure 1-5). This cascade is activated by growth factors signaling through their receptors and activating Ras. Components of the ERK pathway are also frequently mutationally activated or over expressed in cancer cells, leading to over activation of ERK. Active ERK phosphorylates over 160 targets, including Elk1, Ets1, c-Myc, and epidermal growth factor receptor (EGFR). The net result of activation of ERK in cells is proliferation and survival [30]. For this reason, a current focus of cancer researchers is to develop and test therapies that inhibit components or upstream activators or the ERK signaling pathway, including MEK1 and 2, BRAF, EGFR, HER2, and Ras [49-53], reviewed in [30].

The roles of the Ras-Raf-MEK-ERK cascade in DIM's effects on cancer cells are less established than the roles of p38 and JNK, as fewer studies report the effect of DIM on this pathway in cancer cells, and they have conflicting results. McGuire et al. report that 15 μM DIM decreases ERK phosphorylation by 25% after 24 hours in MDA-MB-435-eb cells, breast cancer cells that overexpress HER2 [54]. Co-treatment of 15 μM DIM and 10 nM paclitaxel resulted in an 85% reduction of ERK activation, which suggests that DIM and paclitaxel act synergistically, since the inhibition by the combination of compounds was greater than the sum of the percent inhibition by DIM (25%) and paclitaxel (50%) alone. In Sk-ChA-1 cholangiocarcinoma cells, 25

μM DIM strongly decreased ERK phosphorylation, but not total ERK levels, after 24 h, and this was consistent with decreased Akt activation and increased apoptosis [55].

However, Leong et al. report activation of ERK in endometrial cancer cells [56]. Ishikawa cells treated with 30 μM DIM for 30 minutes showed a strong increase in ERK1 phosphorylation and a modest increase in ERK2 phosphorylation compared to that in cells treated with the vehicle alone. Many factors could account for the differential response of ERK to DIM, including cell type differences, concentrations of DIM used, and the timing of the treatment. It is possible that DIM activates ERK at early time points through a stress-mediated pathway, followed by long-term inactivation of ERK. More studies will be necessary to determine how DIM affects ERK in various cancer types.

DIM's inhibition of this cascade in endothelial cells as it relates to *in vitro* angiogenesis is more established. Two groups have studied the effects of DIM on *in vitro* angiogenesis. Kunimasa and colleagues report that DIM (12.5-25 μM) strongly inhibits tube formation in human umbilical vein endothelial cells (HUVECs), and that the same concentrations inhibit activation of ERK by 86 and 90%, respectively [57]. HUVECs were grown in growth medium containing multiple mitogens that can activate ERK. Because inactivation of ERK by the highly selective MEK inhibitor U0126 also inhibits tube formation in HUVECs, the authors concluded that inhibition of tube formation by DIM is likely mediated in part by inactivation of ERK. A study from our lab reports similar findings, with ERK inhibited by approximately 60 and 80% by 10 and 25 μM DIM, respectively, in HUVECs [58]. However, in this study, cells were incubated in serum-free medium, and individual growth factors were used to activate ERK. DIM inhibited ERK activation by vascular endothelial growth factor (VEGF), platelet-derived growth factor (PDGF), insulin-like growth factor-1 (IGF-1), and epidermal growth factor (EGF). DIM inhibits these signaling pathways at the point of Ras, because VEGF receptor phosphorylation was not affected, but Ras-GTP content and phosphorylation of Raf, MEK1/2, and ERK were all decreased by treatment with DIM. Overexpression of constitutively active mutant Ras (RasG12V) also reversed DIM's inhibition of ERK activation.

The studies on DIM and ERK signaling in cancer cells show conflicting results, possibly due to different cell types or concentrations of DIM. Because ERK is an important mediator of proliferation in cancer cells, it will be worthwhile to determine the cell types or conditions in which DIM inhibits ERK activation.

Akt

Akt is a serine/threonine protein kinase that regulates many normal cellular and cancer processes. Akt is activated by diverse stimuli, including growth factors, integrins, or cytokines. Through various mechanisms, the p85 adapter subunit of phosphatidyl inositol-3 kinase (PI3K) is recruited to the plasma membrane and then allosterically activates the catalytic p110 subunit. Active PI3K phosphorylates the phospholipid substrate phosphatidylinositol-4,5-bisphosphate (PIP_2) to form phosphatidylinositol-3,4,5-trisphosphate (PIP_3). The pleckstrin homology (PH) domain of Akt interacts with PIP_3, causing a conformational change in Akt that exposes threonine 308 and serine 473 of Akt. Phosphatidylinositol-dependent kinase-1 (PDK-1) phosphorylates Akt on threonine 308 and mTORC2 phosphorylates Akt on serine 473 [59-61], fully activating Akt. Negative regulation of Akt signaling is provided by protein tyrosine phosphatases (PTPs) that dephosphorylate receptors, protein phosphatase 2A (PP2A) that

dephosphorylates Akt, and PTEN, which catalyzes the reverse PI3K reaction. Once active, Akt can phosphorylate its substrates, including glycogen synthase kinase-3β (GSK-3β), androgen receptor (AR), mammalian target of rapamycin (mTOR), and members of the forkhead family of transcription factors like FOXO3 . Phosphorylation of Akt can either activate or inactivate its substrates, as shown in figure 1-6.

The net result of activation of the Akt pathway in cancer cells is increased proliferation, motility, invasiveness, and survival through various mechanisms involving Akt's substrates. For example, Akt inactivates GSK-3β by phosphorylating it at serine 9. Active GSK-3β phosphorylates the transcriptional coactivator β-catenin. This phosphorylation targets β-catenin for degradation, preventing β-catenin from activating genes involved in cell proliferation and survival like c-myc and cyclin D [62-64]. Akt phosphorylates AR at serines 213 and 791, and this phosphorylation sensitizes AR and allows it to be activated by lower levels of androgens [65]. FOXO3 is a transcription factor that activates genes involved in cell cycle arrest or apoptosis, such as $p27^{kip1}$. When phosphorylated by Akt at threonine 32 and serines 253 and 315, FOXO3 can no longer bind to DNA and translocates from the nucleus to the cytoplasm [66,67]. Phosphorylation by Akt activates mTOR, which regulates cell growth by promoting translation, phosphorylating the eukaryotic translation initiation factor (eIF) 4E binding protein (4E-BP1) and S6 kinase (S6K). Phosphorylation of 4E-BP1 releases it from eIF4E, allowing eIF4E to participate in the rate limiting step of cap-dependent translation initiation, and phosphorylation of S6K by mTOR activates it, allowing S6K to phosphorylate the 40S ribosomal protein S6, which increases the translation of certain mRNAs [68]. Akt can also activate nuclear factor- κB (NF-κB), a transcription factor, by inducing the degradation of inhibitor of NF-κB (IκB), an inhibitory protein that sequesters NF-κB in the cytoplasm. The exact mechanism of this induction is unknown, although researchers have shown that it involves activation of IκB kinase (IKK), the kinase that phosphorylates IκB, by Akt [69]. Active NF-κB activates or represses genes that mediate proliferation, metastasis, and other cancer processes [70].

Akt inactivation by DIM and its importance have been studied extensively in cancer cells, particularly prostate cancer cells. Bhuiyan et al. first reported Akt inactivation by DIM in androgen-sensitive LNCaP and androgen-insensitive C4-2B prostate cancer cells [71]. When cells were transfected with wild-type or myristoylated (constitutively active) Akt and treated with 50 μM B-DIM, a form of DIM that has higher *in vivo* bioavailability, for 48 hours, both cell lines showed decreased Akt phosphorylation. NF-κB nuclear localization and DNA binding, androgen receptor phosphorylation and nuclear localization, and prostate specific antigen protein expression, all downstream events of Akt activation, were decreased by DIM as well.

Later, the same group followed Akt inhibition by DIM downstream a separate pathway in the same cell lines and investigated the effects of DIM on FOXO3 and GSK-3/β-catenin [72]. For these experiments, the authors used insulin-like growth factor-1 (IGF-1), and not Akt overexpression, to activate Akt. As expected, DIM (50 μM B-DIM for 48 hours) decreased phosphorylation of both Akt and the Akt substrate FOXO3, prevented Akt and FOXO3 complex formation, decreased FOXO3 binding to the *AR* promoter, and increased FOXO3 binding to the $p27^{KIP1}$ promoter. B-DIM also increased GSK-3β binding to β-catenin, and decreased β-catenin protein levels and nuclear translocation.

In PC3 prostate cancer cells stably overexpressing platelet-derived growth factor-D (PDGF-D), B-DIM (5-25 μM) decreased phosphorylation of Akt, mTOR, S6K, and 4E-BP1, and decreased cell growth and invasion after 48 hours [73]. B-DIM also affected phosphorylation of these proteins in cells stably transfected with the empty vector, though to a lesser degree. These

effects were in part due to decreased expression of full-length and activated (cleaved) PDGF-D by B-DIM.

In DU145 prostate cancer cells, Garikapaty et al reported decreased PI3K p85 subunit and Akt protein expression by 25 and 50 μM DIM [74]. This is the first study to show decreased total Akt levels, as the previous studies showed that total Akt levels were not affected by 50 μM B-DIM in LNCaP and C4-2B prostate cancer cells after 48 hours [71]. Furthermore, Akt levels were reduced by DIM and not by I3C. However, in a gene expression study, I3C, but not DIM, decreased expression of *PIK3CA* and *PIK3CB*, the genes encoding the subunits of PI3K, after 6-48 hours in PC-3 prostate cancer cells [47]. The conflicting results on DIM versus I3C's effect and inhibition of gene expression, protein levels, or protein activation may be due to differences in cell type, although androgen sensitivity did not play a role in DIM's effects in two separate studies. The formulation of DIM used and the times of the DIM treatments may also contribute to the varying results. It is interesting however, that studies on Akt activation used extended time points (24-48 hours) despite the rapid kinetics of Akt activation and signaling [75].

Researchers found similar effects of DIM in cholangiocarcinoma cells [55]. Subpopulations of Sk-ChA-1 cells that were sensitive or resistant to Fas-mediated apoptosis were treated with 30 μM DIM and a Fas-activating antibody for 24 h. DIM, but not I3C, induced apoptosis and decreased Akt phosphorylation in both subpopulations of cells.

Both DIM and B-DIM decrease Akt activation in breast cancer cells. DIM at 50-100 μM decreased Akt phosphorylation in MCF10CA1a breast cancer cells, but not in non-tumorigenic MCF10AneoT cells [76]. This resulted in decreased EGF-induced Akt kinase activity and decreased NF-κB activation. The authors also reported decreased EGF-activated PI3K activity, which could be responsible for decreased Akt activity. The same group later reported that lower concentrations of B-DIM (30 μM) for 72 hours decreases Akt phosphorylation in MDA-MB-231 breast cancer cells, and this correlates with growth inhibition and sensitivity of cells to apoptosis by Taxotere [77].

DIM consistently decreases Akt activation in cancer cells, although the kinetics and concentrations vary. While Rahman et al showed that DIM did not affect Akt activation in non-tumorigenic breast epithelial cells, others observed that DIM (12.5-25 μM, 24 h) inhibits Akt activation by about 30% in HUVECs, non-tumorigenic epithelial cells [57], suggesting that more research is necessary to determine the effects of DIM on Akt signaling in non-tumorigenic cells.

Growth Factor Receptor Tyrosine Kinases

Growth factors are secreted proteins or steroid hormones. Receptors for certain growth factors, including EGF, IGF-1, PDGF, VEGF, and hepatocyte growth factor (HGF) have intrinsic protein kinase activity, and are therefore referred to as receptor tyrosine kinases (RTKs). These receptors have extracellular, transmembrane, and intracellular domains. Ligands bind to the extracellular portions, and the kinase activity is intracellular. Growth factor binding induces a conformational change in the receptor that promotes and stabilizes homo- or hetero-dimerization of receptors which leads to trans autophosphorylation of the receptor at tyrosine residues. The phosphotyrosines are binding sites for proteins containing Src homology 2 (SH2) or phosphotyrosine binding domains, including downstream signaling proteins or adapter proteins that recruit other downstream effectors. Figure 1-7 shows phosphotyrosine residues and their specific binding partners on the PDGF receptor α and β forms [78]. This illustrates the

complexity of signaling from RTKs, as well as the diversity between various receptors, even those of the same family that bind the same ligand. Phosphorylated receptors are then internalized by endocytosis and degraded or recycled [78-81].

There are twenty subfamilies of receptor tyrosine kinases [82]. Figure 1-8 illlustrates the domain structures of various RTKs. DIM's effects on EGFR family proteins, the VEGF receptor KDR, and the HGF receptor, Met have been studied. The EGFR family consists of ErbB1, ErbB2, ErbB3, and ErbB4. ErbB1 is also known as EGFR, and ErbB2 is HER2/neu, the oncogene frequently over expressed in breast cancer. Growth factor RTKs are frequently overexpressed, hyperactive, or growth factor independent in cancers, leading to dysregulated growth and proliferation of cells, and are therefore popular targets for new and current therapies including monoclonal antibodies against the receptors, small molecule kinase inhibitors, or inactive compounds that compete with growth factors [83-85].

One study provides evidence that DIM exerts its effects downstream of growth factor receptors because DIM inhibits signaling pathways that are activated by multiple stimuli that activate distinct receptors. Chang et al. reported that DIM inhibits Ras signaling in HUVECs downstream of multiple growth factors including VEGF, EGF, IGF-1, and PDGF [58]. DIM did not affect phosphorylation of the VEGF receptor KDR. However, it is worth noting that HUVECs are primary endothelial cells and not cancer cells, and therefore may respond differently to DIM than cancer cells do.

Other studies implicate specific growth factor receptors in DIM's effects but do not rule out others. For example, DIM decreases expression of full-length and activated PDGF-D in both PC3 prostate cancer cells and in PC3 PDGF-D cells that stably overexpress the growth factor [73], suggesting that the growth inhibition observed in these cells is due to decreased signaling from the PDGF receptor. The same group reported that DIM decreased EGF-activated PI3K and Akt activity in MCF10CA1a breast cancer cells [76]. In MDA-MB-435eB1 breast cancer cells, DIM inhibited cell viability and phosphorylation and expression of HER2/neu, which is overexpressed in this cell line [54]. In each of these studies, only one growth factor pathway was studied.

However, one study showed a role for multiple growth factor receptors in DIM's mechanisms of action in various cancer cell lines [43]. Rahimi's group studied the effects of DIM on cell lines expressing various EGFR mutants, including two breast cancer and two glioma cell lines transfected with either an empty vector or EGFR variant III (EGFRvIII), and two non-small cell lung cancer (NSCLC) cell lines that express EGFR with a mutated tyrosine kinase domain. EGFRvIII is a form of EGFR that has a truncation mutation that results in constitutive phosphorylation and ligand independence. EGFRvIII expression is associated with increased tumorigenicity and poor prognosis in cancer [86,87]. DIM inhibited the growth of all cell lines, though the EGFRvIII-expressing cells were more resistant to DIM. This suggests that while DIM may inhibit EGFR signaling, its antiproliferative activity is largely independent of EGFR. The authors also observed decreased phosphorylation and expression of EGFRvIII and wild type EGFR in all cell lines to different degrees, and decreased activation and expression of HER2 in breast cancer cells and of Met in glioma and NSCLC cells.

More studies are needed to determine how DIM is affecting activation of growth factor receptors. Possible mechanisms worth exploring include inhibition of autophosphorylation, dimerization, or ligand binding, as well as activation of phosphatases or decreased receptor expression.

Conclusions

Overwhelming evidence shows that DIM regulates kinase signaling pathways in cancer cells and that the overall results of inhibited kinase signaling are cell cycle arrest or apoptosis. While most studies focus on the downstream effects of inhibition of these pathways, a few have shed light on mechanisms of DIM's actions, which include ER stress, oxidative stress, or altered calcium signaling.

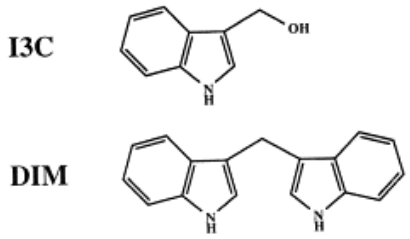

Figure 1-1. Structures of indole-3-carbinol (I3C) and 3,3'-diindolylmethane (DIM) [88]. DIM is the major acid condensation product of *Brassica*-derived I3C.

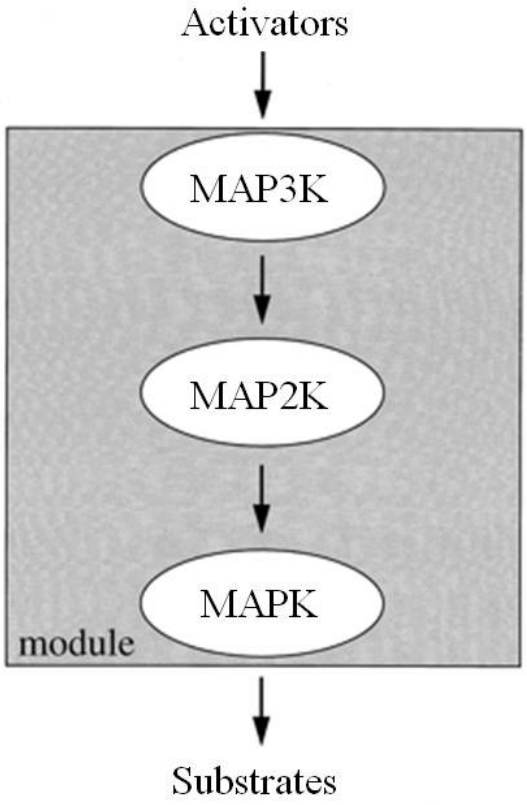

Figure 1-2. General MAPK signaling [34]. MAP3Ks phosphorylate MAP2Ks, and MAP2Ks phosphorylate MAPKs. MAPKs then phosphorylate, and therefore regulate, numerous transcription factors, kinases, and other enzymes on serine and threonine residues. These pathways can be activated by growth factors, cytokines, or various cellular stresses.

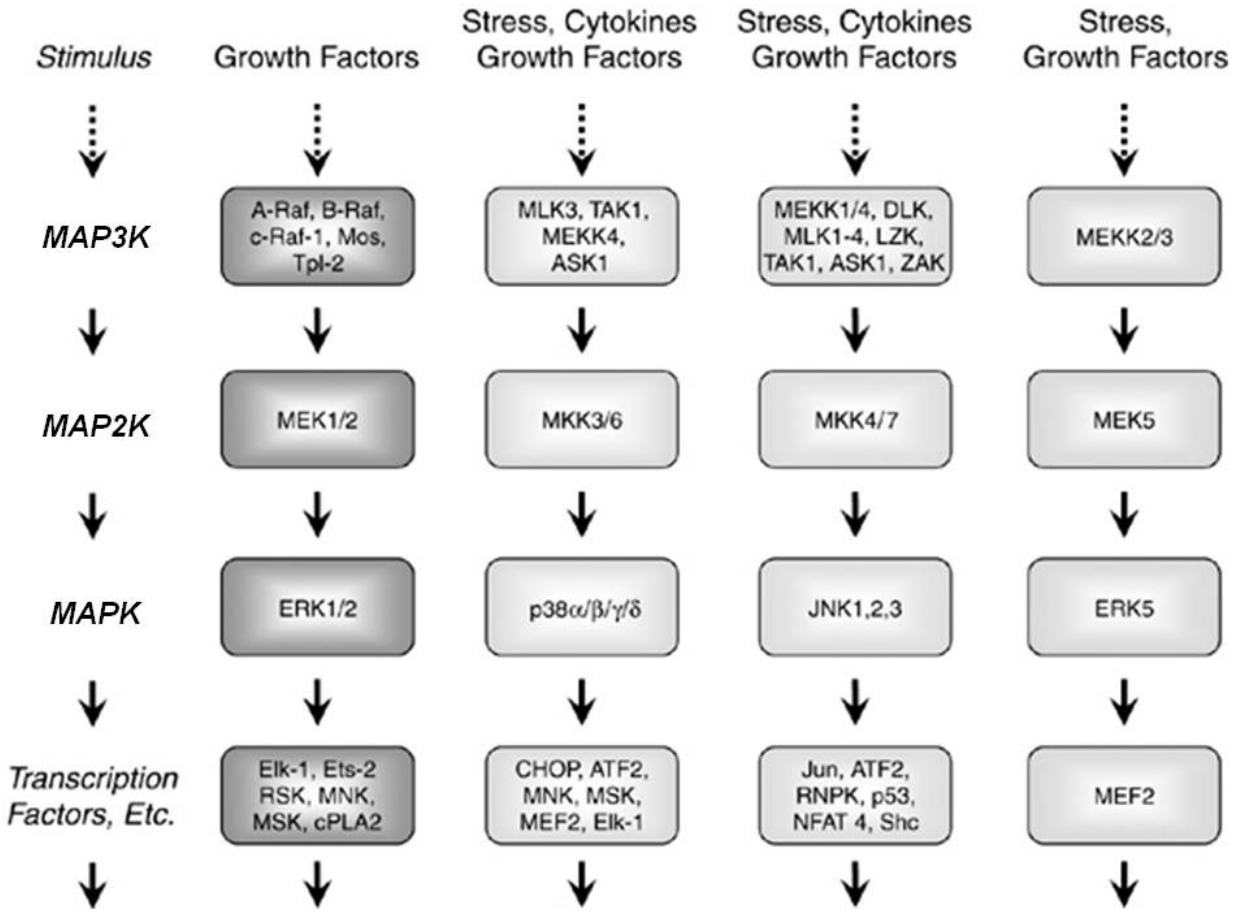

Figure 1-3. MAPK signaling [30]. The MAPKs can be divided in to four groups: extracellular signal-regulated kinases (ERKs), p38s, c-Jun N-terminal kinases (JNKs), and ERK5. DIM's effects on ERK, p38, and JNK kinases have been examined.

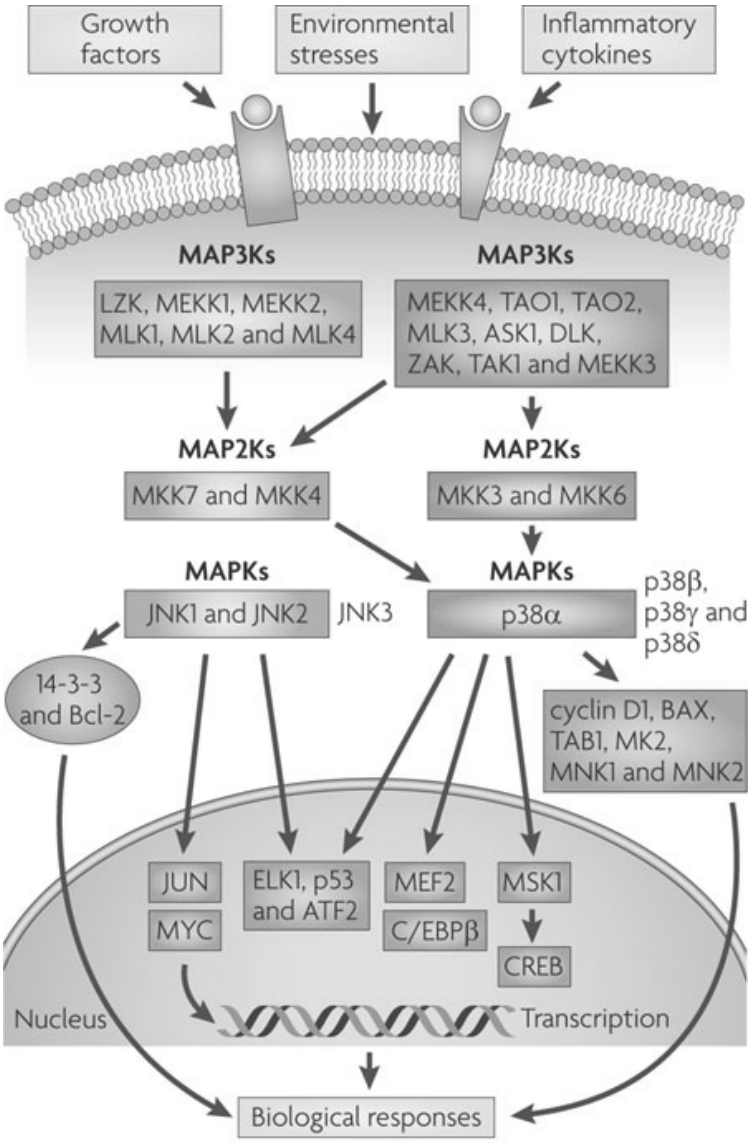

Figure 1-4. p38 and JNK activation and signaling [34]. JNK and p38 are activated by growth factors, stress, or cytokines. These stimuli signal through MAP3Ks and MAP2Ks to phosphorylate p38 and JNK, which regulate various transcription factors that mediate growth, cell division, cytokine production, apoptosis, or differentiation.

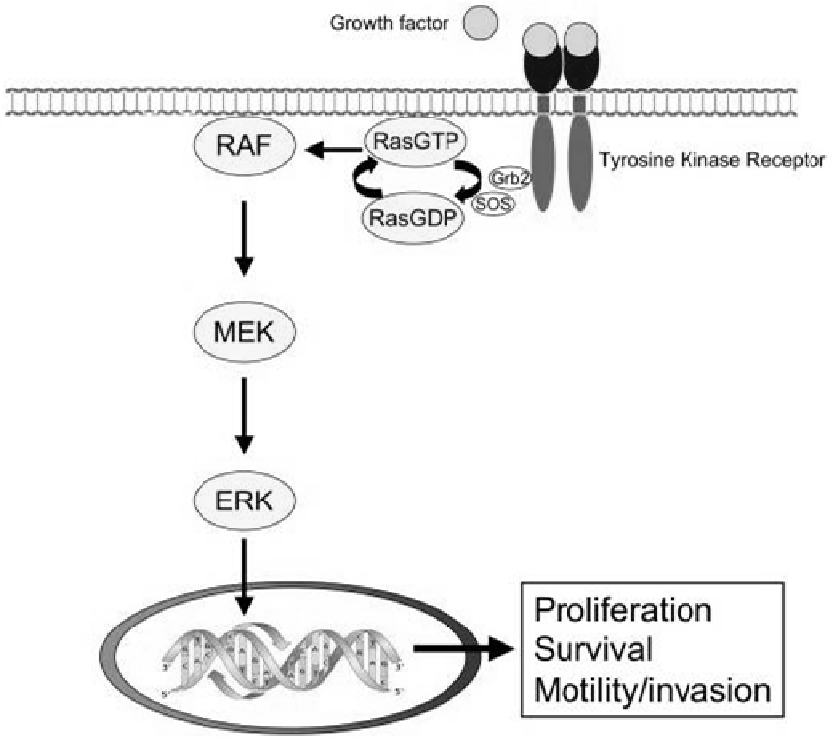

Figure 1-5. The RAF-MEK-ERK cascade [89]. The ERK signaling pathway consists of RAF kinases, the MAP3Ks; MEK1/2, the MAP2Ks; and ERK. This cascade is activated by growth factors signaling through their receptors and activating Ras. Components of the ERK pathway are also frequently mutationally activated or overexpressed in cancer cells, leading to over activation of ERK. Active ERK phosphorylates over 160 targets, including Elk1, Ets1, c-Myc, and EGFR. The net result of activation of ERK in cells is proliferation and survival.

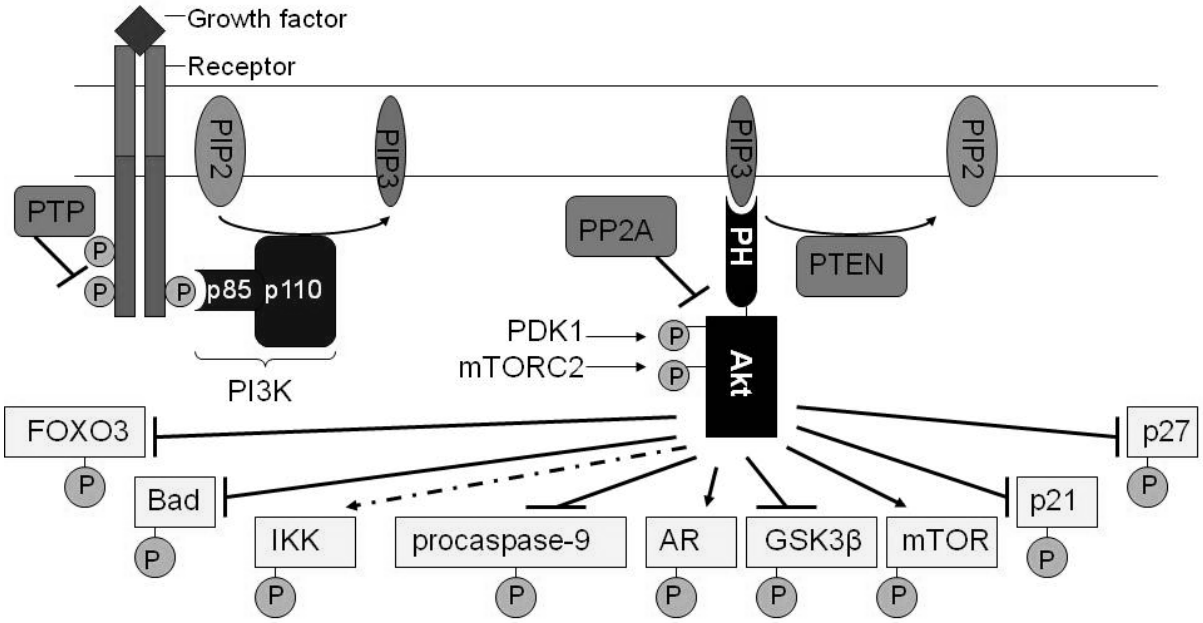

Figure 1-6. Activation of Akt by growth factor receptors/PI3K. Adapted from [90,91]. Through various mechanisms, the p85 adapter subunit of phosphatidyl inositol-3 kinase (PI3K) is recruited to phosphotyrosine residues on activated growth factor receptros and then allosterically activates the catalytic p110 subunit of PI3K. Active PI3K phosphorylates the phospholipid substrate PIP_2 to form PIP_3. The pleckstrin homology (PH) domain of Akt interacts with PIP_3, causing a conformational change in Akt that exposes threonine 308 and serine 473 of Akt. Phosphatidylinositol-dependent kinase-1 (PDK-1) phosphorylates Akt on threonine 308 and mTORC2 phosphorylates Akt on serine 473, fully activating Akt. Negative regulation of Akt signaling is provided by protein tyrosine phosphatases (PTP) that dephosphorylate receptors, protein phosphatase 2A (PP2A) that dephosphorylates Akt, and PTEN, which catalyzes the reverse PI3K reaction. Once active, Akt can phosphorylate its substrates, including glycogen synthase kinase-3β (GSK-3β), androgen receptor (AR), mammalian target of rapamycin (mTOR), and members of the forkhead family of transcription factors like FOXO3 .

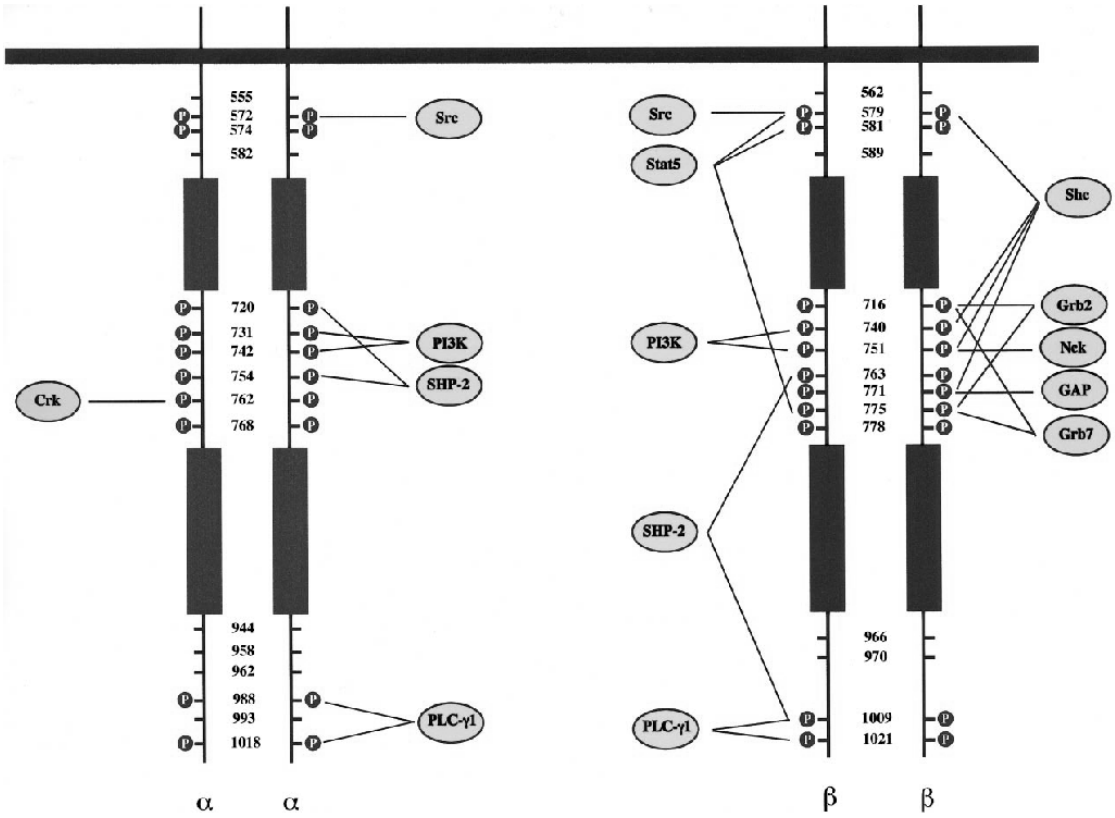

Figure 1-7. Phosphotyrosine residues and recruited signaling proteins on PDGFRα and PDGFRβ [78]. Growth factor binding to receptors induces a conformational change in the receptor that promotes and stabilizes homo- or hetero-dimerization which then leads to trans autophosphorylation at tyrosine residues. The phosphotyrosines are binding sites for proteins containing Src homology 2 (SH2) or phosphotyrosine binding domains, including downstream signaling proteins or adapter proteins that recruit other downstream effectors.

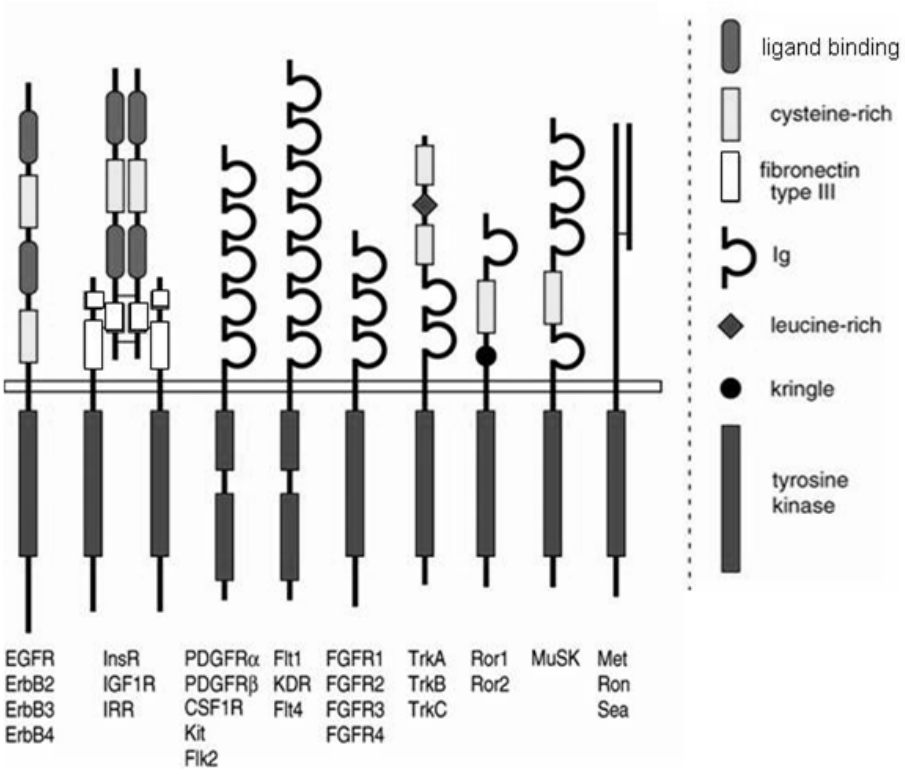

Figure 1-8. Select receptor tyrosine kinase domain structures. Adapted from [92].

CHAPTER 2

DIM inhibits Akt activation, cell cycle progression, survival, and *in vitro* metastasis in MDA-MB-231 breast cancer cells

Introduction

The inverse correlation of consumption of fruits and vegetables and breast cancer risk suggests that bioactive components from these foods represent a promising area of study for breast cancer prevention and treatment [4]. The acid condensation product of *Brassica*-derived indole-3-carbinol, 3,3'-diindolylmethane (DIM), is one such compound that has anti-breast cancer activity. DIM is antitumorigenic against carcinogen-induced breast cancer in Sprague-Dawley rats [17] and against human breast cancer xenografts in nude mice [18]. DIM induces a G1 cell cycle arrest [20] and increases apoptosis in MDA-MB-231 and MCF-7 breast cancer cells via decreased Bcl-2 protein, increased Bax, and decreased Bax/Bcl-2 binding [19]. Pharmacokinetic studies using rodents show that concentrations of 32-200 μM DIM can be achieved in tissues, with the highest levels in the liver, followed by the kidney, lung, heart, and brain [25]. Based on the maximal DIM levels achievable in rodents and on maximum tolerated doses of pure DIM in humans, Howells and colleagues estimate that concentrations of up to 50 μM DIM can be considered physiologically relevant [26]. Thus, DIM may be a promising alternative for breast cancer treatment or prevention because of its efficacy *in vitro* and *in vivo* and because it is widely available, has low toxicity, and is bioavailable.

Signaling in multiple pathways is altered by DIM in breast cancer cells. One of these pathways, Akt signaling, is frequently dysregulated in breast cancer, making Akt an attractive target for therapeutic treatments [93]. Akt is a kinase that is activated by diverse stimuli, including the growth factors EGF, IGF-1, and HGF [94]. Growth factors binding to their receptors activate PI3K, which forms PIP_3, the membrane lipid that recruits Akt and causes a conformational change in Akt that exposes Akt's threonine 308 and serine 473. PDK-1 phosphorylates Akt on threonine 308 and mTORC2 phosphorylates Akt on serine 473 [59-61], fully activating Akt. Once active, Akt can phosphorylate its substrates, including GSK-3α/β. The net result of activation of the Akt pathway in cancer cells is increased proliferation, survival, and motility/invasiveness of cells.

Inhibition of Akt by DIM has been reported in breast, prostate, and cholangiocarcinoma cells [55,71,76]. DIM also inhibits tube formation and induces apoptosis in human vascular cells via inhibition of Akt [57]. In breast cancer cells, this inhibition has many established cellular consequences, including inhibition of the apoptosis inhibitor NF-κB, induction and nuclear localization of the cell cycle inhibitor $p27^{kip}$, induction of apoptosis, and enhanced sensitivity to the chemotherapeutic agent Taxotere [76,77,95]. However, several studies describing this inhibition use very high (50-100 μM) concentrations of DIM that are unlikely to be achieved *in vivo*. Moreover, these published studies report effects on Akt phosphorylation after 24-72 hours, despite the known rapid kinetics of Akt activation and signaling in cancer cells [75]. Furthermore, a mechanism by which DIM inhibits Akt has not yet been defined. We sought to further characterize the inhibitory effects of DIM on Akt signaling and Akt downstream events using physiologically relevant concentrations of the indole and to determine the role of primary upstream activators in these effects.

In this study, we demonstrate that physiologically relevant concentrations of DIM inhibit short- and long-term activation of Akt in the highly invasive MDA-MB-231 breast cancer cells. We also report that DIM selectively inhibits HGF-induced Akt activation, which is one novel mechanism by which DIM inhibits Akt. Finally, we show that DIM induces a G1 cell cycle arrest, apoptosis, and inhibition of *in vitro* metastasis, events that are characteristic of Akt inhibition in cancer cells.

Materials and methods

Cell culture and supplies

MDA-MB-231 cells were purchased from American Type Culture Collection (ATCC) and were grown in Dulbecco's Modified Eagle Medium (DMEM, Invitrogen) supplemented to 4.0 g/L glucose, 3.7 g/L sodium bicarbonate, and 10% FBS (Omega Scientific) in a humidified incubator at 37 °C and 5% CO_2. MCF10AT cells were purchased from ATCC and were grown under similar conditions except they were maintained in DMEM/F12 (Invitrogen) with 10% FBS, 20 ng/mL epidermal growth factor (Sigma), 0.5 μg/mL hydrocortisone (Sigma), 10 μg/mL insulin (Invitrogen), 100 ng/mL cholera toxin (Sigma), and 1% Pen/Strep (Invitrogen). Cells were passaged regularly before reaching 80% confluency, and cells used in experiments were at less than 25 passages. Prior to all experiments, monolayers were washed with PBS and the medium was changed to either medium with 1% FBS or serum-free medium for 24 hours. DIM (LKT Laboratories) or the vehicle control DMSO (Acros Organics) was then added for the indicated times. LY294002 was purchased from Tocris, Matrigel and Annexin V-AlexaFluor488 was purchased from Invitrogen, and propidium iodide and growth factors were purchased from Sigma. Transwell inserts were from BD Biosciences. All other cell culture supplies were purchased from Fisher Scientific.

Western blot analysis

To prepare whole cell lysates, monolayers were scraped directly in protein loading buffer (10% glycerol, 5% 2 mercaptoethanol, 10% SDS, 0.125 M Tris–HCl pH 6.7, 0.15% bromophenol blue), sonicated for 15 s, and heated to 99.9 °C for 5 minutes. Equal amounts of protein were separated by SDS-PAGE and transferred to Immobilon P membranes (Millipore). Membranes were blocked in 5% nonfat dry milk in TBS-Tween for 1 hour and then probed with rabbit anti-Akt (sc-8312), mouse anti-GSK-3α/β (sc-7291), mouse anti-tubulin (sc-5274) from Santa Cruz Biotechnology, rabbit anti-phospho Akt Ser473 (#4058), rabbit anti-phospho GSK-3α/β (#9331) from Cell Signaling Technology or rabbit anti-PARP (214/215) cleavage site (44698G) from Invitrogen overnight at 4 °C. After washing three times in TBST, membranes were incubated in 5% nonfat dry milk in TBST containing the appropriate secondary antibody-HRP conjugates (Santa Cruz Biotechnology), washed again, and exposed to Western Lighting *Plus*-ECL enhanced chemiluminescence substrate (Perkin Elmer) for 1 minute. Immunoreactive proteins were detected using CL-Xposure film (Thermo Scientific). Results shown are representative of at least three independent experiments.

Cell cycle analysis

MDA-MB-231 cells were plated at 10^5 cells/well in 6-well plates. After 24 hours, cells were washed in PBS and switched to medium containing 1% FBS and treated with 0, 15, or 25 μM DIM or 25 μM for 24 hours or LY294002 for 6 hours. Following treatment, cells were

washed with PBS and hypotonically lysed in 0.5 ml of DNA staining solution (0.5 mg/ml propidium, 0.1% sodium citrate, 0.05% Triton X-100). Nuclear-emitted fluorescence with wavelengths of >585 nm was measured with a Coulter® EPICS® XL™ flow cytometer. Ten thousand nuclei were analyzed from each sample at a rate of 300–500 nuclei/s. The percentages of cells within the G_1, S, and G_2/M phases of the cell cycle were determined by analysis with the Multicycle software MPLUS (Phoenix Flow Systems) in the Cancer Research Laboratory Microchemical Facility of the University of California, Berkeley [41].

Annexin V staining

Cells were treated with 0, 15, or 25 μM DIM in DMEM containing 1% FBS for 24 or 48 hours. Live cells were collected by trypsinization, washed with PBS and stained with Annexin V- Alexa Fluor 488 (Invitrogen) and propidium iodide (PI, Sigma) for 15 minutes and then analyzed immediately using a Becton Dickinson FACScan and CellQuest sofware. All Annexin V-binding cells were considered to be apoptotic regardless of PI binding [96].

Invasion and migration assays

Invasion was assessed using the modified transwell Boyden chamber system [18]. Chambers were assembled using 8 μm-pore BD Falcon transwell inserts as the upper chambers and the 12-well plates as the lower chambers. Cell culture inserts were coated with 100 μl/insert Matrigel. The Matrigel was allowed to gel for 4 hours and then was washed with serum-free DMEM. HUVECs were harvested by trypsin/EDTA and resuspended in serum-free DMEM. Medium containing 1% FBS was applied to the lower chamber as a chemoattractant. Cells were then seeded at 0.5 x 10^5 cells/insert in the upper chamber in the presence of 0, 5, 15 or 25 μM DIM and incubated for 8 hours at 37°C and 5% CO_2. At the end of the incubation, the cells in the upper chamber were removed with cotton swabs and cells that traversed the Matrigel to the lower surface of the insert were fixed with 10% formalin/PBS and stained with crystal violet in 10% formalin/PBS, and were photographed under the light microscope at a magnification of x40. Multiple fields from triplicate wells were photographed. Migration was analyzed by the same method except the transwell inserts were not coated with Matrigel.

Wound healing assay

Cell migration was assessed as described [18] with modifications. MDA-MB-231 cells were grown to confluency in 24-well plates. A sterile pipette tip was used to scratch the monolayer and create a gap of constant width. Monolayers were then washed three times with PBS to remove floating cells and debris. DMEM + 1% FBS with increasing concentrations of DIM was added to the cells for 16 hours. Cells were fixed with 10% formalin/PBS and stained with crystal violet in 10% formalin/PBS. Two individual fields from each of three wounds per experiment were photographed using a Nikon Coolpix990 digital camera connected to the Nikon Eclipse TS100 microscope at a 100X magnification.

Results

DIM inhibits Akt activation in MDA-MB-231 cells

DIM has been implicated in the inhibition of Akt signaling in breast cancer cells, but this effect was reported after 24-72 hours and required very high concentrations of DIM [76]. To understand how DIM affects Akt activation in the highly invasive and poorly differentiated MDA-MB-231 cell line at physiologically relevant concentrations, we treated cells with 0-25 μM DIM for 24 hours. As indicated in Figure 2-1A, increasing concentrations of DIM decreased Akt phosphorylation at serine 473 at 24 hours without affecting total Akt levels. These results are consistent with decreased activation of Akt, since Akt must be phosphorylated at serine 473 to be fully active. DIM at 25 μM also decreased Akt phosphorylation in a time-dependent manner, with a slight inhibition appearing at as early as 30 minutes and with a maximal effect by 4 hours (Figure 2-1B). For this reason, we chose 4 hours as our standard time point for DIM treatment. At 4 hours, DIM also inhibited Akt activation in a concentration-dependent manner in MDA-MB-231 cells (Figure 2-1C) without affecting total Akt levels. DIM did not affect Akt phosphorylation in non-tumorigenic, pre-neoplastic MCF10AT cells (Figure 2-1D).

To define a mechanism for DIM's inhibition of Akt activation in invasive breast tumor cells, we sought to determine whether DIM inhibits Akt activation by individual growth factors. We tested EGF, IGF-1 and HGF because each of these growth factors activates Akt and Akt downstream signaling in MDA-MB-231 and other breast cancer cells [97-99]. Moreover, the dysregulation of each growth factor's signaling pathway is implicated in breast cancer pathogenesis in humans [100-103]. In our experiments, each growth factor strongly activated Akt phosphorylation, as demonstrated by the increases in levels of phospho-Akt serine 473 by 25 ng/mL EGF and IGF-1 (Figure 2-2A, bands 3 and 5) and 40-80 ng/mL HGF (Figure 2-2B, bands 2, 4, and 6). DIM did not inhibit Akt activation by either EGF or IGF-1 (Figure 2-2A). However, DIM did decrease levels of HGF-induced phospho-Akt Ser473 (Figure 2-2B). This inhibition was of a degree comparable to that of DIM's inhibition of FBS-induced Akt activation. Treatment with any of these growth factors or DIM did not affect total Akt levels, however.

DIM inhibits phosphorylation of the Akt substrate GSK-3α/β downstream of serum and HGF

Our observation that DIM selectively inhibits Akt activation by HGF suggested that DIM would also inhibit Akt activity. We chose to look at phosphorylation of GSK-3α/β, an established substrate of Akt that is involved in proliferation, by Western blot analysis as a measurable endpoint of Akt activity. Akt is the only known kinase that phosphorylates GSK-3α/β *in vivo* [104]. We used both FBS and HGF to activate Akt for these experiments. DIM produced similar inhibitory effects on GSK-3α/β phosphorylation following treatment with 1% FBS (Figure 2-3A) and 40 ng/mL HGF (Figure 2-3B) in concentration-dependent manners. Levels of total GSK-3α/β were not affected by DIM treatment. These results indicate that physiologically relevant concentrations of DIM inhibit short-term Akt activation and activity, and that the HGF pathway is one pathway involved in this effect.

DIM induces a G1 cell cycle arrest

Inhibition of Akt has been reported to arrest cells in the G1 phase of the cell cycle [105]. We tested whether DIM would arrest the cells in the same way. Cells were treated with increasing concentrations of DIM for 24 hours or with LY294002 (LY) for 6 hours. LY is a PI3K inhibitor and therefore a positive control for inhibition of Akt activation in cells. Cells were then lysed and the nuclei were stained with propidium iodide and analyzed by flow cytometry for DNA content. DIM induced a G1 cell cycle arrest, indicated by an increased percentage of cells in the G1 phase and a decreased percentage of cells in the S phase of the cell cycle (Figure 2-4). LY also induced a G1 cell cycle arrest, suggesting that DIM's effect on the cell cycle is consistent with Akt inactivation.

DIM induces apoptosis

Akt activates survival signaling, and inhibition of Akt can lead to increased apoptosis [106]. Therefore, we tested whether DIM could induce apoptosis in MDA-MB-231 cells. We first assessed apoptosis by detecting cleavage of poly ADP ribose polymerase (PARP). PARP is a DNA repair enzyme that is cleaved by caspase 3 following the committed step of programmed cell death [107]. Using an antibody that reacts with the cleavage site of cleaved PARP but not with full-length PARP, we observed that DIM strongly induces PARP cleavage after 24 and 48 hours, but not after 12 hours (Figure 2-5A). The strongest effect was observed after 24 hours, likely because cells with cleaved PARP will die before they are able to be analyzed at the 48 hour time point. We also measured apoptosis in cells by determining Annexin V binding. In cells treated with 25 μM DIM, but not with 15 μM DIM, we observed an increase in Annexin V binding cells after 24 and 48 hours (Figure 2-5B).

DIM inhibits in vitro *metastasis markers*

In addition to cell cycle arrest and apoptosis, inhibition of cell motility and invasiveness is an established consequence of Akt inhibition [108,109]. Therefore, we tested DIM's ability to inhibit *in vitro* metastasis in MDA-MB-231 cells. To measure motility of cells we used a transwell migration assay. Cells in serum-free medium were seeded into the top of a transwell insert in a 12-well plate. Below the insert in the bottom chamber, we added medium with 1% FBS as a chemoattractant. As a negative control, the chemoattractant was serum-free medium. Figure 2-6A shows representative pictures of the results. FBS (1%) induced migration across the transwell inserts, which was inhibited in a dose-dependent manner by 5-25 μM DIM. This effect was due to inhibition of motility and not loss of viability, as demonstrated by an MTT assay (data not shown). As another measure of *in vitro* metastasis, we tested DIM's ability to inhibit invasion, a process that requires synthesis and secretion of enzymes to degrade an artificial extracellular matrix made of Matrigel before cells can cross the transwell insert. Cells in chamber systems that had serum-free medium in the lower chamber as the chemoattractant did not invade the Matrigel to cross to the lower face of the insert (Figure 2-6B). When 1% FBS was used as the chemoattractant, the cells were much more invasive, and 25 μM DIM in the upper chamber prevented this invasion.

Finally, we used a wound migration assay as an additional measure of cell motility. Confluent monolayers of MDA-MB-231 cells were scratched with a sterile pipette tip, washed, and treated with 0-25 μM DIM or 25 μM LY in DMEM + 1% FBS for 16 hours. The original wounds were photographed and lines delineating the wounds were marked. After the incubation, cells were fixed, stained, and photographed. The borders of the original wounds were artificially overlaid on the new images. Cells that migrated across the original wound borders are shown in Figure 2-6C. Cells treated with the vehicle control DMSO migrated to almost completely close the wound. Fewer cells migrated with increasing concentrations of DIM. LY, which serves as a positive control for inhibition of Akt activation, also resulted in an inhibition of wound migration. Taken together, these data show that DIM inhibits *in vitro* metastasis that is characteristic of Akt inhibition.

Discussion

Although it has been reported that DIM inhibits Akt signaling in breast cancer cells, the mechanism(s) for this action, as well as the kinetics and effects of lower, physiologically relevant concentrations of DIM, have remained unknown. We report here that DIM inhibits short- and long-term Akt activation by serum and by HGF in MDA-MB-231 breast cancer cells. In addition, DIM inhibited cell cycle progression and *in vitro* metastasis and induced apoptosis, which are all consistent with Akt inhibition.

We have shown that DIM inhibits activation of Akt, a proto-oncogene which contributes to growth, survival, metastasis, and chemotherapy resistance in breast cancer cells. Components of this pathway are frequently mutated or over expressed in breast cancer. The gene encoding the catalytic subunit of PI3K, *PIK3CA,* is one of the most common mutations in breast cancer, and these mutations are associated with poor prognosis [110]. HER2, an EGF receptor that activates the PI3K/Akt pathway, is amplified in 10-30% of breast cancers. Activation of the PI3K/Akt pathway also plays a role in resistance to current breast cancer therapies like trastuzimab and tamoxifen [90,111,112]. Compounds like DIM that inhibit this central pathway could be effective against breast cancers with a variety of genetic aberrations and could help to overcome resistance to chemotherapy.

We have also identified the HGF pathway as a target of DIM. DIM selectively inhibited Akt activation by HGF, and not by EGF or IGF-1. Additional studies will determine the mechanism whereby DIM inhibits HGF signaling (see chapter 3). The observation that DIM inhibits Akt downstream of one growth factor and not others suggests that DIM is not acting to inhibit Akt at any point of the pathway where signaling from different growth factors converges, such as PI3K. However, it is still likely that DIM has additional mechanisms of inhibition of Akt, since DIM inhibits Akt activation by fetal bovine serum, of which human hepatocyte growth factor is not a known component.

Other phytochemicals have also been reported to inhibit Akt activation in breast cancer cells through various mechanisms. Adams et al. report that blueberry extract also inhibits HGF-induced Akt activation and cell migration in MDA-MB-231 cells *in vitro* and in MDA-MB-231 xenografts [113]. However, it is unknown if this effect is selective for HGF since the authors did not report the effects of blueberry extract on Akt activation by other growth factors or serum. Green tea polyphenols also inhibit HGF-induced Akt activation in MDA-MB-231 cells [114]. Because diverse compounds with varying structures can all inhibit HGF-induced Akt activation,

this suggests that a general cellular stress response to anticancer phytochemicals may be involved. Still, other phytochemicals like genistein or curcumin inhibit Akt activation and activity downstream of EGF or serum, which contains a variety of components that can activate Akt [115-117].

In summary, DIM strongly and selectively inhibited Akt activation and activity in tumor-derived breast cancer cells by a mechanism that involves the blockade of HGF signaling. Consistent with Akt inactivation, DIM also induced a G1 cell cycle arrest, apoptosis, and inhibition of migration. These effects make DIM an attractive candidate for further study as a breast cancer treatment, particularly in breast cancers in which components of the HGF/PI3K/Akt pathway are activated by mutation, amplification, or over expression.

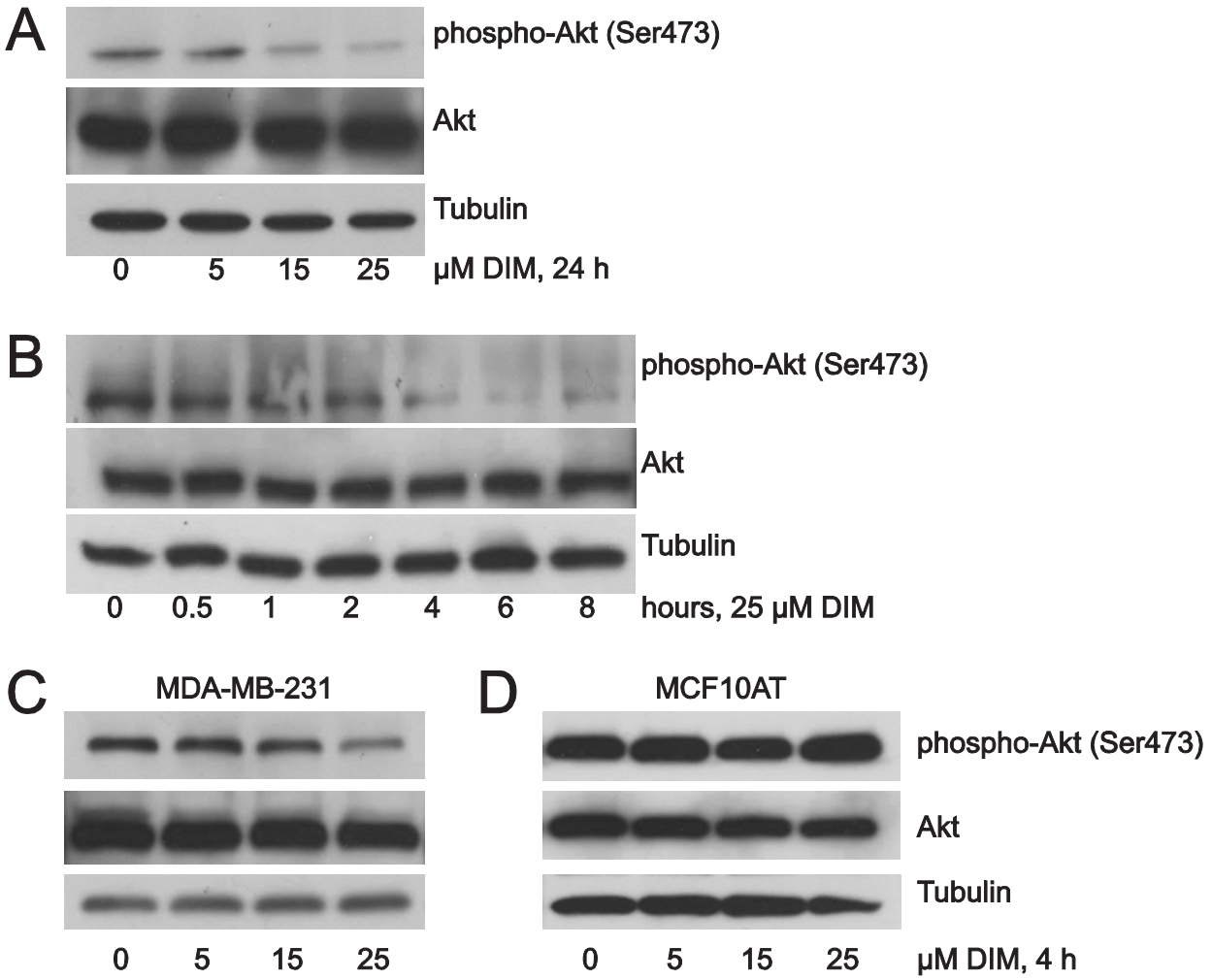

Figure 2-1. DIM inhibits Akt activation in MDA-MB-231 cells but not in nontumorigenic MCF10AT cells. (A) Western blot analysis of phosphorylated and total Akt protein from cells incubated in 1% FBS overnight and then treated with increasing concentrations of DIM for 24 hours. (B) Western blot analysis of phosphorylated and total Akt protein from cells treated with 25 μM DIM for 0-8 hours. (C) and (D) Same as (A) except MDA-MB-231 cells (C) or MCF10AT cells (D) were treated with DIM for 4 hours, the optimal time for Akt inhibition. For all experiments, tubulin was used as a loading control. Results are representative of three independent experiments.

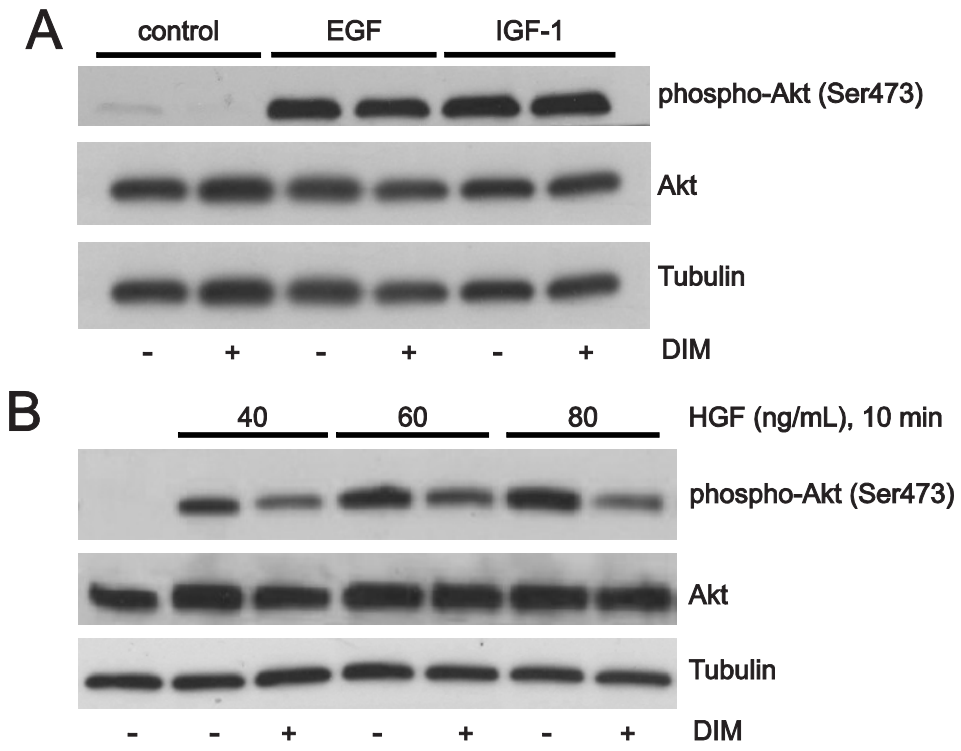

Figure 2-2. DIM inhibits Akt activation by HGF but not by EGF or IGF-1. (A) MDA-MB-231 cells were incubated overnight in serum-free medium, treated with DIM for 4 hours, and then epidermal growth factor (EGF, 25 ng/mL) or insulin-like growth factor-1 (IGF-1, 25 ng/mL) for 10 minutes. (B) Cells were incubated overnight in serum-free medium, and treated with DIM for 4 hours, and HGF (40 ng/mL) for 10 minutes. Total cell lysates were collected and analyzed by Western blotting for phospho Akt Ser473 and total Akt. Tubulin was used as a loading control in all experiments, and results are representative of three independent experiments.

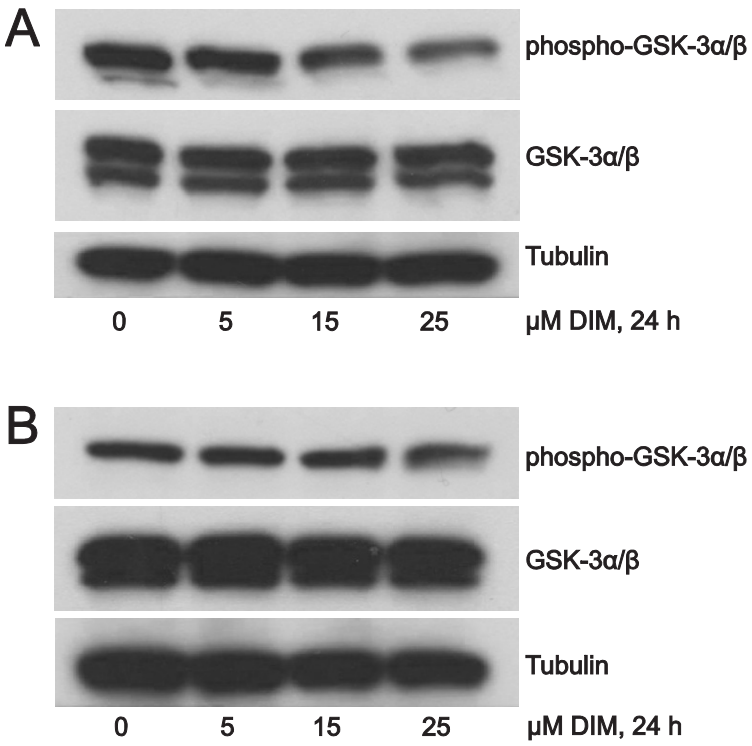

Figure 2-3. DIM decreases Akt activity in cells. (A) Cells were incubated in medium containing 1% FBS overnight and then treated with increasing concentrations of DIM for 4 hours. (B) Cells were serum-starved overnight and then treated with increasing concentrations of DIM for 4 hours and then 40 ng/mL HGF was added for 10 minutes. In both experiments, total cell lysates were collected and analyzed by Western blotting for phospho and total GSK-3α/β and the loading control tubulin. Results are representative of three independent experiments.

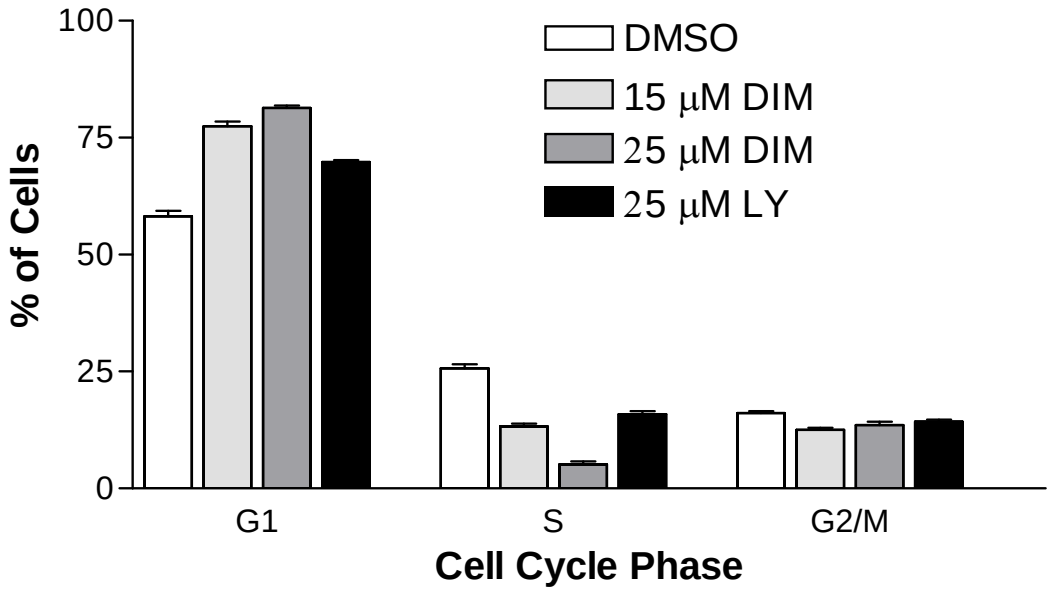

Figure 2-4. DIM induces a G1 cell cycle arrest in MDA-MB-231 cells. Cells were treated with increasing concentrations of DIM or 25 μM for 24 hours or with LY294002 (LY) for 6 hours before the nuclei were stained with propidium iodide and analyzed by flow cytometry for DNA content. DIM induced a G1 cell cycle arrest, indicated by an increased percentage of cells in the G1 phase and a decreased percentage of cells in the S phase of the cell cycle. LY, the positive control for Akt inhibition, also induced a G1 cell cycle arrest.

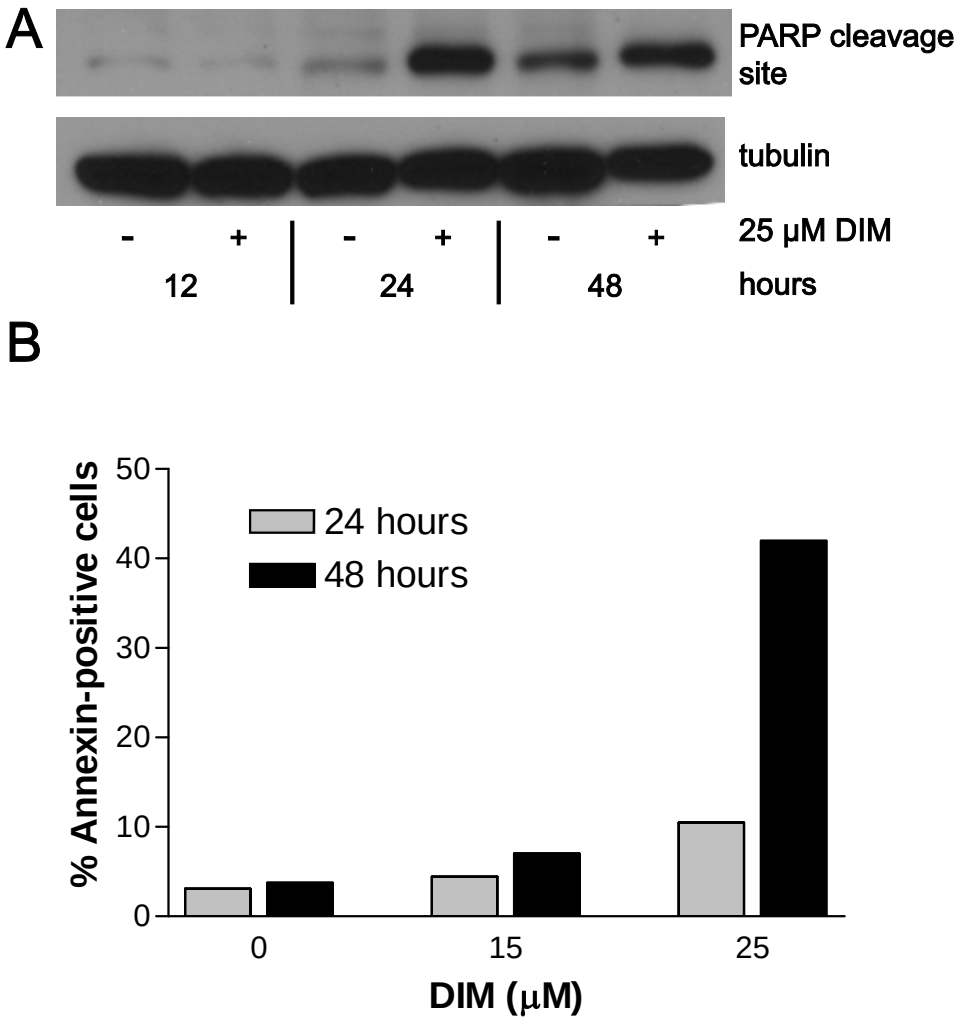

Figure 2-5. DIM induces apoptosis in MDA-MB-231 cells. (A) Cells were treated with 0 or 25 μM DIM in DMEM + 1% FBS for 12, 24, and 48 hours. Total cell lysates were collected and analyzed by Western blotting for PARP cleavage site and the loading control tubulin. Results are representative of three independent experiments. (B) Cells were treated with 0, 15, or 25 μM DIM in DMEM + 1% FBS for 24 or 48 hours. Live cells were stained with propidium iodide (PI) and Annexin V-FITC and analyzed by flow cytometry. Annexin V binding cells, both PI-negative (early apoptotic) and PI-positive (late apoptotic) were counted.

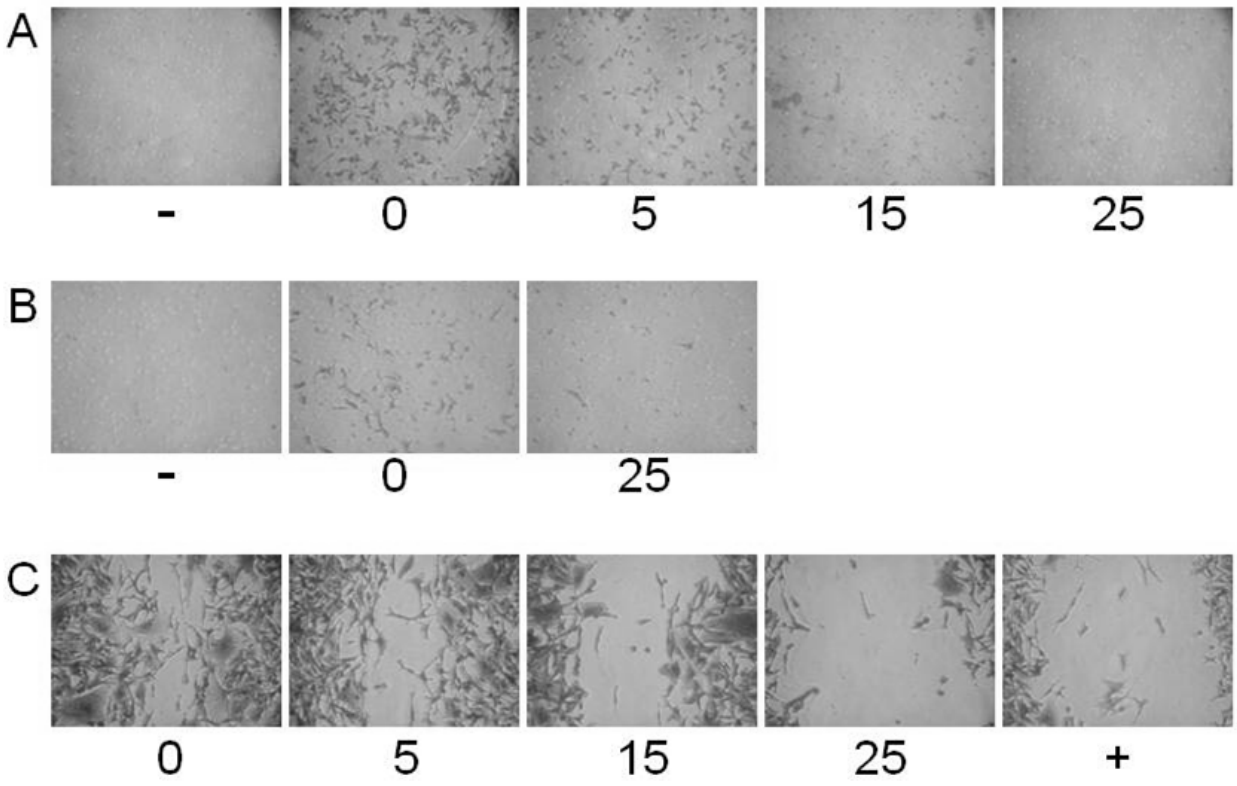

Figure 2-6. DIM inhibits *in vitro* metastasis in MDA-MB-231 cells. (A) Migration. MDA-MB-231 cells in serum-free medium were seeded onto transwell inserts in modified Boyden chamber systems in the presence of 0-25 μM DIM, indicated by the numbers above. DMEM containing 1% FBS was added to the bottom chamber as a chemoattractant. After 8 hours, cells in the upper chamber were removed and cells that migrated to the lower face of the insert were fixed and stained. As a negative control (-), serum-free DMEM was used as a chemoattractant. (B) Invasion. Same as (A) except the inserts were coated with Matrigel. (C) Wound migration. Monolayers of MDA-MB-231 cells were scratched with a sterile pipette tip. Floating cells and debris were washed away with PBS and DMEM containing 1% FBS and 0-25 μM DIM or 25 μM LY (+) was added to the cells for 16 hours. Cells were then fixed, stained and photographed. Each photograph shows the area of the wound that was removed during the initial scratch, and each cell shown is a cell that migrated across the wound border. All pictures shown are representative fields from triplicate wells from at least 3 independent experiments.

CHAPTER 3

DIM inhibits c-Met phosphorylation and induces ligand-dependent degradation of c-Met in MDA-MB-231 breast cancer cells to selectively inhibit HGF/c-Met signaling

Introduction

In chapter 2 we demonstrated that physiologically relevant concentrations of DIM inhibit short- and long-term activation of Akt in breast cancer cells and that DIM selectively inhibits HGF-induced Akt activation. To follow up on those studies, our goal was to determine a mechanism by which DIM inhibits Akt activation by HGF. To do this, we began by examining the expression and activation of the HGF receptor, c-Met.

C-Met is a receptor tyrosine kinase for which HGF is the only known endogenous ligand. HGF binding to c-Met induces homodimerization of c-Met and trans auto-phosphorylation of several tyrosine residues, including Y1234/1235, Y1003, Y1349, and Y1356. Phosphorylations at Y1234/1235 are necessary for full activation of the receptor [118]. Phospho-Y1349 recruits Gab1 and Phospho-Y1356 recruits Grb2 [119]. These scaffolding proteins recruit PI3K and Sos, and activate the Erk and Akt pathways, respectively. HGF also regulates termination of c-Met signaling by inducing internalization of c-Met. Phospho-Y1003 recruits the ubiquitin E3 ligase Cbl, which mono-ubiquinates c-Met [120]. This mono-ubiquitination is a signal for binding of HGF-regulated tyrosine kinase substrate (Hrs), which is involved in retaining c-Met in clathrin-coated pits [121]. C-Met undergoes endocytosis and internalized c-Met receptors are then delivered to sorting endosomes and either recycled back to the plasma membrane or degraded in the lysosomes [122] (Figure 3-1).

The net result of Akt activation by HGF in cancer cells is an invasive growth phenotype characterized by increased proliferation, survival, and motility of the cancer cells [119,123,124]. Cell lines that overexpress HGF and/or c-Met are tumorigenic in nude mice, and downregulation of these proteins decreases the tumorigenic potential of the cells [125,126]. HGF and c-Met are frequently overexpressed in breast cancer, and c-Met overexpression is a strong and independent predictor of poor prognosis [103,119,127,128]. Patients with high HGF levels in tumor extracts have significantly shorter disease-free and overall survival times compared to patients with low HGF levels [102]. Because of these observations, researchers have considerable interest in c-Met and HGF as targets for breast cancer drug development. Current clinical strategies to inhibit HGF/c-Met signaling include development of monoclonal antibodies against c-Met or HGF, c-Met or HGF antagonists, c-Met kinase inhibitors, or compounds that inhibit downstream effectors of c-Met signaling [85,129,130].

Although we and others have reported that DIM inhibits Akt activation and cell proliferation and motility, the roles of specific upstream activators of this pathway, including HGF/c-Met, in this activity have not been investigated. In this study, we demonstrate that DIM selectively inhibits HGF signaling, which is one novel mechanism by which DIM inhibits Akt. DIM inhibits HGF signaling by decreasing phosphorylation of c-Met and inducing HGF-dependent degradation of c-Met.

Materials and Methods

Cell culture and supplies

MDA-MB-231 cells were purchased from American Type Culture Collection (ATCC) and were grown in Dulbecco's Modified Eagle Medium (DMEM, Invitrogen) supplemented to 4.0 g/L glucose, 3.7 g/L sodium bicarbonate, and 10% FBS (Omega Scientific) in a humidified

incubator at 37 °C and 5% CO_2. Cells were passaged regularly before reaching 80% confluency, and cells used in experiments were at less than 25 passages. Prior to all experiments, monolayers were washed with PBS and the medium was changed to serum-free medium for 24 hours. DIM (LKT Laboratories) or the vehicle control DMSO (Acros Organics) was then added for the indicated times. Lactacystin, phenylarsine oxide, ascorbic acid, α-tocopherol, N-(tert-Butyl) hydroxylamine HCL, cyclosporin A and sodium orthovanadate were purchased from Sigma and SB202190 was purchased from Tocris. All other cell culture supplies were purchased from Fisher Scientific.

Wound healing assay

Cell migration was assessed as described [18] with modifications. MDA-MB-231 cells were grown to confluency in 24-well plates. A sterile pipette tip was used to scratch the monolayer and create a gap of constant width. Monolayers were then washed three times with PBS to remove floating cells and debris. Serum-free medium with or without HGF (60 ng/mL) and with increasing concentrations of DIM was added to the cells for 16 h. Cells were fixed with 10% formalin/PBS and stained with crystal violet in 10% formalin/PBS. Wounds were photographed using a Nikon Coolpix990 digital camera connected to the Nikon Eclipse TS100 microscope at a 100X magnification. Artificial lines delineating the outline of the wound were drawn on images of the original wounds and then overlaid on final wound images. Cells that migrated across the lines in each of two images from duplicate wells of three independent experiments were counted.

Thymidine incorporation assay

Cell proliferation was determined by a thymidine incorporation assay as described [41], with modifications. At 50% confluency, MDA-MB-231 cells in 12-well plates were washed with PBS, incubated in serum-free medium overnight, and then treated with varying concentrations of DIM for 4 h and HGF (60 ng/mL) for 1 h. After the incubation, cells were washed and fresh serum-free medium containing 10 μCi of [^{3}H]-thymidine (Perkin Elmer) was added to each well and allowed to incubate at 37 °C for 4 h. The medium was removed and cells were washed three times with ice-cold 10% trichloroacetic acid. Cells were lysed in 0.3 N NaOH, and [^{3}H]-thymidine incorporation into DNA was determined by scintillation counting of the lysates.

Western blot analysis

To prepare whole cell lysates, monolayers were scraped directly in protein loading buffer (10% glycerol, 5% 2 mercaptoethanol, 10% SDS, 0.125 M Tris–HCl pH 6.7, 0.15% bromophenol blue), sonicated for 15 s, and heated to 99.9 °C for 5 min. Equal amounts of protein were separated by SDS-PAGE and transferred to Immobilon P membranes (Millipore). Membranes were blocked in 5% nonfat dry milk in TBST for 1 h and then probed with mouse anti-tubulin (sc-5274) from Santa Cruz Biotechnology, rabbit anti-phospho Akt Ser473 (#4058)

or rabbit anti-phospho Met Tyr1234/1235 (#3077) from Cell Signaling Technology, or rabbit anti-Met from Abcam (ab51067) overnight at 4 °C. After washing three times in TBST, membranes were incubated in 5% nonfat dry milk in TBS-Tween containing the appropriate secondary antibody-HRP conjugates (Santa Cruz Biotechnology), washed again, and exposed to Western Lighting *Plus*-ECL enhanced chemiluminescence substrate (Perkin Elmer) for 1 min. Immunoreactive proteins were detected using CL-Xposure film (Thermo Scientific). Densitometry was performed using ImageJ Software (NIH). Results shown are representative of at least three independent experiments.

Statistics

The results are expressed as means $\pm$ SD for at least three replicate determinations for each assay. Data were analyzed using one-way ANOVA and Tukey's honest significance post-test for multiple comparisons using GraphPad Prism Software. The levels of significance are noted for $p < 0.05$ and $p < 0.001$.

Results

DIM inhibits HGF-activated cell motility

Activation of Akt by HGF in breast cancer cells results in cell motility [99,114]. Because we know that DIM inhibits Akt activation by HGF, we hypothesized that DIM treatment would result in less motile cells. To test this possibility, we used a wound migration assay. Confluent monolayers of MDA-MB-231 cells were uniformly wounded with a sterile pipette tip and then washed and incubated in fresh serum-free medium with or without DIM and HGF. The first panel of Figure 3-2 shows a representative picture of wounded cells in serum-free medium with no HGF. Relatively few cells migrated to close the wound. When 60 ng/mL HGF was added, approximately twice the number of cells migrated across the wound borders, partially closing the wound. Cells treated with 5-15 μM DIM showed a 34 and 100% decrease in HGF-induced migration, respectively. DIM at 25 μM produced the most striking effect, with inhibition of migration below baseline levels (Figure 3-2), indicating decreased cell motility with increasing concentrations of DIM.

DIM inhibits HGF-stimulated cellular proliferation

Another response to HGF stimulation in breast cancer cells is proliferation. We performed a [^{3}H]-thymidine incorporation assay to measure DIM's inhibition of HGF-induced proliferation. Figure 3-3 shows that 60 ng/mL significantly ($p<0.05$) increased the uptake of [^{3}H]-thymidine by cells compared to cells in serum-free medium, and that DIM strongly inhibited this uptake in a concentration-dependent manner. Treatment of MDA-MB-231 cells with 5 and 15 μM DIM led to a 80% and 100% inhibition of the HGF-induced response. Incubation of cells with 25 μM DIM produced an inhibition of thymidine uptake to below baseline levels. These results indicate that DIM strongly inhibits HGF-induced cellular proliferation.

DIM induces ligand-dependent degradation of c-Met

To examine the potential role of c-Met in DIM's effects, we began by looking at c-Met expression. We used a time point of 4 hours, because that is the optimal time for inhibition of HGF-activated Akt by DIM. DIM alone did not affect c-Met expression, but when 40 ng/mL HGF was added to the medium for an additional hour, we observed decreased c-Met levels in DIM-treated cells (Figure 3-4A). We then treated the cells with DIM for 4 hours and HGF for various time points ranging from 10 minutes through 2 hours. With 10 minutes of HGF treatment, DIM-treated cells showed slightly decreased c-Met (Figure 3-4B). The longer the cells were treated with HGF, the less c-Met protein we observed. Because DIM does not affect c-Met levels in the absence of HGF, this suggests that DIM does not affect translation of c-Met, but rather promotes degradation by HGF. We confirmed by QPCR that DIM does not affect c-Met message levels (data not shown).

DIM acts to induce degradation of c-Met at or upstream of endocytosis

Next we wanted to explore how DIM might act to promote degradation of c-Met by HGF. To assess the role of ROS in DIM's effects, we pre-treated cells with antioxidants for 30 minutes before adding DIM and HGF. We also pre-treated cells with a lysosomal proton pump inhibitor, lactacystin, and an inhibitor of endocytosis, phenylarsine oxide (PAO), to determine the point in the degradation pathway at which DIM is acting. As shown in Figure 3-5, DIM alone again did not affect c-Met protein levels. When 40 ng/mL HGF was added for one hour, DIM strongly decreased c-Met levels. Antioxidants did not reverse this effect; they decreased c-Met levels on their own, even without DIM. Lactacystin pre-treatment had no obvious effect, indicating that DIM acts before the step of lysosomal degradation. However, PAO prevented DIM-induced degradation of c-Met, suggesting that DIM acts at or upstream of the endocytosis step of c-Met degradation.

DIM decreases tyrosine phosphorylation of c-Met

Because HGF is necessary for DIM-induced c-Met degradation, we tested whether DIM affects HGF induced phosphorylation of c-Met at Y1003, the tyrosine residue necessary for recruiting the ubiquitin ligase Cbl. Increased Y1003 phosphorylation would lead to increased ubiquitination and ultimately degradation of c-Met. To our surprise, we saw that DIM actually decreased phosphorylation of Y1003 at each time point studied (Figure 3-6, top row). This suggests that DIM acts downstream of receptor phosphorylation and upstream of endocytosis to promote c-Met degradation. Therefore, decreases in c-Met phosphorylation at y1003 by DIM are likely not important.

However, decreased phosphorylation of the c-Met receptor is intriguing, given that a current research focus of many investigators is to develop compounds that inhibit c-Met activation. HGF activates downstream signaling by binding to c-Met and inducing homodimerization and trans-autophosphorylation of tyrosines Y1234 and Y1235 in the activation loop of c-Met's kinase domain. These tyrosine phosphorylations are required for full activation of c-Met's kinase activity [118]. To investigate whether DIM inhibits activation of c-

Met by HGF, we determined the degree of tyrosine phosphorylation of c-Met at Tyr1234/1235 after treatment with DMSO or 25 μM DIM for 4 hours and 40 ng/mL HGF for 0-30 minutes via Western blotting (Figure 3-6, second row). We observed phosphorylation of c-Met after one minute and increased phosphorylation levels after 5, 10, 20, and 30 minutes, with the strongest phosphorylation observed at 30 minutes. At each time point, DIM strongly decreased phosphorylation of c-Met at Tyr1234/1235, but total c-Met levels did not change.

Involvement of protein tyrosine phosphatases, p38, and calcineurin in DIM's effects on c-Met phosphorylation

Previous studies from our group showed that p38 and calcineurin are important mediators of some of DIM's effects in breast cancer cells. Inhibition of p38 prevents DIM-induced upregulation of the CDK inhibitor $p21^{cip1/waf1}$ [27], and either p38 inhibition by SB202190 (SB) or calcineurin inhibition by cyclosporin A (CsA) prevents DIM's upregulation of interferon-gamma expression [28]. To determine the possible involvement of p38, calcineurin, and protein tyrosine phosphatases in DIM's effect of decreased c-Met tyrosine phosphorylation, we pretreated cells with inhibitors of each of these proteins before treatment with DIM and HGF. Pretreatment of cells with 100 μM sodium orthovanadate (SOV) had no effect on DIM-induced decrease in c-Met phosphorylation (Figure 3-7A). Pretreatments with 10 μM SB and 10 μM CsA decreased HGF-induced c-Met phosphorylation and DIM did not further decrease phospho-c-Met levels in cells pretreated with these inhibitors.

To further test the possible involvement of calcineurin in DIM's effect, we pretreated cells with increasing concentrations of the calcineurin inhibitor, CsA, before adding DIM for 4 hours and HGF for 10 minutes (Figure 3-7B). CsA at concentrations of 10 and 30 μM again decreased HGF-induced c-Met phosphorylation, and DIM did not further decrease phospho-c-Met levels, suggesting that DIM may decrease phospho-c-Met through activation of calcineurin.

Discussion

Here we report that DIM inhibits motility and proliferation of MDA-MB-231 breast cancer cells downstream of HGF, and that DIM promotes ligand-dependent degradation of c-Met and inhibits c-Met activation.

Our results suggest that DIM is a promising treatment possibility for breast cancers that have dysregulated HGF/c-Met signaling. These strong effects were seen at physiologically relevant concentrations of DIM, suggesting that DIM could be effective with low toxicity, and it would be worthwhile to explore synergistic effects of DIM and other inhibitors of c-Met signaling to allow clinicians to use lower concentrations of other more toxic compounds.

We found that DIM promotes HGF-induced degradation of c-Met. Using compounds that inhibit various steps in the pathway, we conclude that DIM is acting to promote degradation between c-Met Y1003 phosphorylation and internalization of the receptor. Possibilities for mechanisms include upregulation of Cbl, increased recruitment or activity of Cbl, or increased expression or activity of Hrs. However, the more promising effect of DIM on c-Met is decreased phosphorylation of the receptor. Compounds with this activity have great clinical relevance as potential treatments for multiple cancers, including breast cancer.

Other phytochemicals also decrease c-Met tyrosine phosphorylation or c-Met signaling in various systems. Orally administered pomegranate fruit extract resulted in decreased phospho-c-Met levels in lungs of benzo(a)pyrene-treated A/J mice [131]. The flavonols quercitin, myricetin, and kaempferol decrease HGF-induced c-Met phosphorylation, Akt phosphorylation, cell migration, and cell morphology changes in DAOY human medulloblastoma cells [132]. In MDA-MB-231 cells, berbamine decreases FBS-induced c-Met phosphorylation [133], and green tea catechins inhibit HGF-induced c-Met activation and signaling [114]. Because diverse compounds with varying structures can all inhibit c-Met signaling by decreasing phosphorylation of the receptor, this suggests that a general cellular stress response to anticancer phytochemicals may be involved.

In support of this hypothesis, we observed that p38 and calcineurin, both of which are stress signaling factors, may play a role in DIM's mechanism of action on c-Met signaling. It is interesting to note that treatment with SB and CsA to inhibit p38 and calcineurin, respectively, decreases c-Met activation, as demonstrated by decreased levels of phospho-c-Met Tyr1234/1235. This is consistent with a report showing that increased intracellular calcium inhibits c-Met tyrosine phosphorylation independent of PKC in GTL-16 gastric carcinoma cells [134], and also suggests other potential mechanisms of regulation of c-Met activity that have not yet been reported and are worthy of further study. Regardless of the decrease in HGF-induced activation of c-Met in SB- and CsA-pretreated cells, however, treatment with DIM did not further inhibit c-Met activation. This indicates that inhibition of p38 or calcineurin abolishes DIM's effects.

It is unknown whether DIM's effects on c-Met degradation and activation are related; however, it is likely because both events involve phosphorylation of c-Met. Inhibition of phosphorylation of the receptor could prevent recruitment of various scaffolding or signaling proteins necessary for the internalization and degradation of c-Met.

In summary, DIM inhibits activation of, promotes degradation of, and inhibits motility and proliferation downstream of the HGF receptor c-Met, making DIM an attractive candidate for further study as a breast cancer treatment.

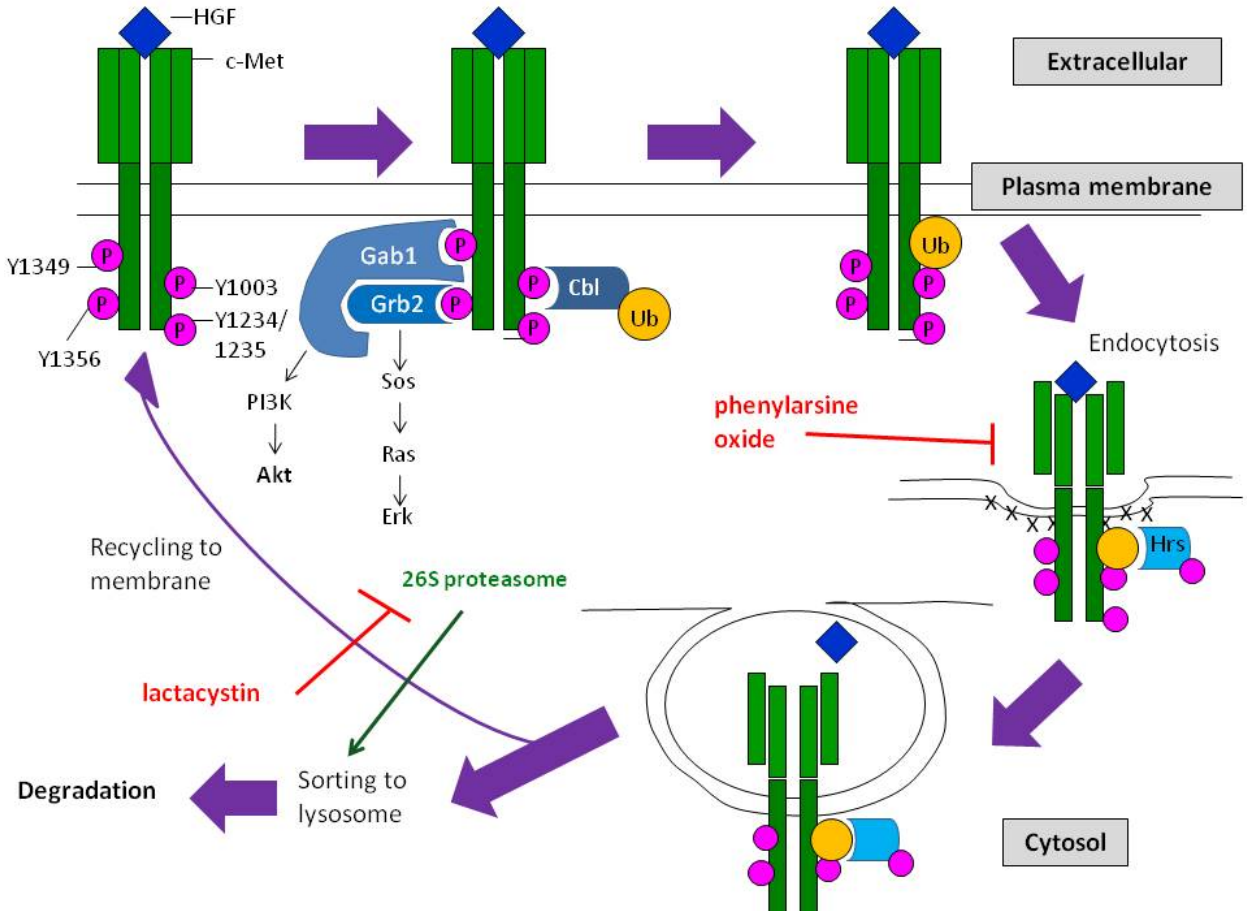

Figure 3-1. HGF-induced activation and degradation of c-Met. HGF binding to c-Met induces dimerization of c-Met and trans auto-phosphorylation of several tyrosine residues, including Y1234/1235, Y1003, Y1349, and Y1356. Phosphorylations at Y1234/1235 are necessary for full activation of the receptor. Phospho-Y1349 recruits Gab1 and Phospho-Y1356 recruits Grb2. These scaffolding proteins recruit PI3Kand Sos, and activate the Erk and Akt pathways, respectively. HGF also regulates termination of c-Met signaling by inducing internalization of c-Met. Phospho-Y1003 recruits the ubiquitin E3 ligase Cbl, which mono-ubiquinates c-Met. Mono-ubiquitination of c-Met is a signal for binding of Hrs, which is involved in retaining c-Met in clathrin-coated pits. Internalized c-Met receptors are then delivered to sorting endosomes, dissociated from HGF, and either recycled back to the plasma membrane or degraded in the lysosomes. Pink circles = phosphate groups, Yellow circles = ubiquitin monomers, red compounds = inhibitors, green compounds = activators.

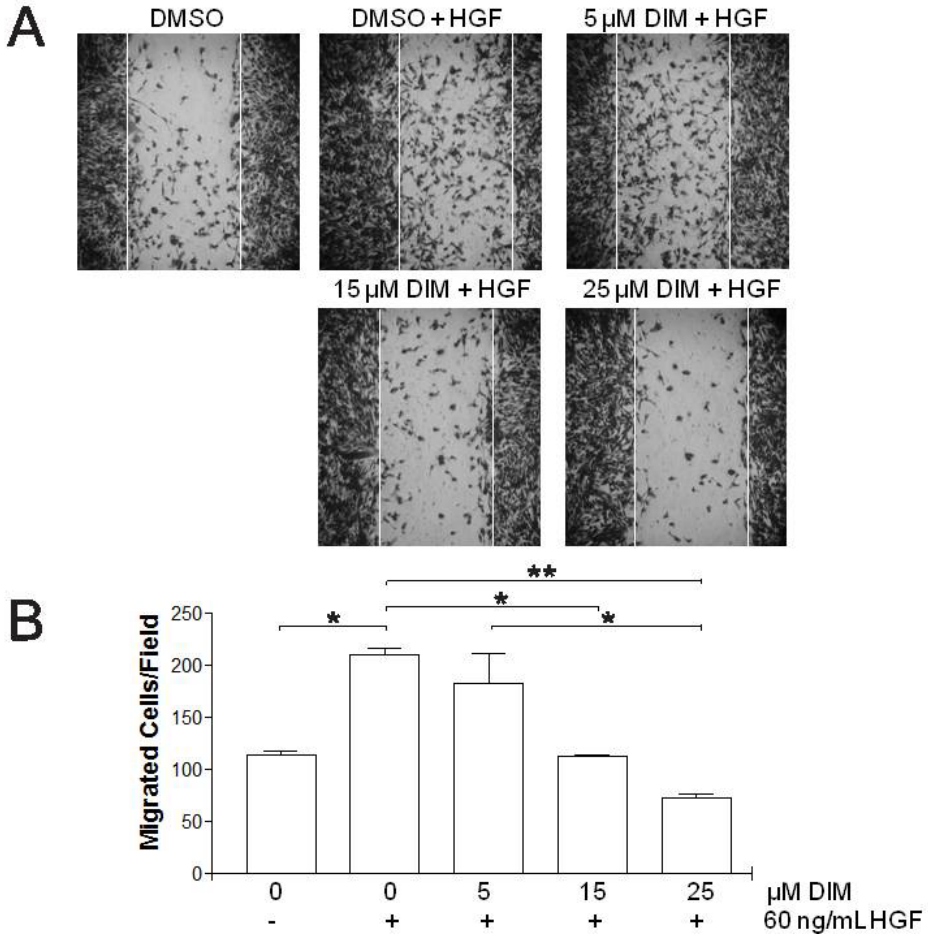

Figure 3-2. DIM inhibits HGF-activated cell motility. (A) Confluent monolayers of MDA-MB-231 cells were scratched with a sterile pipette tip, creating gaps of fixed width. Floating cells and debris were washed away with PBS, and serum-free medium or serum-free medium containing HGF (60 ng/mL) and 0, 5, 15, or 25 μM DIM was added. After 16 h, the wounds were photographed. Photographs are representative of 2 independent fields from duplicate wells. (B) Cells that migrated across the original wound borders were counted. Results are representative of three independent experiments. *, $p < 0.05$; **, $p < 0.001$.

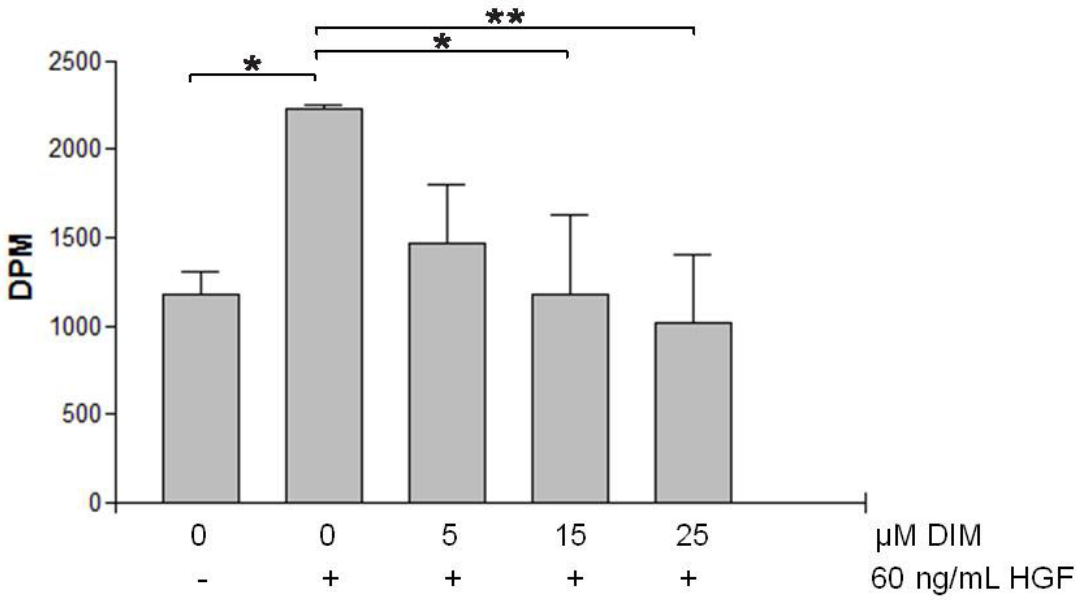

Figure 3-3. DIM inhibits HGF-stimulated cellular proliferation. Cells were serum-starved overnight and then treated with DMSO or DIM for 4 hours. HGF (60 ng/mL) was added to cells for 1 hour and the cells were then washed with PBS. Fresh serum-free medium containing [^{3}H]-thymidine was added for an additional 4 hours. Excess [^{3}H]-thymidine was removed and cells were lysed in 0.3 N NaOH. Incorporation of [^{3}H]-thymidine into DNA, as a measure of proliferation, was determined by scintillation counting of the lysates. *, $p < 0.05$; **, $p < 0.001$.

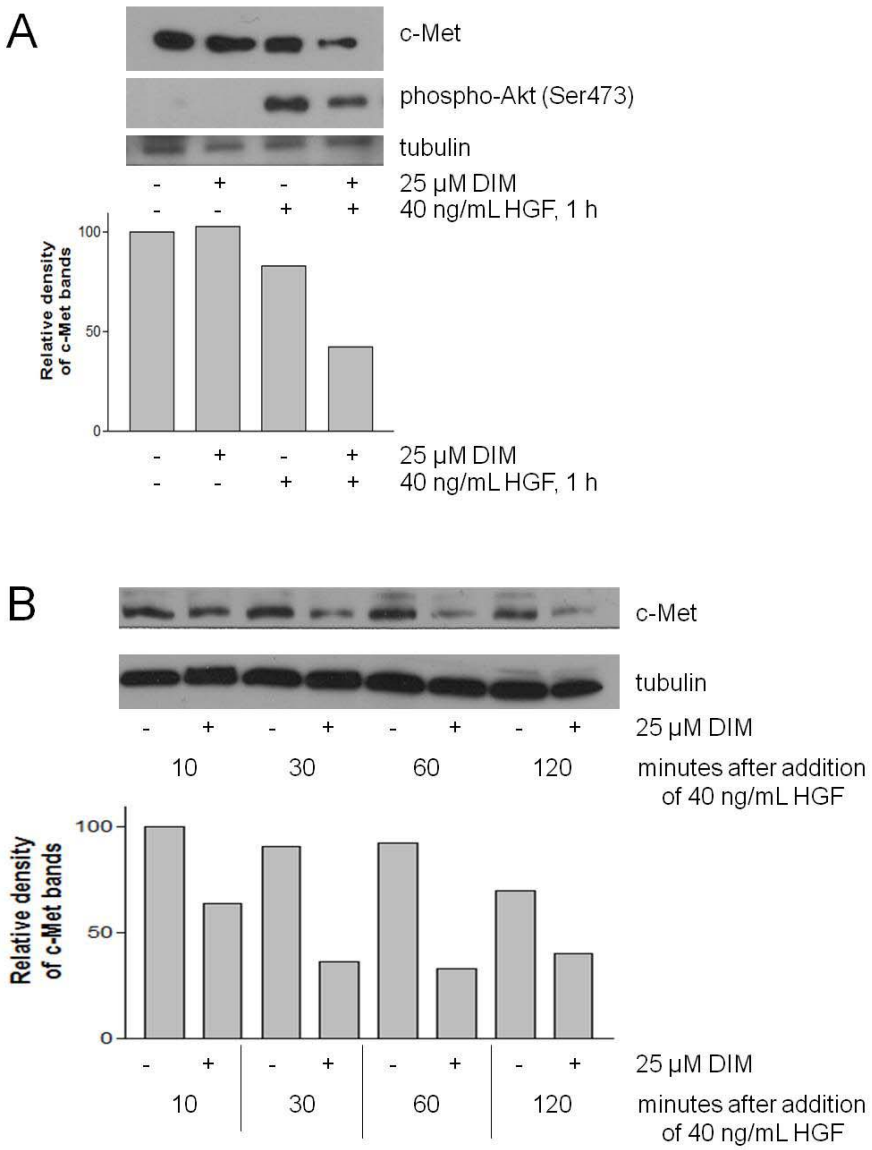

Figure 3-4. DIM induces ligand-dependent degradation of c-Met. Cells were serum-starved overnight and treated with DMSO or 25 µM DIM for 4 hours. HGF was then added for one hour (A) or for 10-120 minutes (B). Total cell lysates were collected and analyzed by Western blotting for c-Met, phospho-Akt S473 and the loading control tubulin. Results are representative of three independent experiments. Histograms indicate relative densities of c-Met bands normalized to tubulin.

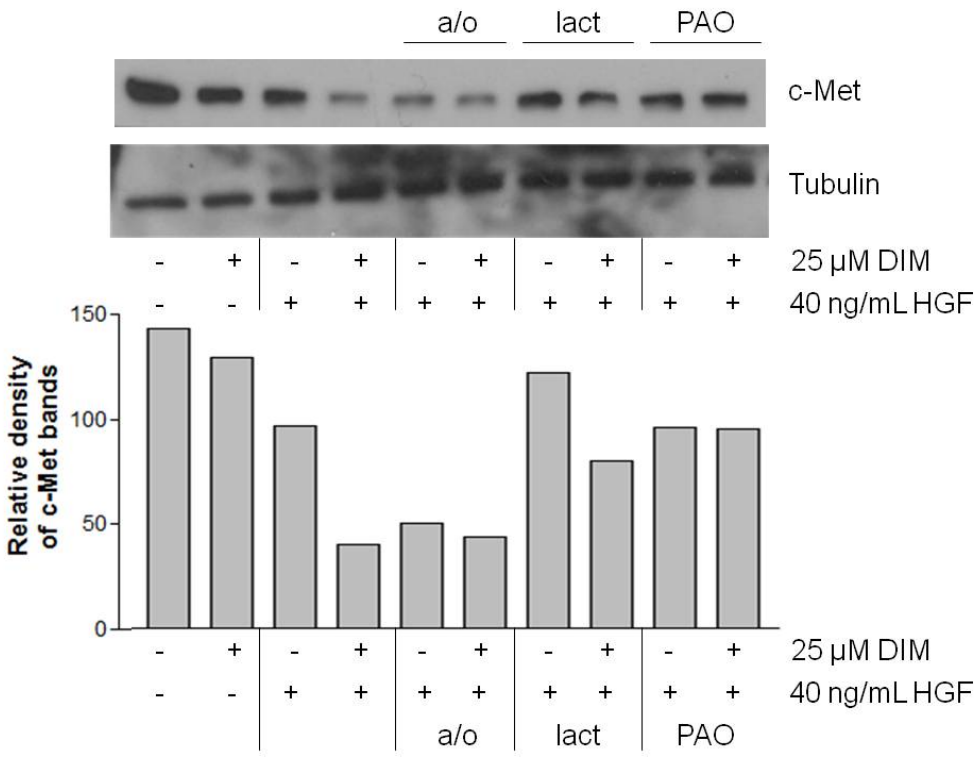

Figure 3-5. DIM acts to induce degradation of c-Met at or upstream of endocytosis. Cells pre-treated with antioxidants (a/o), 10 μM lactacystin (lact), or 20 mM phenylarsine oxide (PAO) for 30 minutes and then treated with DMSO or DIM for 4 hours and HGF for 1 hour. Total cell lysates were collected and analyzed by Western blotting for c-Met and the loading control tubulin. Results are representative of three independent experiments. Histograms indicate relative densities of c-Met bands normalized to tubulin.

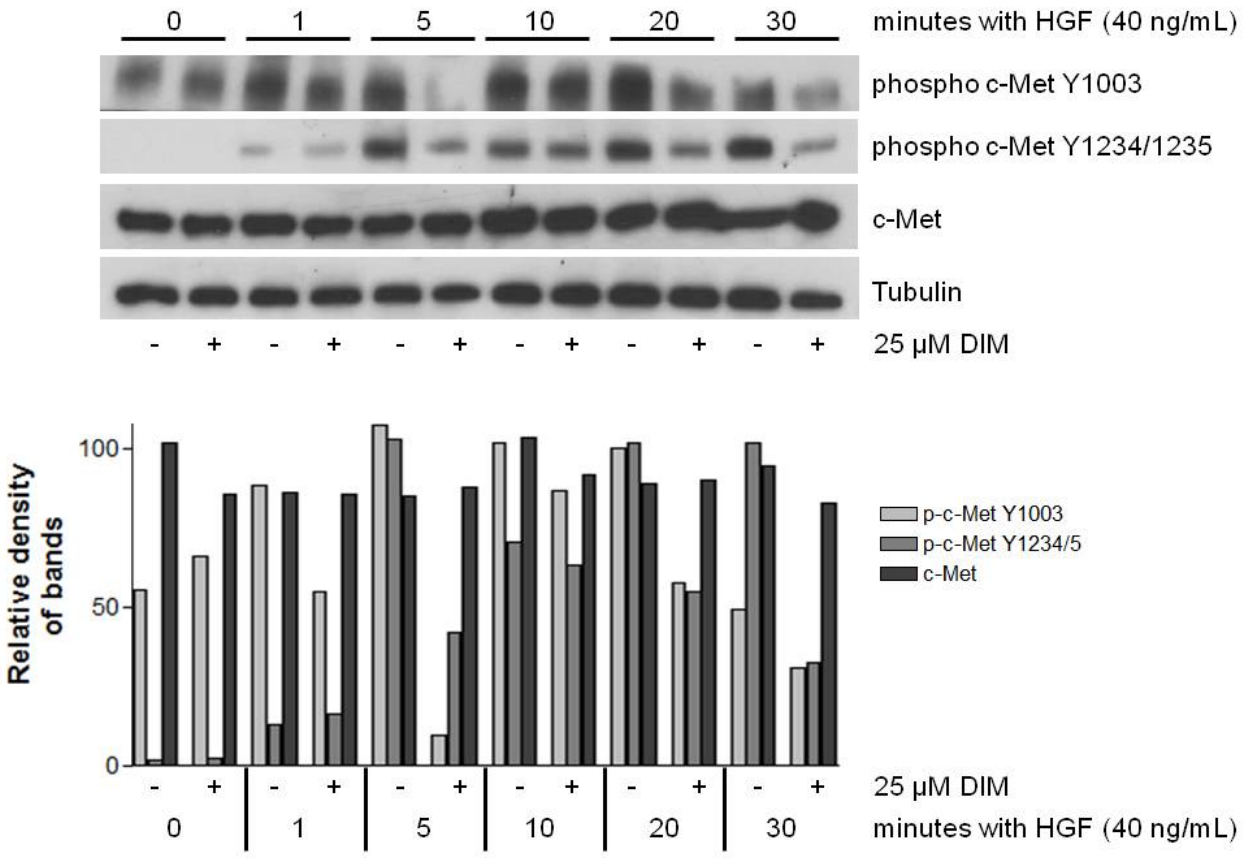

Figure 3-6. DIM decreases phosphorylation of c-Met. Cells were incubated in serum-free medium overnight and then treated with DMSO or 25 μM DIM for 4 h, followed by HGF treatment for 0-30 min. Total cell lysates were collected and analyzed by Western blotting for phospho-c-Met Y1003, phospho-c-Met Y1234/1235, c-Met and the loading control tubulin. Results are representative of three independent experiments. Histograms indicate relative densities of bands normalized to tubulin.

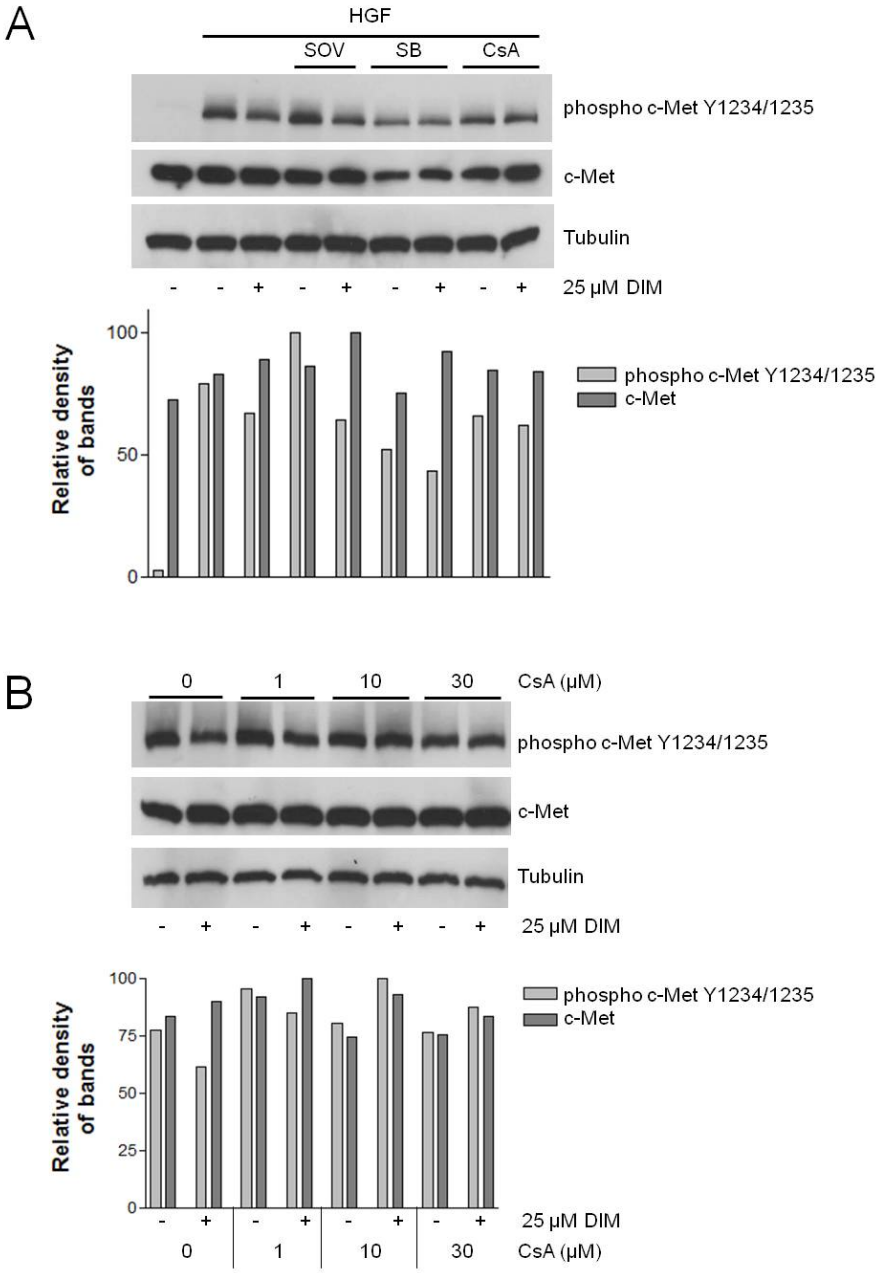

Figure 3-7. Involvement of protein tyrosine phosphatases, p38, and calcineurin in DIM's effects on c-Met phosphorylation. (A) MDA-MB-231 cells were serum-starved overnight, then pretreated with 100 μM sodium orthovanadate (SOV), 10 μM SB202190 (SB) or 10 μM cyclosporin A (CsA) for 30 minutes, followed by DMSO or 25 μM DIM for 4 h and 40 ng/mL HGF for 10 min. (B) Same as (A) except cells were pretreated with increasing concentrations of CsA before addition of DIM and HGF. In both experiments, total cell lysates were collected and analyzed by Western blotting for phospho-c-Met Tyr1234/1235, total c-Met, and the loading control tubulin. Results are representative of three independent experiments. Histograms indicate relative densities of bands normalized to tubulin.

CHAPTER 4

p38 is a key mediator of DIM's effects on gene expression

Introduction

3,3'-Diindolylmethane (DIM) is a promising anti-breast cancer phytochemical that inhibits proliferation and angiogenesis and induces apoptosis in breast cancer cells *in vitro* and in rodent models [17-20]. DIM exerts its effects in cells in part by modulating various cell signaling pathways, including the c-Met/PI3K/Akt pathway (see chapters 2 and 3) and the p38 pathway. DIM activates p38 in various cancer cells, including breast, prostate, cervical, and non-small cell lung cancer cells, and glioma cells [27,28,40-43]. In breast cancer cells, this activation has been observed from 30 minutes to 5 hours after treatment with 50 μM DIM, but activation of p38 in breast cancer cells by lower, more physiologically relevant concentrations has not been reported.

Regulation of gene expression has also been shown to play a role in DIM's effects in breast cancer cells [27,28,48]. Our lab has shown that DIM induces the expression of $p21^{cip1/waf1}$, which leads to a G1 cell cycle arrest and that DIM also induces interferon-γ, which results in immune activation. Using microarray technology, Rahman et al. have shown that DIM at 30 μM regulates the expression of 1,238 genes in MDA-MB-231 cells at 6, 24, and 48 hours. One goal of the current study was to expand on this finding by analyzing the short-term (4 hours) gene expression profile of MDA-MB-231 cells treated with DIM under the conditions that we have determined to be physiologically relevant and the most effective for inhibiting cell cycle progression and inducing apoptosis. We also sought to determine potential common mechanisms for DIM's effects on gene expression.

Here we demonstrate that 25 μM DIM for 4 hours regulates the expression of over 400 genes in MDA-MB-231 cells. We also show that DIM activates p38 and this activation is partly responsible for DIM-induced up regulation of several genes and for DIM's induction of apoptosis.

Materials and methods

Cell Culture and supplies

MDA-MB-231 cells were purchased from American Type Culture Collection (ATCC) and were grown in Dulbecco's Modified Eagle Medium (DMEM, Invitrogen) supplemented to 4.0 g/L glucose, 3.7 g/L sodium bicarbonate, and 10% FBS (Omega Scientific) in a humidified incubator at 37 °C and 5% CO_2. Cells were passaged regularly before reaching 80% confluency, and cells used in experiments were at less than 25 passages. Prior to all experiments, monolayers were washed with PBS and the growth medium was changed to medium with 1% FBS for 20 hours. DIM (LKT Laboratories), DMSO (Acros Organics), SB202190, SB239063, SB203580, SP600125, Gö6983 (Tocris), ascorbic acid, α-tocopherol, or N-(tert-Butyl) hydroxylamine HCL (Sigma) were added for the indicated times. All other cell culture supplies were purchased from Fisher Scientific.

Microarrays

MDA-MB-231 cells were plated in 6-well plates in growth medium. When the cells reached 70% confluency they were washed in PBS and incubated in DMEM containing 1% FBS for 20 hours and then treated with 25 μM DIM or the vehicle control DMSO for 4 hours at 37 °C. Total cellular RNA was isolated with the Aurum RNA isolation kit (Bio-Rad) according to the manufacturer's protocol. Total RNA was first quantitated by 260/280 absorbance spectrophotometry, and then qualitatively evaluated by capillary electrophoresis using the Bio-Rad Experion system. Biotin-labeled cRNA samples were hybridized overnight against Illumina HumanWG-6 v3.0 BeadChips. The array hybridizations, washing, staining, and scanning were performed at the UCSF Genomics Core (San Francisco, CA). Treatments were done in triplicate.

Microarray data analysis

The Illumina arrays were pre-processed using lumi package [135]. The differential expression analysis was performed using limma package [136]. Data analysis was performed as described [137], except fold change threshold 1.7 was used. The canonical pathways were generated through the use of Ingenuity Pathways Analysis (Ingenuity® Systems, www.ingenuity.com).

Quantitative reverse transcriptase PCR

MDA-MB-231 cells were serum-starved in 1% FBS for 20 h and then treated for 4 h with DMSO or 25 μM DIM. Total RNA was extracted with the Aurum RNA isolation kit (BioRad) and 2 μg of total RNA were subjected to reverse transcription using the Superscript II Reverse Transcriptase kit (Invitrogen). Real time PCR analysis was performed in duplicate using EVA QPCR Supermix (BioChain Institute) with an Applied Biosystems 7500 Real-Time PCR System. Primer sequences are listed in Table 2-1. The data were collected and analyzed using the comparative Ct (threshold cycle) method using *RPL19* as the reference gene. The results are expressed as means $\pm$ SEM for at least three replicate determinations for each assay. Data were analyzed using GraphPad Prism Software.

Western blot analysis

MDA-MB-231 cells were serum-starved in 1% FBS for 20 h and then treated for the indicated times with DMSO or DIM. To prepare whole cell lysates, monolayers were scraped directly in protein loading buffer (10% glycerol, 5% 2 mercaptoethanol, 10% SDS, 0.125 M Tris–HCl pH 6.7, 0.15% bromophenol blue), sonicated for 15 seconds, and heated to 99.9 °C for 5 minutes. Equal amounts of protein were separated by SDS-PAGE and transferred to Immobilon P membranes (Millipore). Membranes were blocked in 5% nonfat dry milk in TBS-Tween for 1 hour and then probed with rabbit anti-p38 (#9212) or rabbit anti-phospho-p38 (#9215) from Cell Signaling Technology or rabbit anti-PARP (214/215) cleavage site (44698G) from Invitrogen overnight at 4 °C. After washing three times in TBST, membranes were incubated in 5% nonfat dry milk in TBST containing the appropriate secondary antibody-HRP

conjugates (Santa Cruz Biotechnology), washed again, and exposed to Western Lighting *Plus*-ECL enhanced chemiluminescence substrate (Perkin Elmer) for 1 minute. Immunoreactive proteins were detected using CL-Xposure film (Thermo Scientific). Results shown are representative of at least three independent experiments.

Results

Regulation of gene expression by DIM

In MDA-MB-231 cells, 25 μM DIM regulated the expression of 434 distinct genes; 283 were up regulated and 151 were down regulated (Table 4-2, Figure 4-1). Of these genes, many were expected to be regulated by DIM, including the AhR-activated genes *CYP1a1* and *CYP1b1* and the cyclin-dependent kinase inhibitors *CDKN1a* and *CDKN1b*, which encode $p21^{cip1/waf1}$ and $p27^{kip1}$, respectively. We also identified genes whose regulation by DIM have not previously been reported, including the genes for the vitamin D receptor *VDR,* the pro-apoptotic interleukin *IL24,* and cyclooxygenase-2, *PTGS2*.

Gene ontology analysis shows that DIM regulates the expression of genes across a wide variety of biological processes, including cell death and proliferation (Figure 4-2). We also used a canonical pathway analysis to identify cell signaling pathways whose known components were altered by DIM. We saw that DIM, not surprisingly, regulates a significant number of genes involved in aryl hydrocarbon receptor signaling, G1/S cell cycle checkpoint regulation, and p38 MAPK signaling, among others (Figure 4-3). It was, however, surprising to see that the second most statistically significant pathway to be modified by DIM was VDR/RXR activation.

Validation of microarray results with quantitative PCR (QPCR)

To confirm our microarray results, we analyzed the expression of *CCNE2, CDKN1a, CDKN1b, CEBPB, CYP1a1, CYP1b1, DDIT3, IL24, MAPK14, MEF2A, NCOA7, NFE2L2, PTGS2, RUNX2,*and *TXNIP* by QPCR (Figure 4-4). We chose these genes based on relevance, degree of upregulation, and whether they belonged to a canonical pathway or function that was up regulated by DIM. AhR signaling genes include *CYP1a1, CYP1b1, CCNE2* (cyclin E2)*, NCOA7* and *NFE2L2* (the gene that encodes Nrf2). VDR/RXR activation genes include *VDR, RUNX2, CDKN1a, CDKN1b, TXNIP*, also known as vitamin D3 up regulated protein (*VDUP*), and *CEBPB*, a transcriptional co-activator. Genes involved in the G1/S checkpoint include *CCNE2, CDKN1a* and *CDKN1b.* Genes in the p38 MAPK signaling canonical pathway are *MAPK14* (the gene for p38)*, DDIT3* (the gene for the proapoptotic GADD153, or CHOP)*,* and *MEF2A*, a p38 substrate. The results of the QPCR analysis were in agreement with the microarray data (Table 4-2). Though the fold changes were not exactly the same for each gene between the microarray and QPCR data, the degrees of induction or repression were similar.

Induction of IL24 *is p38- and ROS-dependent*

We chose to use *IL24* as a model gene for studying potential mechanisms of up regulation by DIM because *IL24* is strongly up regulated by DIM and because it is a relevant gene that encodes a pro-apoptotic protein. Our lab has previously reported that DIM activates p38 and JNK in different cell lines and this activation is responsible for various downstream events [27,28,41]. Additionally, *IL24* was first identified using subtraction hybridization in melanoma cells treated with a combination of interferon β and the PKC activator mezerein [138]. Therefore, we pre-treated cells with inhibitors of either p38, JNK, or PKC for 30 minutes before treating cells with DIM to determine whether these pathways were involved in DIM's effects. As expected, DIM induced *IL24* by approximately 20-fold. As shown in Figure 4-5A, pretreatment with either SP600125 (SP, JNK inhibitor) or Gö6983 (Go, PKC inhibitor) did not reverse DIM-induced *IL24* up regulation. However, pretreatment of cells with 10 μM SB202190 (SB, p38 inhibitor) completely blocked DIM's effect. To confirm the role of p38, we pretreated cells with a panel of p38 inhibitors, including SB202190, SB239063, and SB203580 (Figure 4-5B). Each inhibitor blocked DIM's effect and SB202190 and SB239063 reversed DIM's effect in concentration-dependent manners, further confirming the involvement of p38 in DIM's mechanism of action on *IL24*.

Because our lab previously showed that DIM induces the formation of reactive oxygen species (ROS) in cells, and these ROS are responsible for activating p38 [27], we tested whether or not antioxidants could reverse DIM's induction of *IL24*. We pretreated cells with antioxidants, including water soluble ascorbic acid (vitamin C), lipid soluble α-tocopherol (vitamin E), mitochondria-specific N-(tert-Butyl) hydroxylamine HCL (BHA), or combinations of the three (Figure 4-5C). Vitamins C and E together and BHA alone reversed DIM's effect by 68% and 58%, respectively. All three antioxidants in combination reversed DIM's effect by 86%. Taken together, these data show that DIM induces *IL24* via a mechanism involving ROS and p38.

DIM activates p38 in MDA-MB-231 cells

We next wanted to confirm that DIM activates p38 in MDA-MB-231 cells within the same time frame as the gene expression analyses. We treated cell with or without 25 μM DIM for various time points and analyzed p38 phosphorylation by Western blotting (Figure 4-6A,B). DIM activated p38 at 15 minutes, the earliest time point studied, and this activation was sustained for 8 hours, the latest time point studied. We also observed strong p38 activation at 4 hours, the time point used for all of the gene expression experiments. We assessed p38 activation by various concentrations of DIM after 30 minutes and observed that 5 μM DIM did not activate p38, 10 μM DIM had a minimal effect, and 15-25 μM DIM activated p38 in a concentration-dependent manner.

The p38 inhibitor reverses DIM's effects on gene expression

Since DIM induces *IL24* via activation of p38, we wanted to know if p38 inhibition would reverse DIM's effect on other genes. Therefore, we pretreated cells with SB, treated them with DIM, and analyzed gene expression of several genes that were regulated by DIM in the

microarray experiment. SB reversed DIM's effects on several genes to various degrees, from 7-78% reversal (Figure 4-7). Generally, the stronger the induction by DIM was, the stronger the reversal by SB was. We also observed that SB reversed DIM's effects on genes that were activated by DIM, and not on genes that were repressed by DIM, including *CCNE2*.

The p38 inhibitor reverses DIM-induced PARP cleavage after 24 and 48 h

DIM at 25 μM induces the expression of several genes via activation of p38 after 4 hours, and the same concentration of DIM induces apoptosis at longer time points (see Chapter 2). To see if there was a possible connection between these effects, we treated cells with or without DIM and SB and measured apoptosis via detection of PARP cleavage by Western blotting (Figure 4-8). DIM induces PARP cleavage after 24 and 48 hours. After 24 hours, SB partially blocked DIM's apoptotic effect, and after 48 hours, PARP cleavage was almost completely reversed by the p38 inhibitor, demonstrating that DIM induces apoptosis in part through activation of p38.

Discussion

We have reported the early changes in gene expression that result from treatment of MDA-MB-231 cells with 25 μM DIM. DIM regulates the expression of over 400 genes after 4 hours. While this number differs from the 1,238 genes that were differentially regulated by DIM in a similar study, this could be due to the differences in concentrations (25 vs. 30 μM), the differences in serum levels (1% vs. 10%), the difference in the fold change cutoffs used (1.7 vs. 1.5) or the time point differences (4 hours vs. 48 hours). Rahman et al.'s study reported the effects of DIM after 6, 24, and 48 hours, but the specific number of genes that were regulated were only reported for 48 hours, and it is likely that fewer genes were affected after the 6 hour time point. Both studies show similar results, with DIM affecting many genes in the same way. One major difference between the two studies is that we see almost twice as many genes up regulated as we do down regulated genes, while Rahman et al. shows approximately the same number genes up and down regulated.

In this study, we confirmed many known effects of DIM, including the up regulation of the genes for $^{p21cip1/waf1}$ and $p27^{kip1}$, and we also observed some surprising results. We identified *IL24* as a DIM-induced gene that shows strong up regulation after 4 hours. *IL24* encodes a pro-apoptotic interleukin that selectively kills cancer cells without harming normal cells; thus, this gene should be the focus of extensive follow-up experiments. We also identified the gene for the vitamin D receptor, *VDR,* and the VDR/RXR activation pathway as DIM targets. While the research is still inconclusive, vitamin D status may be associated with lower risks of certain cancers in humans, including breast cancer. Potential mechanisms for VDR's anticancer effects include 1,25-dihydroxyvitamin D signaling through VDR/RXR to activate the expression of genes involved in differentiation, growth arrest, apoptosis, or detoxification [139-142]. Therefore, the effects of DIM on the vitamin D pathway and how this relates to DIM's anti-breast cancer effects are worthy of further study.

We used a panel of p38 inhibitors and antioxidants and found that inhibition of p38 reverses DIM's effects on up regulation of several genes and on apoptosis. It is possible that DIM-induced apoptosis is mediated by changes in gene expression. DIM regulates 41 genes involved in cell death (Figure 4-2). Gene expression experiments at later time points and gene knock down experiments will be necessary to confirm the roles of individual genes in DIM's pro-apoptotic activities.

In conclusion, DIM regulates the expression of over 400 genes after 4 hours, with 283 genes up regulated. DIM strongly activates p38, and p38 is a key mediator of DIM's up regulation of several of these genes and of DIM-induced apoptosis.

Table 4-1. Primer Sequences for QPCR

Gene Name	Forward Sequence	Reverse Sequence
CCNE2	TCTTCACTGCAAGCACCATC	ACCTCATTATTCATTGCTTCCAA
CDKN1a	GCCATTAGCGCATCACAGT	TGCGTTCACAGGTGTTTCTG
CDKN1b	CATTCCATGAAGTCAGCGAT	CGTCAAACGTAAACAGCTCG
CEBPB	AACAAGCCCGTAGGAACATC	TTTCGAAGTTGATGCAATCG
CYP1a1	GAGGCCAGAAGAAACTCCGT	CCCAGCTCAGCTCAGTACCT
CYP1b1	ACCTGATCCAATTCTGCCTG	TATCACTGACATCTTCGGCG
DDIT3	TGGATCAGTCTGGAAAAGCA	AGCCAAAATCAGAGCTGGAA
IL24	GCACAACCATCTGCATTTGA	TTTCAACAGAGGCTGCAAAG
MAPK14	TGGAGAGCTTCTTCACTGCC	CGAGCGTTACCAGAACCTGT
MEF2A	TGAAGTATCAGGGTCTGGGC	CCTCATGAAAGCAGAACCAAC
NCOA7	GCTGAGGCTGTCTCTGCATT	CAAGGAAGAGAAGAAGGAACG
NFE2L2	TCTTGCCTCCAAAGTATGTCAA	ACACGGTCCACAGCTCATC
PTGS2	GGTGGGAACAGCAAGGATT	CCCTCAGACAGCAAAGCCTA
RUNX2	CCTAAATCACTGAGGCGGTC	CAGTAGATGGACCTCGGGAA
TXNIP	TTGAAGGATGTTCCCAGAGG	CTTCGGAGTACCTGCGCTAT
VDR	ATTGCCTCCATCCCTGAAG	GGAACAGCTTGTCCACCC

Table 4-2. Genes regulated by 25 µM DIM after 4 hours in MDA-MB-231 cells. Genes whose regulation by DIM was confirmed by QPCR are shaded grey.

Gene	Accession	GeneDescription	Fold Change	p-value
CYP1A1	NM_000499.2	cytochrome P450, family 1, subfamily A, polypeptide 1	30.685	3.90E-12
TMEM46	NM_001007538.1	transmembrane protein 46	10.726	6.51E-10
CYP1B1	NM_000104.2	cytochrome P450, family 1, subfamily B, polypeptide 1	9.798	6.51E-10
PTGS2	NM_000963.1	prostaglandin-endoperoxide synthase 2 (prostaglandin G/H synthase and cyclooxygenase)	10.162	8.86E-10
IL24	NM_181339.1	interleukin 24	16.212	1.21E-09
IL1A	NM_000575.3	interleukin 1, alpha	10.09	1.81E-09
GDF15	NM_004864.1	growth differentiation factor 15	6.779	5.11E-09
SIPA1L2	NM_020808.1	signal-induced proliferation-associated 1 like 2	8.704	5.11E-09
MGC59937	NM_199001.1	Similar to RIKEN cDNA 2310002J15 gene	5.031	1.95E-08
HECW2	NM_020760.1	HECT, C2 and WW domain containing E3 ubiquitin protein ligase 2	5.13	3.19E-08
VIPR1	NM_004624.2	vasoactive intestinal peptide receptor 1	4.704	4.06E-08
TIPARP	NM_015508.2	TCDD-inducible poly(ADP-ribose) polymerase	4.29	8.02E-08
APM-1	XM_113971.4	PREDICTED: Homo sapiens BTB/POZ-zinc finger protein-like (APM-1), mRNA.	4.188	8.82E-08
GPR68	NM_003485.3	G protein-coupled receptor 68	4.047	1.09E-07
RND1	NM_014470.2	Rho family GTPase 1	4.661	1.62E-07
IL24	NM_006850.2	interleukin 24	7.135	2.21E-07
SERTAD4	NM_019605.2	SERTA domain containing 4	0.275	2.21E-07
SERPINB2	NM_002575.1	serpin peptidase inhibitor, clade B (ovalbumin), member 2	3.767	2.33E-07
F2RL3	NM_003950.2	coagulation factor II (thrombin) receptor-like 3	4.279	2.37E-07
PTGS2	NM_000963.1	prostaglandin-endoperoxide synthase 2 (prostaglandin G/H synthase and cyclooxygenase)	5.338	6.00E-07
BMF	NM_001003942.1	Bcl2 modifying factor	3.272	6.46E-07
SPRY1	NM_005841.1	sprouty homolog 1, antagonist of FGF signaling (Drosophila)	0.298	7.78E-07
SESN2	NM_031459.3	sestrin 2	3.756	8.64E-07
SPRY1	NM_005841.1	sprouty homolog 1, antagonist of FGF signaling (Drosophila)	0.316	8.89E-07
APOLD1	NM_030817.1	apolipoprotein L domain containing 1	3.465	8.91E-07
FBN2	NM_001999.3	fibrillin 2 (congenital contractural arachnodactyly)	3.805	8.91E-07
FBXO32	NM_148177.1	F-box protein 32	3.112	8.91E-07
ATF3	NM_001040619.1	activating transcription factor 3	3.625	1.05E-06
OTUB2	NM_023112.2	OTU domain, ubiquitin aldehyde binding 2	3.389	1.09E-06
KIAA1644	XM_376018.3	KIAA1644 protein	3.251	1.37E-06
DDIT3	NM_004083.4	DNA-damage-inducible transcript 3	3.303	1.37E-06
CXCL2	NM_002089.1	chemokine (C-X-C motif) ligand 2	4.259	1.37E-06
PLEKHF1	NM_024310.2	pleckstrin homology domain containing, family F (with FYVE domain) member 1	3.105	1.44E-06
CYGB	NM_134268.3	cytoglobin	3.538	1.72E-06
HEY1	NM_012258.2	hairy/enhancer-of-split related with YRPW motif 1	3.287	1.95E-06
GPR175	NM_016372.1	G protein-coupled receptor 175	2.836	1.95E-06
CDKN1A	NM_078467.1	cyclin-dependent kinase inhibitor 1A (p21, Cip1)	2.775	2.35E-06
CYR61	NM_001554.3	cysteine-rich, angiogenic inducer, 61	0.339	2.49E-06
TSC22D1	NM_183422.1	TSC22 domain family, member 1	4.617	2.70E-06
C8ORF13	NM_053279.1	chromosome 8 open reading frame 13	2.741	3.05E-06
C9ORF150	NM_203403.1	chromosome 9 open reading frame 150	3.032	3.20E-06
TMEM156	NM_024943.1	transmembrane protein 156	2.786	3.94E-06
STC2	NM_003714.2	stanniocalcin 2	2.8	3.94E-06
NFIL3	NM_005384.2	nuclear factor, interleukin 3 regulated	3.334	3.94E-06
CTH	NM_153742.3	cystathionase (cystathionine gamma-lyase)	3.291	3.94E-06
TSC22D1	NM_183422.1	TSC22 domain family, member 1	3.09	4.85E-06
FLJ23152	XM_376469.2	hypothetical gene supported by AK026805	2.882	5.84E-06
VEGFA	NM_003376.4	vascular endothelial growth factor A	2.614	6.05E-06

IL1B	NM_000576.2	interleukin 1, beta	2.811	6.13E-06
RUNX2	NM_001024630.1	runt-related transcription factor 2	2.778	6.13E-06
HSPA6	NM_002155.3	heat shock 70kDa protein 6 (HSP70B')	4.068	6.80E-06
BAIAP2L2	NM_025045.3	BAI1-associated protein 2-like 2	2.595	6.80E-06
TSC22D3	NM_004089.3	TSC22 domain family, member 3	2.704	8.08E-06
CTH	NM_153742.3	cystathionase (cystathionine gamma-lyase)	2.916	8.51E-06
PPFIA4	NM_015053.1	protein tyrosine phosphatase, receptor type, f polypeptide (PTPRF), interacting protein (liprin), alpha 4	0.35	8.64E-06
KLF9	NM_001206.2	Kruppel-like factor 9	2.569	8.64E-06
FOSB	NM_006732.1	FBJ murine osteosarcoma viral oncogene homolog B	2.582	9.55E-06
VEGF	NM_001025366.1	vascular endothelial growth factor A	2.509	9.97E-06
MAFF	NM_012323.2	v-maf musculoaponeurotic fibrosarcoma oncogene homolog F (avian)	2.393	1.43E-05
FST	NM_013409.1	follistatin	0.416	1.46E-05
CDRT1	NM_006382.1	CMT1A duplicated region transcript 1	2.481	1.50E-05
LHX4	NM_033343.2	LIM homeobox 4	2.635	1.62E-05
THBD	NM_000361.2	thrombomodulin	2.509	1.68E-05
KLF4	NM_004235.3	Kruppel-like factor 4 (gut)	2.725	1.80E-05
PPP1R15A	NM_014330.2	protein phosphatase 1, regulatory (inhibitor) subunit 15A	2.383	1.92E-05
DKK1	NM_012242.2	dickkopf homolog 1 (Xenopus laevis)	0.406	1.97E-05
HMOX1	NM_002133.1	heme oxygenase (decycling) 1	2.743	2.05E-05
ENC1	NM_003633.1	ectodermal-neural cortex (with BTB-like domain)	0.4	2.05E-05
FST	NM_006350.2	follistatin	0.412	2.06E-05
SMOX	NM_175840.1	spermine oxidase	2.304	2.06E-05
SOX9	NM_000346.2	SRY (sex determining region Y)-box 9 (campomelic dysplasia, autosomal sex-reversal)	0.389	2.12E-05
RGL1	NM_015149.2	ral guanine nucleotide dissociation stimulator-like 1	2.601	2.18E-05
CTH	NM_001902.4	cystathionase (cystathionine gamma-lyase)	2.435	2.18E-05
CEBPB	NM_005194.2	CCAAT/enhancer binding protein (C/EBP), beta	2.429	2.19E-05
TMEM156	NM_024943.1	transmembrane protein 156	2.522	2.23E-05
KRT17	NM_000422.1	keratin 17	3.16	2.37E-05
IRXL1	NM_173576.1	mohawk homeobox	2.64	2.39E-05
SCG5	NM_003020.1	secretogranin V (7B2 protein)	2.498	2.39E-05
E2F7	NM_203394.1	E2F transcription factor 7	2.606	2.57E-05
ANKRD37	NM_181726.1	ankyrin repeat domain 37	0.44	2.59E-05
NFE2	NM_006163.1	nuclear factor (erythroid-derived 2), 45kDa	2.35	2.95E-05
TCP11L2	NM_152772.1	t-complex 11 (mouse)-like 2	2.6	3.09E-05
HS.397465	BX538009	Homo sapiens mRNA; cDNA DKFZp686F1546 (from clone DKFZp686F1546)	2.229	3.10E-05
BMF	NM_001003943.1	Bcl2 modifying factor	2.412	3.20E-05
ADM2	NM_024866.3	adrenomedullin 2	2.569	3.40E-05
PFKFB3	NM_004566.2	6-phosphofructo-2-kinase/fructose-2,6-biphosphatase 3	0.448	3.53E-05
IRAK2	NM_001570.3	interleukin-1 receptor-associated kinase 2	2.301	3.55E-05
SPRY1	NM_199327.1	sprouty homolog 1, antagonist of FGF signaling (Drosophila)	0.329	3.86E-05
CTGF	NM_001901.2	connective tissue growth factor	0.435	4.21E-05
DSCR1	NM_203418.1	regulator of calcineurin 1	0.321	4.21E-05
HEY2	NM_012259.1	hairy/enhancer-of-split related with YRPW motif 2	2.232	4.31E-05
GTF2IRD1	NM_005685.2	GTF2I repeat domain containing 1	2.259	4.31E-05
ELF3	NM_004433.3	E74-like factor 3 (ets domain transcription factor, epithelial-specific)	2.277	4.31E-05
BMP4	NM_001202.2	bone morphogenetic protein 4	0.366	4.37E-05
ARL4C	NM_005737.3	ADP-ribosylation factor-like 4C	2.348	4.43E-05
SLITL2	NM_138440.1	vasorin	2.151	4.54E-05
BCL3	NM_005178.2	B-cell CLL/lymphoma 3	2.346	4.96E-05
NUPR1	NM_001042483.1	nuclear protein 1	2.299	5.01E-05
ZNF165	NM_003447.2	zinc finger protein 165	2.359	5.01E-05
MGC19764	NM_144975.2	schlafen family member 5	2.326	5.01E-05
TSC22D1	NM_006022.2	TSC22 domain family, member 1	2.687	5.01E-05

PCK2	NM_004563.2	phosphoenolpyruvate carboxykinase 2 (mitochondrial)	2.296	5.31E-05
JARID2	NM_004973.2	jumonji, AT rich interactive domain 2	2.405	5.31E-05
MTSS1	NM_014751.2	metastasis suppressor 1	2.306	5.34E-05
HS.570308	BX099724	Homo sapiens cDNA clone IMAGp998F201004, mRNA sequence	0.448	5.35E-05
PSCD4	NM_013385.2	pleckstrin homology, Sec7 and coiled-coil domains 4	2.206	6.12E-05
SLC3A2	NM_001012661.1	solute carrier family 3 (activators of dibasic and neutral amino acid transport), member 2	2.513	6.85E-05
TRIB3	NM_021158.3	tribbles homolog 3 (Drosophila)	2.274	6.90E-05
PFKFB4	NM_004567.2	6-phosphofructo-2-kinase/fructose-2,6-biphosphatase 4	0.485	7.09E-05
ASB7	NM_024708.2	ankyrin repeat and SOCS box-containing 7	2.414	7.28E-05
NEUROG2	NM_024019.2	neurogenin 2	2.543	7.36E-05
SGK	NM_005627.2	serum/glucocorticoid regulated kinase 1	0.444	7.83E-05
HS.551128	AF176921	Homo sapiens MSTP131 (MST131) mRNA, complete cds	2.456	8.15E-05
BIRC3	NM_001165.3	baculoviral IAP repeat-containing 3	2.169	8.16E-05
TFAP2A	NM_001032280.2	transcription factor AP-2 alpha (activating enhancer binding protein 2 alpha)	2.065	8.16E-05
LOC651309	XM_942586.1	PREDICTED: Homo sapiens hypothetical protein LOC651309 (LOC651309), mRNA.	2.583	8.16E-05
CTGF	NM_001901.2	connective tissue growth factor	0.436	8.28E-05
ANKRA2	NM_023039.2	ankyrin repeat, family A (RFXANK-like), 2	2.281	8.52E-05
TNFRSF11B	NM_002546.2	tumor necrosis factor receptor superfamily, member 11b (osteoprotegerin)	0.462	8.64E-05
SKP2	NM_032637.2	S-phase kinase-associated protein 2 (p45)	0.363	8.91E-05
TRAF1	NM_005658.3	TNF receptor-associated factor 1	2.23	8.91E-05
EDN1	NM_001955.2	endothelin 1	0.397	8.91E-05
NADK	NM_023018.3	NAD kinase	2.014	8.92E-05
SLC37A2	NM_198277.1	solute carrier family 37 (glycerol-3-phosphate transporter), member 2	2.227	9.86E-05
HS.444290	AK124776	Homo sapiens cDNA FLJ42786 fis, clone BRAWH3006761	0.431	1.00E-04
SMAD7	NM_005904.2	SMAD family member 7	2.058	0.000100824
C9ORF132	NM_203305.1	family with sequence similarity 102, member A	2.255	0.000102139
VDR	NM_000376.2	vitamin D (1,25- dihydroxyvitamin D3) receptor	2.291	0.000102139
NDP	NM_000266.1	Norrie disease (pseudoglioma)	0.486	0.000108035
C14ORF4	NM_024496.2	chromosome 14 open reading frame 4	2.062	0.000108216
MXD1	NM_002357.2	MAX dimerization protein 1	2.053	0.000111148
SSH1	NM_018984.2	slingshot homolog 1 (Drosophila)	2.707	0.000111148
LOC153222	NM_153607.1	chromosome 5 open reading frame 41	2.154	0.000119174
TSC22D3	NM_004089.3	TSC22 domain family, member 3	2.441	0.000130421
CXYORF3	NM_005088.2	splicing factor, arginine/serine-rich 17A	2.052	0.000140532
SLC7A5	NM_003486.5	solute carrier family 7 (cationic amino acid transporter, y+ system), member 5	1.946	0.000160695
PRDM1	NM_001198.2	PR domain containing 1, with ZNF domain	2.856	0.000160695
ALDH1A3	NM_000693.1	aldehyde dehydrogenase 1 family, member A3	1.947	0.000167524
JUNB	NM_002229.2	jun B proto-oncogene	2.072	0.000174837
LYST	NM_001005736.1	lysosomal trafficking regulator	0.491	0.000177498
PGBD3	NM_170753.1	piggyBac transposable element derived 3	1.989	0.000193777
WT1	NM_000378.3	Wilms tumor 1	0.477	0.000200664
FLJ14166	NM_024565.4	cyclin J-like	2.017	0.000203608
P8	NM_012385.1	nuclear protein 1	2.047	0.000212875
EGR2	NM_000399.2	early growth response 2 (Krox-20 homolog, Drosophila)	2.01	0.000217304
FLJ11000	NM_018295.1	transmembrane protein 140	1.923	0.000219946
A4GALT	NM_017436.4	alpha 1,4-galactosyltransferase (globotriaosylceramide synthase)	2.18	0.000219946
LMCD1	NM_014583.2	LIM and cysteine-rich domains 1	2.026	0.000219946
LPXN	NM_004811.1	leupaxin	1.99	0.000224496
RASD1	NM_016084.3	RAS, dexamethasone-induced 1	1.927	0.00022684
C10ORF73	XM_937528.1	chromosome 10 open reading frame 73	2.056	0.00022684
GPR81	NM_032554.2	G protein-coupled receptor 81	0.519	0.000231204
IL24	NM_181339.1	interleukin 24	3.318	0.000236407
HAS3	NM_005329.2	hyaluronan synthase 3	2.401	0.000236689

LOC283050	XM_944265.1	hypothetical protein LOC283050	1.999	0.000236745
OSR1	NM_145260.2	odd-skipped related 1 (Drosophila)	0.495	0.000236745
HS.444692	BM999001	Homo sapiens cDNA clone IMAGE:5881642 3, mRNA sequence	0.464	0.000236745
MID1IP1	NM_021242.3	MID1 interacting protein 1 (gastrulation specific G12 homolog (zebrafish))	2.081	0.000236745
ZFP36	NM_003407.1	zinc finger protein 36, C3H type, homolog (mouse)	1.972	0.000236745
IER3	NM_052815.1	immediate early response 3	1.957	0.00024195
CACNG6	NM_031897.2	calcium channel, voltage-dependent, gamma subunit 6	2.156	0.000259758
HKDC1	NM_025130.2	hexokinase domain containing 1	2.038	0.000265773
KIAA1434	NM_019593.2	hypothetical protein KIAA1434	2.017	0.000265773
EPHA2	NM_004431.2	EPH receptor A2	0.493	0.00026941
NCOA7	NM_181782.2	nuclear receptor coactivator 7	1.887	0.000277123
HS.132578	BX100705	Homo sapiens cDNA clone IMAGp998F18724, mRNA sequence	1.897	0.000277745
LOC153222	NM_153607.1	chromosome 5 open reading frame 41	1.92	0.000289506
CDC25A	NM_001789.2	cell division cycle 25 homolog A (S. pombe)	0.513	0.000297004
HSD3B1	NM_000862.1	hydroxy-delta-5-steroid dehydrogenase, 3 beta- and steroid delta-isomerase 1	0.511	0.000303392
OSGIN1	NM_013370.3	oxidative stress induced growth inhibitor 1	2.021	0.000303392
CCNE2	NM_057735.1	cyclin E2	0.47	0.000303392
EMX1	NM_001040404.1	empty spiracles homeobox 1	1.926	0.000303392
NFE2L2	NM_006164.2	nuclear factor (erythroid-derived 2)-like 2	2.02	0.000314
F2RL1	NM_005242.3	coagulation factor II (thrombin) receptor-like 1	1.963	0.00031879
DHRS3	NM_004753.4	dehydrogenase/reductase (SDR family) member 3	1.913	0.000341838
FAM43A	NM_153690.4	family with sequence similarity 43, member A	2.165	0.000344874
XAF1	NM_199139.1	XIAP associated factor-1	2.297	0.000355631
FLJ35767	NM_207459.1	FLJ35767 protein	1.966	0.000360887
CCNE1	NM_057182.1	cyclin E1	0.508	0.000371128
RASGRP3	NM_170672.1	RAS guanyl releasing protein 3 (calcium and DAG-regulated)	1.863	0.000371128
SKP2	NM_032637.2	S-phase kinase-associated protein 2 (p45)	0.513	0.00040447
FEN1	NM_004111.4	flap structure-specific endonuclease 1	0.503	0.00040447
DNAJB9	NM_012328.1	DnaJ (Hsp40) homolog, subfamily B, member 9	1.992	0.000405023
CSTF3	NM_001033506.1	cleavage stimulation factor, 3' pre-RNA, subunit 3, 77kDa	0.545	0.000408511
LOC399942	XM_934471.1	PREDICTED: Homo sapiens similar to Tubulin alpha-2 chain (Alpha-tubulin 2), transcript variant 5 (LOC399942)	0.317	0.000408511
SLC3A2	NM_001012661.1	solute carrier family 3 (activators of dibasic and neutral amino acid transport), member 2	2.048	0.000413694
TNFAIP3	NM_006290.2	tumor necrosis factor, alpha-induced protein 3	1.98	0.00041493
DHDH	NM_014475.2	dihydrodiol dehydrogenase (dimeric)	1.944	0.000415078
GLDN	NM_181789.1	gliomedin	2.004	0.000435936
DDIT4L	NM_145244.2	DNA-damage-inducible transcript 4-like	1.971	0.000436036
MGC52057	NM_194317.2	LY6/PLAUR domain containing 6	0.528	0.000439624
CDKN2D	NM_001800.3	cyclin-dependent kinase inhibitor 2D (p19, inhibits CDK4)	0.514	0.000448928
INHBE	NM_031479.3	inhibin, beta E	1.872	0.000448928
UGCG	NM_003358.1	UDP-glucose ceramide glucosyltransferase	1.936	0.000461193
SLC6A6	NM_003043.2	solute carrier family 6 (neurotransmitter transporter, taurine), member 6	1.924	0.000462777
PRDM13	NM_021620.2	PR domain containing 13	2.024	0.00050355
SIX1	NM_005982.1	SIX homeobox 1	0.519	0.000519118
BTG1	NM_001731.1	B-cell translocation gene 1, anti-proliferative	1.802	0.000519118
GPR110	NM_153840.2	G protein-coupled receptor 110	1.997	0.000519118
SLC14A1	NM_015865.1	solute carrier family 14 (urea transporter), member 1 (Kidd blood group)	1.878	0.000519118
MUC5AC	XM_495860.2	PREDICTED: Homo sapiens mucin 5, subtypes A and C, tracheobronchial/gastric (MUC5AC), mRNA.	2.082	0.000519118
AGPAT5	NM_018361.2	1-acylglycerol-3-phosphate O-acyltransferase 5 (lysophosphatidic acid acyltransferase, epsilon)	0.509	0.000519118
CABLES1	NM_138375.1	Cdk5 and Abl enzyme substrate 1	1.846	0.000519118
TMEM45B	NM_138788.2	transmembrane protein 45B	2.039	0.000529383
ERN1	NM_152461.2	endoplasmic reticulum to nucleus signaling 1	1.835	0.000529383

CXYORF3	NM_005088.2	splicing factor, arginine/serine-rich 17A	1.803	0.000529792
BMP4	NM_130851.1	bone morphogenetic protein 4	0.51	0.000529792
IRF1	NM_002198.1	interferon regulatory factor 1	1.93	0.000529792
TXNIP	NM_006472.1	thioredoxin interacting protein	1.916	0.00053685
RRAD	NM_004165.1	Ras-related associated with diabetes	2.122	0.000541243
HSPA1A	NM_005345.4	heat shock 70kDa protein 1A	2.234	0.00054427
C14ORF28	NM_001017923.1	chromosome 14 open reading frame 28	1.823	0.00054464
FBLN1	NM_006486.2	fibulin 1	1.916	0.00054648
HERPUD1	NM_001010990.1	homocysteine-inducible, endoplasmic reticulum stress-inducible, ubiquitin-like domain member 1	1.931	0.000571646
MID1IP1	NM_021242.3	MID1 interacting protein 1 (gastrulation specific G12 homolog (zebrafish))	1.999	0.000577699
SLC7A2	NM_003046.2	solute carrier family 7 (cationic amino acid transporter, y+ system), member 2	1.935	0.000577699
SCHIP1	NM_014575.1	schwannomin interacting protein 1	0.531	0.000614999
KRTAP2-1	XM_937100.1	PREDICTED: Homo sapiens keratin associated protein 2-1, transcript variant 3 (KRTAP2-1), mRNA.	2.19	0.000617075
LOC644979	XM_928051.1	hypothetical LOC644979	0.541	0.000631312
MGC26963	NM_152621.3	sphingomyelin synthase 2	1.842	0.000696426
CDCA7	NM_145810.1	cell division cycle associated 7	0.56	0.000717308
FAIM3	NM_005449.3	Fas apoptotic inhibitory molecule 3	1.8	0.00075044
ZNF114	NM_153608.1	zinc finger protein 114	0.532	0.000768551
IL1RN	NM_173842.1	interleukin 1 receptor antagonist	1.872	0.000775444
ASNS	NM_133436.1	asparagine synthetase	1.97	0.000783863
ARHGEF2	NM_004723.2	rho/rac guanine nucleotide exchange factor (GEF) 2	1.805	0.000789338
ZFP36L1	NM_004926.2	zinc finger protein 36, C3H type-like 1	2.146	0.000789338
GPR110	NM_153840.2	G protein-coupled receptor 110	1.881	0.000795629
DSCR1	NM_203417.1	regulator of calcineurin 1	0.48	0.000797288
CEBPG	NM_001806.2	CCAAT/enhancer binding protein (C/EBP), gamma	1.841	0.000797288
INSIG1	NM_198336.1	insulin induced gene 1	1.852	0.000831075
CDK5R1	NM_003885.2	cyclin-dependent kinase 5, regulatory subunit 1 (p35)	0.558	0.000867331
FLRT3	NM_013281.2	fibronectin leucine rich transmembrane protein 3	1.775	0.000885747
NR3C1	NM_001020825.1	nuclear receptor subfamily 3, group C, member 1 (glucocorticoid receptor)	1.9	0.000888088
TSPYL2	NM_022117.1	TSPY-like 2	1.91	0.000896679
HS.492187	AL136588	chromosome 8 open reading frame 57	1.79	0.00090333
CXORF6	NM_005491.1	chromosome X open reading frame 6	0.565	0.00090333
LOC387763	XM_373497.4	hypothetical LOC387763	1.868	0.0009293
BMP4	NM_001202.2	bone morphogenetic protein 4	0.5	0.000938253
BIRC3	NM_001165.3	baculoviral IAP repeat-containing 3	1.844	0.000938253
LARP6	NM_018357.2	La ribonucleoprotein domain family, member 6	1.747	0.000949865
CEBPD	NM_005195.2	CCAAT/enhancer binding protein (C/EBP), delta	1.905	0.000971874
MAFG	NM_002359.2	v-maf musculoaponeurotic fibrosarcoma oncogene homolog G (avian)	1.737	0.000981528
HS.568951	BU561024	Homo sapiens cDNA clone IMAGE:6591845 5, mRNA sequence	1.753	0.000988871
LOC440993	NM_001013714.1	hypothetical gene supported by AK128346	1.893	0.000991871
PDK4	NM_002612.2	pyruvate dehydrogenase kinase, isozyme 4	1.83	0.000991871
SLC38A2	NM_018976.3	solute carrier family 38, member 2	1.8	0.001025487
CHAC1	NM_024111.2	ChaC, cation transport regulator homolog 1 (E. coli)	1.887	0.001025487
EREG	NM_001432.1	epiregulin	1.855	0.001028166
NTN4	NM_021229.3	netrin 4	1.77	0.001053927
HS.583454	BE439741	HTM1-598F HTM1 Homo sapiens cDNA, mRNA sequence	1.735	0.001105362
GTPBP2	NM_019096.3	GTP binding protein 2	1.805	0.001113096
RASD2	NM_014310.3	RASD family, member 2	1.81	0.001113096
FAM102A	NM_001035254.1	family with sequence similarity 102, member A	1.783	0.001128644
C8ORF72	NM_147189.1	family with sequence similarity 110, member B	1.897	0.001133262
CREB3L3	NM_032607.1	cAMP responsive element binding protein 3-like 3	1.928	0.001135207
TFAP2A	NM_001032280.1	transcription factor AP-2 alpha (activating enhancer binding protein 2 alpha)	1.895	0.001206702

CBX2	NM_005189.1	chromobox homolog 2 (Pc class homolog, Drosophila)	0.564	0.001223314
PDE7B	NM_018945.3	phosphodiesterase 7B	1.796	0.001236223
C10ORF10	NM_007021.2	chromosome 10 open reading frame 10	0.545	0.001241241
RELB	NM_006509.2	v-rel reticuloendotheliosis viral oncogene homolog B, nuclear factor of kappa light polypeptide gene enhancer in B-cells 3 (avian)	1.771	0.001279984
DST	NM_183380.1	dystonin	0.532	0.001279984
LOC650495	XM_939583.1	PREDICTED: Homo sapiens hypothetical LOC650495 (LOC650495), mRNA.	0.556	0.001279984
C3ORF59	NM_178496.2	chromosome 3 open reading frame 59	1.78	0.001279984
TXNDC5	NM_030810.2	thioredoxin domain containing 5	0.446	0.001281796
TBC1D2	NM_018421.2	TBC1 domain family, member 2	0.56	0.001301905
FZD7	NM_003507.1	frizzled homolog 7 (Drosophila)	1.827	0.001384567
FAM107A	NM_007177.1	family with sequence similarity 107, member A	1.884	0.001415733
ALDH1A3	NM_000693.1	aldehyde dehydrogenase 1 family, member A3	1.761	0.001422
ST7L	NM_138729.2	suppression of tumorigenicity 7 like	1.77	0.001437306
WNT7B	NM_058238.1	wingless-type MMTV integration site family, member 7B	1.849	0.001492824
MCM7	NM_182776.1	minichromosome maintenance complex component 7	0.512	0.001496624
TNFSF4	NM_003326.2	tumor necrosis factor (ligand) superfamily, member 4 (tax-transcriptionally activated glycoprotein 1, 34kDa)	1.77	0.00151134
BDNF	NM_001709.3	brain-derived neurotrophic factor	0.558	0.001528765
TNFRSF10D	NM_003840.3	tumor necrosis factor receptor superfamily, member 10d, decoy with truncated death domain	0.562	0.001528765
HCP5	NM_006674.2	HLA complex P5	1.752	0.001605762
LDOC1L	NM_032287.2	leucine zipper, down-regulated in cancer 1-like	1.702	0.001605762
LOC653110	XM_926584.1	PREDICTED: Homo sapiens similar to annexin A8, transcript variant 1 (LOC653110), mRNA.	0.58	0.001634991
ERCC6	NM_000124.1	excision repair cross-complementing rodent repair deficiency, complementation group 6	1.839	0.001634991
PXK	NM_017771.2	PX domain containing serine/threonine kinase	1.913	0.001634991
EFNA1	NM_004428.2	ephrin-A1	1.747	0.001634991
SLC16A6	NM_004694.2	solute carrier family 16, member 6 (monocarboxylic acid transporter 7)	1.875	0.00164359
RPS26	NM_001029.3	ribosomal protein S26	0.553	0.001661921
MAFG	NM_002359.2	v-maf musculoaponeurotic fibrosarcoma oncogene homolog G (avian)	1.711	0.001688612
ARNTL	NM_001030272.1	aryl hydrocarbon receptor nuclear translocator-like	1.8	0.001727721
MGC4677	XM_939115.1	PREDICTED: Homo sapiens hypothetical protein MGC4677 (MGC4677), mRNA.	0.543	0.001732915
ZNF295	NM_020727.3	zinc finger protein 295	1.842	0.001736207
FLJ14213	NM_024841.2	hypothetical protein FLJ14213	0.578	0.00173778
ANKRD1	NM_014391.2	ankyrin repeat domain 1 (cardiac muscle)	2.137	0.001755183
DOC1	NM_014890.1	filamin A interacting protein 1-like	0.578	0.0017658
CARD10	NM_014550.3	caspase recruitment domain family, member 10	1.804	0.0017658
DHRS9	NM_005771.3	dehydrogenase/reductase (SDR family) member 9	1.898	0.001792106
RBCK1	NM_006462.3	RanBP-type and C3HC4-type zinc finger containing 1	1.774	0.001792106
FBXO30	NM_032145.4	F-box protein 30	1.739	0.001792106
ABCA1	NM_005502.2	ATP-binding cassette, sub-family A (ABC1), member 1	1.95	0.001827319
ABTB2	NM_145804.1	ankyrin repeat and BTB (POZ) domain containing 2	1.923	0.00183486
INSIG2	NM_016133.2	insulin induced gene 2	0.575	0.001898059
CCDC58	NM_001017928.2	coiled-coil domain containing 58	0.542	0.001915239
SSBP2	NM_012446.2	single-stranded DNA binding protein 2	1.707	0.00192241
RCC1	NM_001269.2	regulator of chromosome condensation 1	0.499	0.001946176
WDSUB1	NM_152528.1	WD repeat, sterile alpha motif and U-box domain containing 1	1.796	0.002003211
LOC653752	XM_933660.1	PREDICTED: Homo sapiens similar to dexamethasone-induced transcript (LOC653752), mRNA.	1.714	0.002003211
GCOM1	NM_001018096.1	GRINL1A combined protein	1.725	0.002049488
FLJ39827	NM_152424.1	family with sequence similarity 123B	0.559	0.002092167
PIM3	NM_001001852.2	pim-3 oncogene	1.863	0.002132648
ID1	NM_181353.1	inhibitor of DNA binding 1, dominant negative helix-loop-helix protein	0.583	0.002261677

MEST	NM_177524.1	mesoderm specific transcript homolog (mouse)	0.475	0.002368064
ROR1	NM_005012.1	receptor tyrosine kinase-like orphan receptor 1	1.716	0.002478639
PRSS1	NM_002769.2	protease, serine, 1 (trypsin 1)	1.73	0.002527158
SPRY2	NM_005842.2	sprouty homolog 2 (Drosophila)	1.744	0.002538311
SIN3B	NM_015260.1	SIN3 homolog B, transcription regulator (yeast)	1.739	0.002585678
HS.566710	AW591174	Homo sapiens cDNA clone IMAGE:2703687 3 similar to contains element OFR repetitive element ;, mRNA sequence	1.736	0.00268159
ACPL2	NM_152282.3	acid phosphatase-like 2	0.584	0.002720457
EPIM	NM_194356.1	syntaxin 2	0.569	0.002778942
APOBEC3B	NM_004900.3	apolipoprotein B mRNA editing enzyme, catalytic polypeptide-like 3B	0.581	0.002823183
BIRC3	NM_182962.1	baculoviral IAP repeat-containing 3	1.853	0.002842517
TUBB6	NM_032525.1	tubulin, beta 6	0.539	0.002915521
TUBA1A	NM_006009.2	tubulin, alpha 1a	0.509	0.002947559
PDE9A	NM_001001567.1	phosphodiesterase 9A	1.918	0.002956519
C3ORF58	NM_173552.2	chromosome 3 open reading frame 58	0.579	0.002962221
ZNF167	NM_018651.2	zinc finger protein 167	1.706	0.002994923
MTHFD2	NM_006636.2	methylenetetrahydrofolate dehydrogenase (NADP+ dependent) 2, methenyltetrahydrofolate cyclohydrolase	1.862	0.003012662
C17ORF44	NM_173621.1	Homo sapiens chromosome 17 open reading frame 44 (C17orf44), mRNA.	1.751	0.003109897
DYRK1B	NM_006484.1	dual-specificity tyrosine-(Y)-phosphorylation regulated kinase 1B	1.74	0.003136695
ODC1	NM_002539.1	ornithine decarboxylase 1	1.76	0.003156163
MEF2A	NM_005587.1	myocyte enhancer factor 2A	1.851	0.003207015
C9ORF91	NM_153045.2	chromosome 9 open reading frame 91	1.758	0.00333076
SLC37A3	NM_207113.1	solute carrier family 37 (glycerol-3-phosphate transporter), member 3	0.455	0.00333076
KLHL24	NM_017644.3	kelch-like 24 (Drosophila)	1.706	0.003395235
LOC653994	XM_944429.1	PREDICTED: Homo sapiens similar to Eukaryotic translation initiation factor 4H (eIF-4H) (Williams-Beuren syndrome chromosome region 1 protein homolog), transcript variant 2 (LOC653994), mRNA.	0.485	0.003498742
ALDH3A1	NM_000691.3	aldehyde dehydrogenase 3 family, memberA1	1.812	0.003498742
SLC7A11	NM_014331.2	solute carrier family 7, (cationic amino acid transporter, y+ system) member 11	2.059	0.003550726
MTMR7	NM_004686.2	myotubularin related protein 7	1.821	0.003551238
PDE4B	NM_002600.3	phosphodiesterase 4B, cAMP-specific (phosphodiesterase E4 dunce homolog, Drosophila)	0.563	0.003642659
TCP11L2	NM_152772.1	t-complex 11 (mouse)-like 2	1.949	0.003711882
PGAM1	NM_002629.2	phosphoglycerate mutase 1 (brain)	0.496	0.003711882
DHX9	NM_001357.2	DEAH (Asp-Glu-Ala-His) box polypeptide 9	0.454	0.003711882
FAM59A	NM_022751.1	family with sequence similarity 59, member A	1.947	0.003787237
SNF1LK	NM_173354.2	SNF1-like kinase	1.796	0.003901886
HIST2H4A	NM_003548.2	histone cluster 2, H4a	2.015	0.003927298
CNN2	NM_004368.2	calponin 2	0.489	0.004139047
IGFBP1	NM_000596.2	insulin-like growth factor binding protein 1	1.787	0.004154193
TSPYL2	XM_944226.1	PREDICTED: Homo sapiens TSPY-like 2, transcript variant 3 (TSPYL2), mRNA.	1.709	0.004160815
KRCC1	NM_016618.1	lysine-rich coiled-coil 1	1.857	0.004309465
LOC338758	XM_931359.1	hypothetical protein LOC338758	1.743	0.004315309
SORD	NM_003104.3	sorbitol dehydrogenase	0.511	0.004402991
HIF1A	NM_181054.1	hypoxia-inducible factor 1, alpha subunit (basic helix-loop-helix transcription factor)	1.742	0.004424519
LOC128439	NM_139016.2	chromosome 20 open reading frame 198	1.71	0.004530394
HS.207531	BX111417	BX111417 NCI_CGAP_Pr28 Homo sapiens cDNA clone IMAGp998N105566, mRNA sequence	1.759	0.004767106
TUBE1	NM_016262.3	tubulin, epsilon 1	1.9	0.004861231
KRCC1	NM_016618.1	lysine-rich coiled-coil 1	1.741	0.00521528
PPM1G	NM_177983.1	protein phosphatase 1G (formerly 2C), magnesium-dependent, gamma isoform	0.566	0.005476109
CDC25A	NM_001789.2	cell division cycle 25 homolog A (S. pombe)	0.554	0.005575417

MLXIPL	NM_032953.2	MLX interacting protein-like	1.948	0.005575417
AP1S1	NM_001283.2	adaptor-related protein complex 1, sigma 1 subunit	0.577	0.005575417
BATF	NM_006399.2	basic leucine zipper transcription factor, ATF-like	1.75	0.005633505
LOC641765	XM_935531.1	similar to General transcription factor II-I repeat domain-containing protein 1 (GTF2I repeat domain-containing protein 1) (Muscle TFII-I repeat domain-containing protein 1) (General transcription factor III) (Slow-muscle-fiber enhancer binding pro...	1.734	0.005774984
HS.559705	DA529130	DA529130 FEBRA2 Homo sapiens cDNA clone FEBRA2021739 5, mRNA sequence	0.564	0.005774984
PCNA	NM_182649.1	proliferating cell nuclear antigen	0.583	0.005903172
PDLIM5	NM_001011515.1	PDZ and LIM domain 5	0.543	0.006222921
CTBP1	NM_001012614.1	C-terminal binding protein 1	0.441	0.006237728
LOC644391	XM_932163.1	PREDICTED: Homo sapiens hypothetical protein LOC644391 (LOC644391), mRNA.	1.856	0.006297818
SLC4A7	NM_003615.2	solute carrier family 4, sodium bicarbonate cotransporter, member 7	1.761	0.006300549
NBPF15	NM_173638.2	neuroblastoma breakpoint family, member 15	0.555	0.006307611
MRFAP1L1	NM_203462.1	Morf4 family associated protein 1-like 1	0.583	0.006411913
EFEMP1	NM_004105.2	EGF-containing fibulin-like extracellular matrix protein 1	0.533	0.006411913
BTBD7	NM_018167.3	BTB (POZ) domain containing 7	0.529	0.006411913
FBXO32	NM_058229.2	F-box protein 32	1.701	0.006461822
ECOP	NM_030796.3	EGFR-coamplified and overexpressed protein	0.532	0.006657234
RNU30	NR_002561.1	small nucleolar RNA, C/D box 30	0.586	0.006816437
TNPO1	NM_153188.1	transportin 1	0.492	0.006847217
MUC4	NM_018406.3	mucin 4, cell surface associated	1.756	0.006934646
STARD7	NM_020151.2	StAR-related lipid transfer (START) domain containing 7	0.454	0.007238384
PSAT1	NM_021154.3	phosphoserine aminotransferase 1	1.709	0.007432434
FBLN1	NM_001996.2	fibulin 1	1.75	0.007763336
IBRDC3	NM_153341.1	ring finger protein 19B	1.91	0.007839727
TUBB	NM_178014.2	tubulin, beta	0.505	0.007852799
ALG1	NM_019109.3	asparagine-linked glycosylation 1 homolog (S. cerevisiae, beta-1,4-mannosyltransferase)	0.585	0.008004156
UHRF1	NM_013282.2	ubiquitin-like, containing PHD and RING finger domains, 1	0.491	0.008173663
HNRPM	NM_005968.2	heterogeneous nuclear ribonucleoprotein M	0.549	0.008864222
KIAA1622	NM_058237.1	KIAA1622	1.735	0.00897787
HNRPA1	NM_002136.1	heterogeneous nuclear ribonucleoprotein A1	0.549	0.009203219
USP4	NM_003363.2	ubiquitin specific peptidase 4 (proto-oncogene)	0.541	0.009726145
HIATL2	NM_032318.1	Homo sapiens hippocampus abundant gene transcript-like 2 (HIATL2), mRNA.	0.58	0.009726145
MCM7	NM_005916.3	minichromosome maintenance complex component 7	0.483	0.010026638
AMD1	NM_001634.4	adenosylmethionine decarboxylase 1	0.537	0.010703825
CASP2	NM_032982.2	caspase 2, apoptosis-related cysteine peptidase (neural precursor cell expressed, developmentally down-regulated 2)	0.4	0.011118827
SORD	NM_003104.3	sorbitol dehydrogenase	0.538	0.0111653
DDB1	XM_943551.1	PREDICTED: Homo sapiens damage-specific DNA binding protein 1, 127kDa, transcript variant 4 (DDB1), mRNA.	0.52	0.012835903
NUP155	NM_153485.1	nucleoporin 155kDa	0.475	0.013265633
CPNE1	NM_003915.2	copine I	0.579	0.013422389
LOC644063	XM_931572.1	PREDICTED: Homo sapiens similar to heterogeneous nuclear ribonucleoprotein K isoform a, transcript variant 2 (LOC644063), mRNA.	0.536	0.013446501
HSPD1	NM_002156.4	heat shock 60kDa protein 1 (chaperonin)	0.586	0.014401086
ARPC4	NM_001024960.1	actin related protein 2/3 complex, subunit 4, 20kDa	0.574	0.01472231
CDK2	NM_001798.2	cyclin-dependent kinase 2	0.558	0.014923232
HS.569340	DA483022	DA483022 FCBBF1 Homo sapiens cDNA clone FCBBF1000024 5, mRNA sequence	0.414	0.014954122
WBSCR1	NM_022170.1	eukaryotic translation initiation factor 4H	0.546	0.015023474
LOC652903	XM_942634.1	PREDICTED: Homo sapiens similar to Bcl-XL-binding protein v68 (LOC652903), mRNA.	0.561	0.015591345
HNRPK	NM_031263.1	heterogeneous nuclear ribonucleoprotein K	0.581	0.015649546
TRIM6-TRIM34	NM_001003819.1	TRIM6-TRIM34	0.537	0.01583005
LYPLA2P1	NR_001444.1	lysophospholipase II pseudogene 1	0.521	0.015854274

RBM4	NM_002896.1	RNA binding motif protein 4	0.587	0.015854274
DKFZP434A013 1	NM_018991.2	stromal antigen 3-like 1	0.588	0.016308928
TGFB2	NM_003238.1	transforming growth factor, beta 2	0.526	0.01687665
DPAGT1	NM_001382.2	dolichyl-phosphate (UDP-N-acetylglucosamine) N-acetylglucosaminephosphotransferase 1 (GlcNAc-1-P transferase)	0.584	0.019517767
MAPK14	NM_139013.1	mitogen-activated protein kinase 14	0.539	0.020412636
ZDHHC9	NM_016032.2	zinc finger, DHHC-type containing 9	0.549	0.020469744
CXCR4	NM_003467.2	chemokine (C-X-C motif) receptor 4	0.588	0.021015074
MAP2K3	XM_944206.1	PREDICTED: Homo sapiens mitogen-activated protein kinase kinase 3 (MAP2K3), mRNA.	0.578	0.021333218
CDKN1B	NM_004064.2	cyclin-dependent kinase inhibitor 1B (p27, Kip1)	1.704	0.021712637
HCAP-H2	NM_014551.3	non-SMC condensin II complex, subunit H2	0.578	0.022915677
TBRG4	NM_004749.2	transforming growth factor beta regulator 4	0.588	0.023739217
LGALS3	NM_002306.1	lectin, galactoside-binding, soluble, 3	1.734	0.023750925
PAPPA	NM_002581.3	pregnancy-associated plasma protein A, pappalysin 1	1.717	0.024578627
OAS2	NM_016817.2	2'-5'-oligoadenylate synthetase 2, 69/71kDa	0.573	0.024680234
TCF19	NM_007109.1	transcription factor 19 (SC1)	0.575	0.024982499
LRCH4	NM_002319.2	leucine-rich repeats and calponin homology (CH) domain containing 4	0.568	0.025317784
NNT	NM_012343.3	nicotinamide nucleotide transhydrogenase	0.563	0.025753504
P4HA2	NM_001017974.1	procollagen-proline, 2-oxoglutarate 4-dioxygenase (proline 4-hydroxylase), alpha polypeptide II	0.536	0.026003743
HS.143018	BX105338	BX105338 Soares_pregnant_uterus_NbHPU Homo sapiens cDNA clone IMAGp998C114347, mRNA sequence	1.831	0.026522
ZDHHC13	NM_019028.2	zinc finger, DHHC-type containing 13	0.573	0.029118234
KUA-UEV	NM_199203.1	TMEM189-UBE2V1	0.52	0.029767318
MCRS1	NM_006337.3	microspherule protein 1	0.541	0.029914141
DUSP4	NM_001394.5	dual specificity phosphatase 4	0.518	0.029934444
GOLPH2	NM_177937.1	golgi membrane protein 1	0.576	0.030381267
MAFF	NM_012323.2	v-maf musculoaponeurotic fibrosarcoma oncogene homolog F (avian)	1.774	0.030805497
C14ORF150	NM_080666.2	WD repeat domain 89	0.585	0.032186163
GTF2I	XM_939506.1	PREDICTED: Homo sapiens general transcription factor II, i (GTF2I), mRNA.	0.528	0.035382017
NET1	NM_005863.2	neuroepithelial cell transforming gene 1	0.519	0.036700043
LBR	NM_002296.2	lamin B receptor	0.489	0.037959584
PRIM2A	XM_942683.1	PREDICTED: Homo sapiens primase, polypeptide 2A, 58kDa, transcript variant 2 (PRIM2A), mRNA.	0.579	0.040979238
ASNS	NM_133436.1	asparagine synthetase	1.847	0.041553359
MGAT4B	NM_014275.2	mannosyl (alpha-1,3-)-glycoprotein beta-1,4-N-acetylglucosaminyltransferase, isozyme B	0.561	0.041866583
ANAPC7	NM_016238.1	anaphase promoting complex subunit 7	0.588	0.045185676

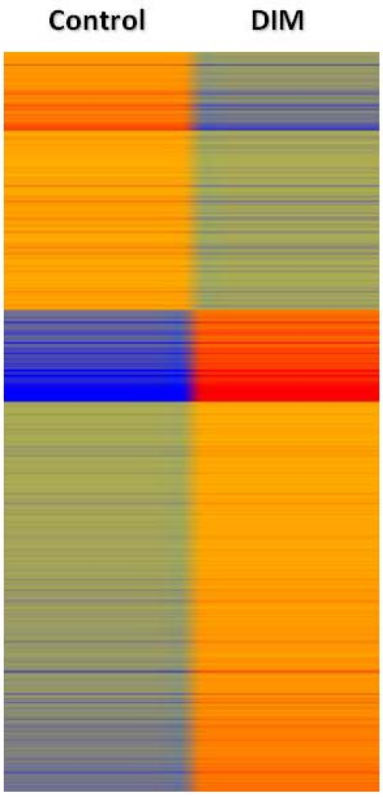

Figure 4-1. Heatmap of log-intensities of the regulated genes by DIM in MDA-MB-231 cells. Genes regulated by DIM are shown in rows. For each gene, the average log intensities are colored yellow, relatively higher expression are colored with reds of increasing intensity, and relatively lower expression are colored with blues of increasing intensity. The controls and treated samples for microarrays were done in triplicate. Each activated gene was 1.7-fold or greater and each repressed gene was 0.7-fold or less with p-values <0.05.

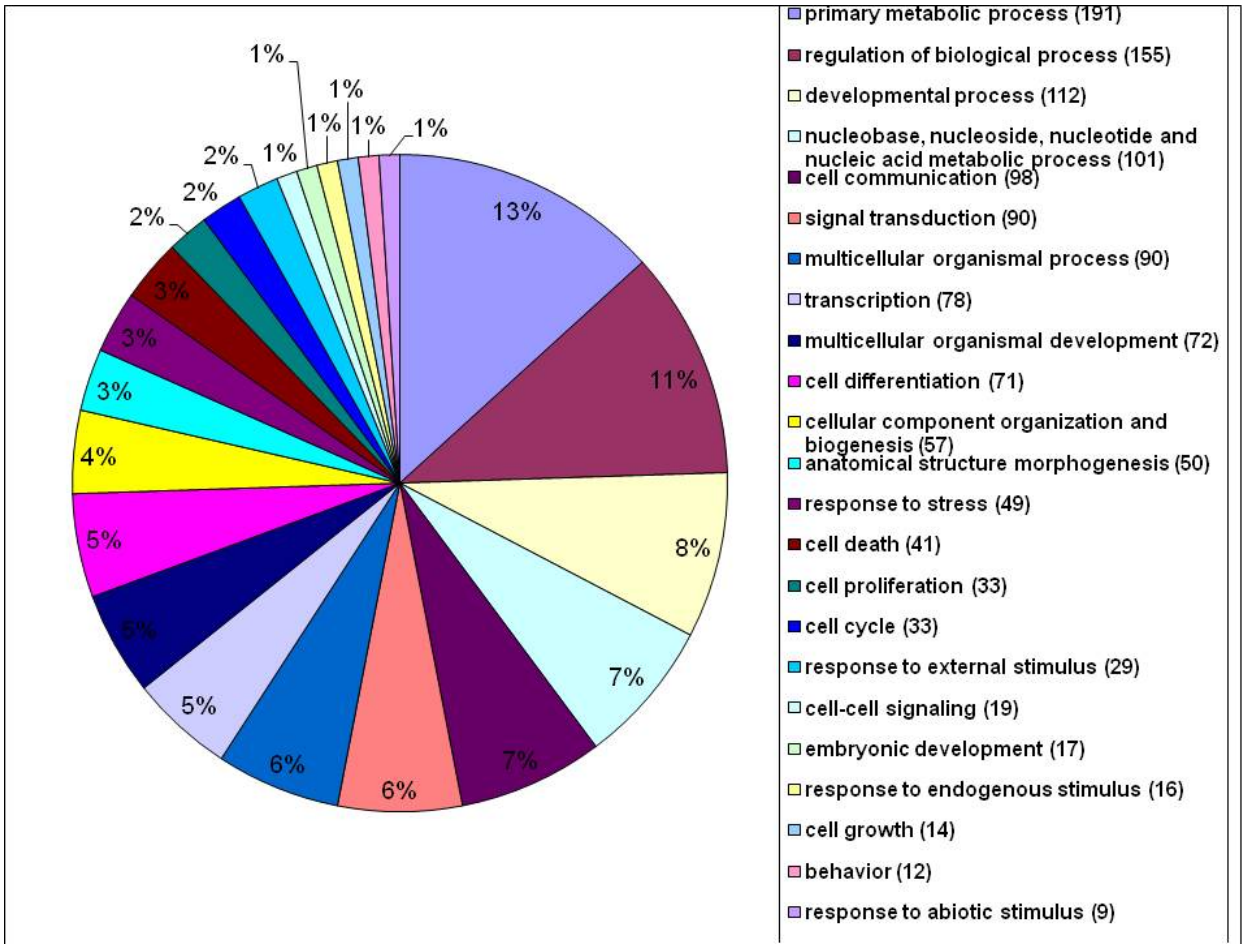

Figure 4-2. Significantly enriched GO terms for genes regulated by DIM in MDA-MB-231 cells. Gene ontology (GO) terms significantly enriched in various biological processes for genes regulated by DIM in MDA-MB-231 cells. Threshold 0.05 was used for selecting GO terms using BH-adjusted *p*-values. Significant GO slim terms are presented in the pie chart. The number of genes regulated in the each biological class is shown in parentheses.

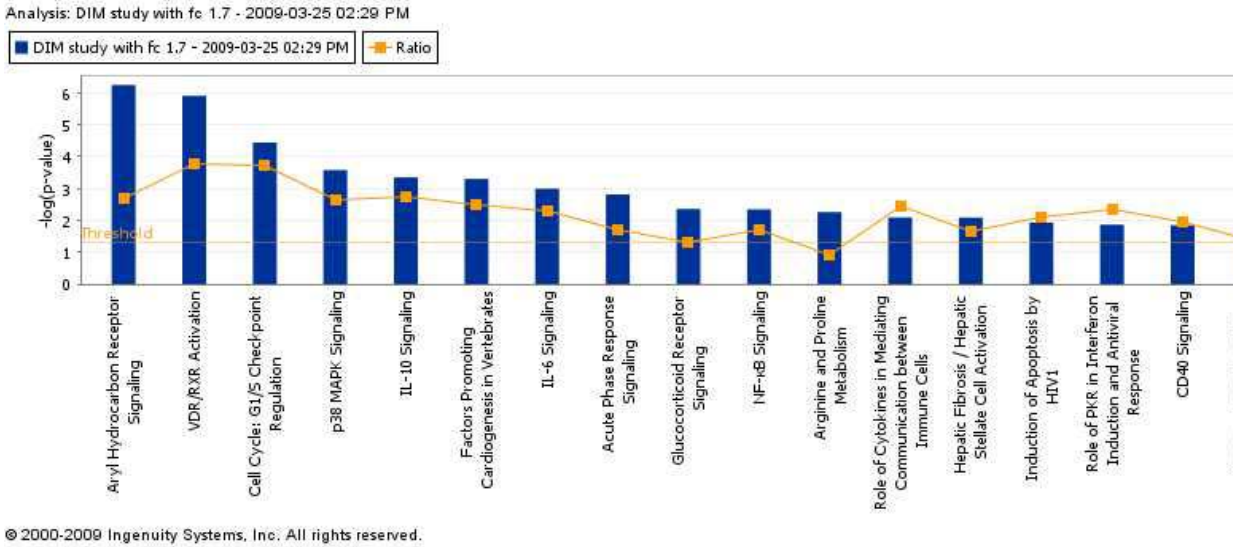

Figure 4-3. DIM regulates genes involved in various canonical pathways. Canonical pathways analysis identified the pathways from the Ingenuity Pathways Analysis library of canonical pathways that were most significant to the data set. Molecules from the data set that met the gene expression cutoff of $p<0.05$ and were associated with a canonical pathway in Ingenuity's Knowledge Base were considered for the analysis. The significance of the association between the data set and the canonical pathway was measured in 2 ways: 1) A ratio of the number of molecules from the data set that map to the pathway divided by the total number of molecules that map to the canonical pathway is displayed (orange squares). 2) Fisher's exact test was used to calculate a p-value determining the probability that the association between the genes in the dataset and the canonical pathway is explained by chance alone (blue bars = -log(p-values)). The top 16 of 119 pathways are shown.

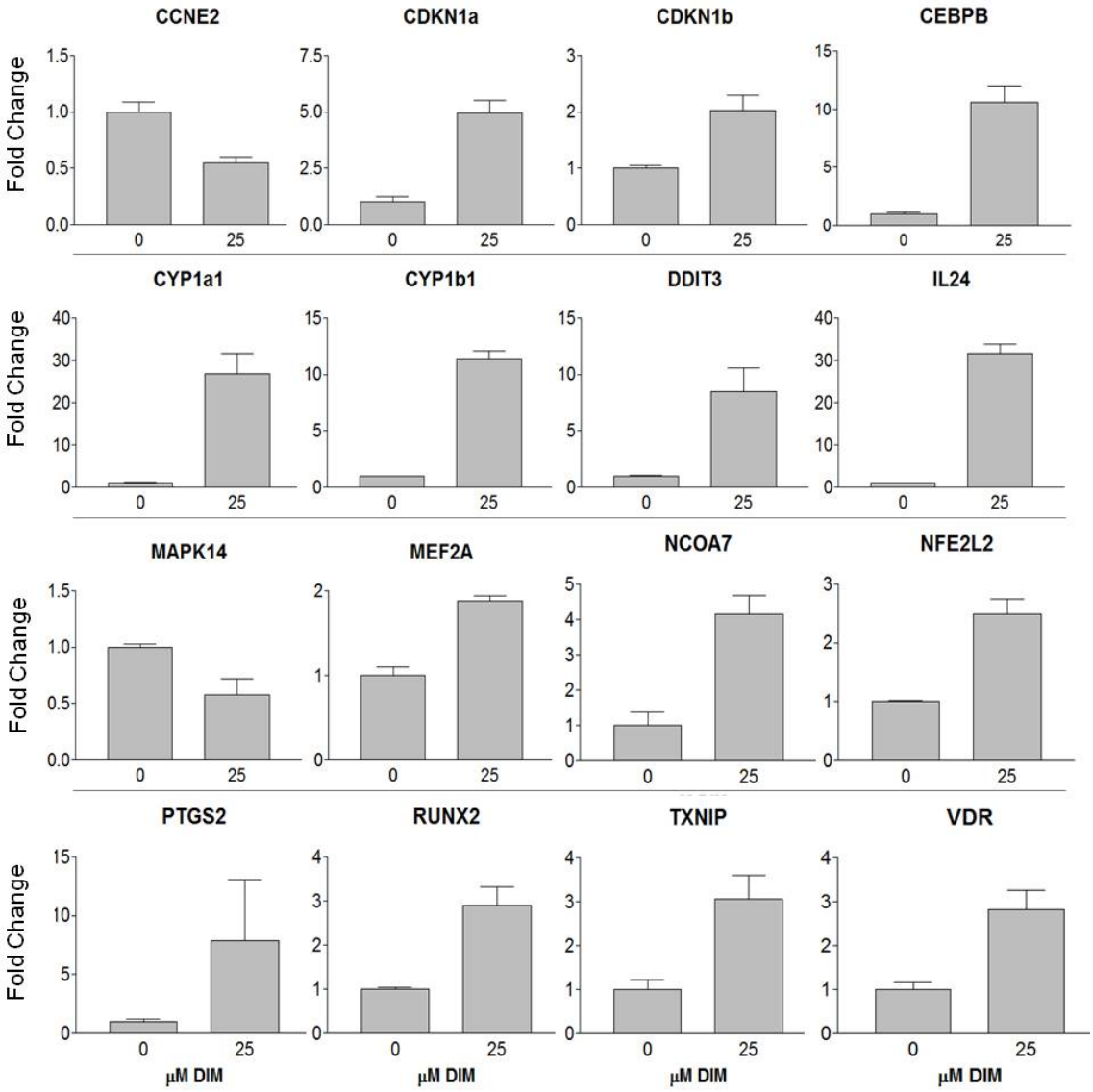

Figure 4-4. Validation of microarray results with quantitative reverse transcriptase PCR (QPCR). MDA-MB-231 cells were serum-starved in 1% serum for 20 hours and treated with 0 or 25 μM DIM for 4 hours before total RNA was collected and gene expression was analyzed by QPCR. Fifteen individual genes were analyzed and results matched those from the microarray analysis. Each experiment tested triplicate samples and was repeated three times. For all genes, $p<0.05$ for the fold changes of DMSO versus 25 μM DIM. Bars = average fold change + SEM.

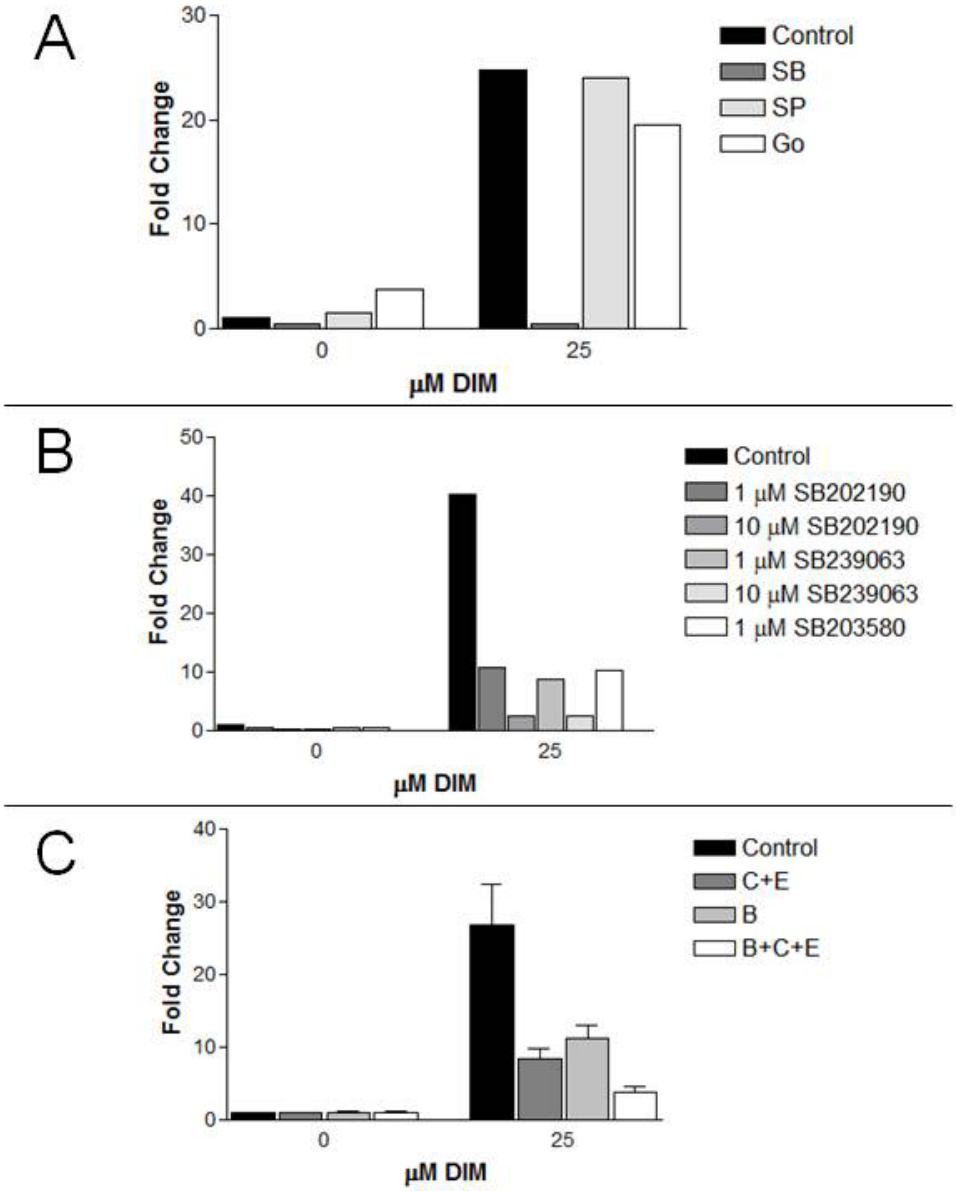

Figure 4-5. ***IL24*** **induction by DIM is reversed by p38 inhibitors and antioxidants, but is not reversed by inhibition of JNK or PKC. A.** MDA-MB-231 cells in medium containing 1% FBS were pre-treated with DMSO (control), 10 µM SB202190 (SB, p38 inhibitor), 8 µM SP600125 (SP, JNK inhibitor), or 5 µM Gö6983 (Go, PKC inhibitor) for 30 minutes and then treated with DMSO or 25 µM DIM for 4 hours. **B.** Cells were pretreated with DMSO or 1 or 10 µM of various p38 inhibitors for 30 minutes and then treated with DMSO or 25 µM DIM for 4 hours. **C.** Cells were pretreated with an antioxidants including 500 µM ascorbic acid (C), 300 µM α-tocopherol (E), and 0.1 mM N-(tert-Butyl) hydroxylamine HCl (B) for 30 minutes, and then treated with DMSO or 25 µM DIM for 4 hours. For all experiments, total RNA was isolated and subjected to reverse transcription and gene expression was assessed by QPCR. Bars = average fold change of 1-3 replicates + SEM.

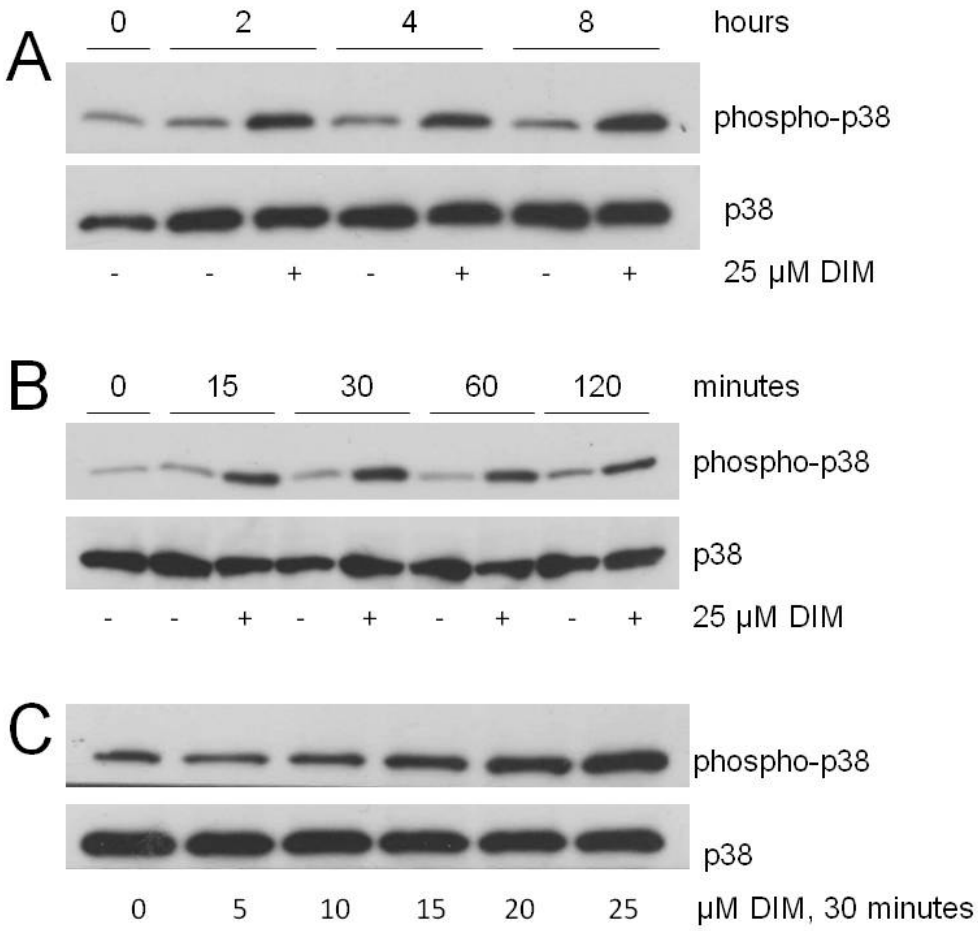

Figure 4-6. DIM activates p38. A. MDA-MB-231 cells were serum-starved in 1% FBS for 20 hours and treated with 0 or 25 µM DIM for 2, 4, or 8 hours or **B.** 0, 15, 30, 60, or 120 minutes. **C.** Cells were serum-starved in 1% FBS for 20 hours and then treated with increasing concentrations of DIM for 30 minutes. Total cell lysates were collected and analyzed by Western blotting for phospho-p38 or total p38. Results are representative of three independent experiments.

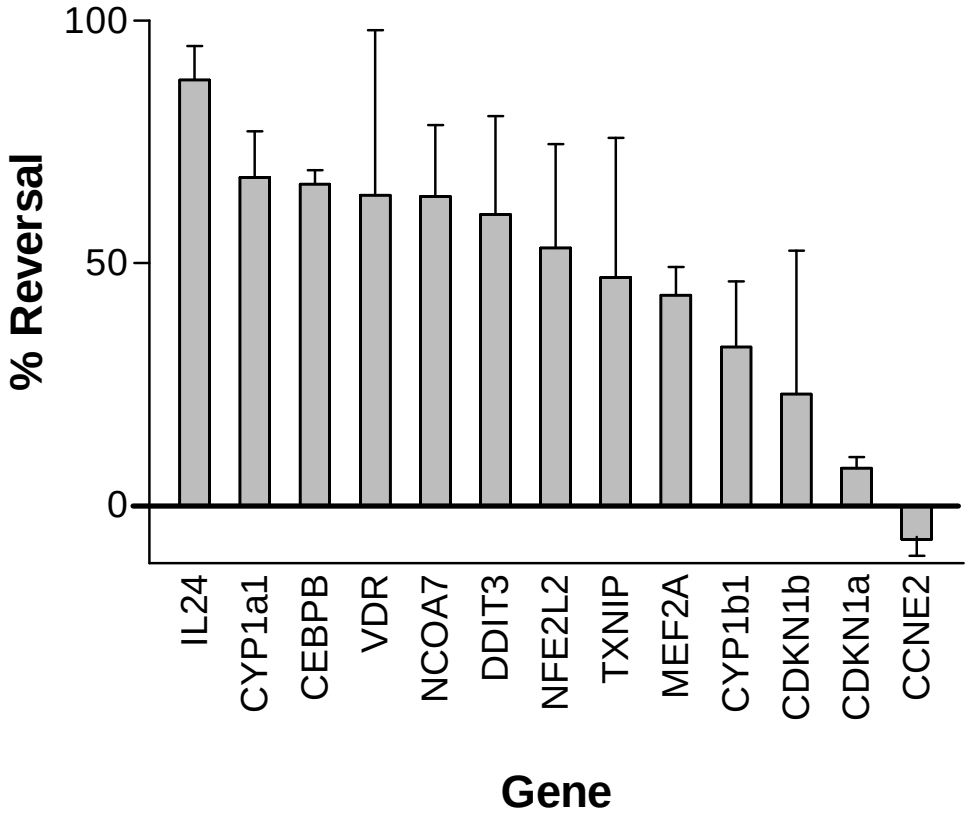

Figure 4-7. SB202190 reverses DIM's effects on expression of several genes. MDA-MB-231 cells in medium containing 1% FBS were pre-treated with 10 μM SB202190 (SB) or DMSO for 30 minutes and then treated with DMSO or 25 μM DIM for 4 hours. Total RNA was isolated and subjected to reverse transcription and gene expression was assessed by QPCR. % Reversal of DIM's effects by SB was calculated using the following formula:

% Reversal = (FC DIM – FC DIM+SB) / FC DIM,

where FC = fold change, DIM = cells treated with 25 μM DIM, and DIM+SB = cells treated with 10 μM SB and 25 μM DIM. Pre-treatment of cells with SB reversed DIM's effects on expression of several activated genes by 7-78%, but had no effect on repressed genes. Bars = Average % Reversal + SEM.

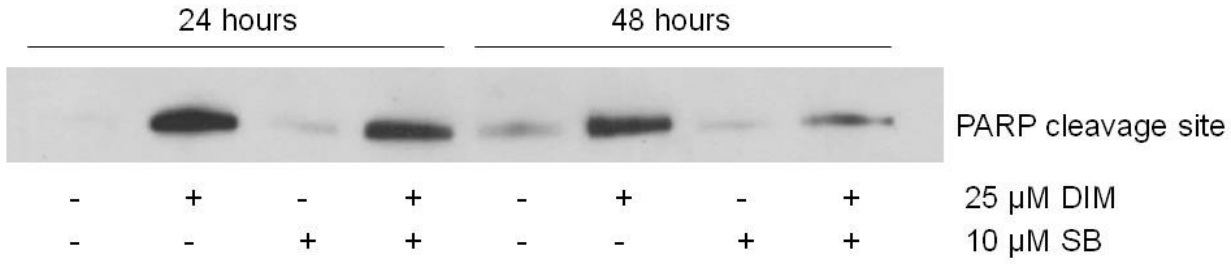

Figure 4-8. SB202190 reverses DIM's induction of apoptosis. MDA-MB-231were treated with or without 25 μM DIM and 10 μM SB202190 (SB) in DMEM containing 1% FBS for 24 or 48 hours. Total cell lysates were collected and analyzed by Western blotting for PARP cleavage site. Results are representative of three independent experiments.

CHAPTER 5

Future Direction

Future experiments should focus on determining more specific mechanisms by which DIM inhibits c-Met and should establish the relationship between c-Met inhibition and Akt inhibition, as well as between c-Met/Akt inhibition and cell cycle progression, proliferation, apoptosis, and motility in MDA-MB-231 breast cancer cells. The gene expression profiling study also opens up many opportunities for follow up experiments. The most relevant future experiments are described below.

Determine if DIM inhibits cell cycle progression, survival, and motility via inhibition of Akt

For these experiments, we can use a constitutively active Akt to try to override DIM's effects on cell cycle progression, survival, and motility. We hypothesize that DIM's cytostatic effects can be at least partially reversed and inhibition of GSK will be completely reversed by constitutively active Akt. To test this, we can stably transfect MDA-MB-231 cells, which do not express ERα, with a plasmid encoding a 4-hydroxytamoxifen (4OHT) -inducible Akt (iAkt) construct [143,144]. In this construct, the PH domain of Akt has been deleted to remove PIP_3 dependence, and the myristoylation sequence from the src-family protein Fyn has been added to induce constitutive membrane localization. This protein is fused to a mutated estrogen receptor ligand binding domain called ER-T2, which gives iAkt a 10-fold increased sensitivity to 4OHT compared to estrogen or tamoxifen. We can treat these stably transfected cells with 4OHT to induce Akt activity, treat with DIM, and then assess GSK phosphorylation, cell cycle progression, survival, and motility.

It will also be important to measure the degree of inhibition of other immediate downstream effectors of c-Met, like Ras.

Determine specificity of DIM's effects on c-Met inhibition

We have shown that DIM inhibits activation of Akt by HGF, and not by EGF or IGF-1. It is therefore necessary to determine whether inhibition of c-Met is responsible for DIM's inhibition of Akt or if other receptors or factors are also involved. Akt can be activated by many different stimuli besides the three growth factors studied. One way to address this is to test activation of Akt by other compounds, including various growth factors or cytokines. We could also use a constitutively active c-Met to reverse DIM's effects on Akt. We expect that in serum-free medium with HGF added as the activator, such a construct would block DIM's effects. However, in medium containing serum, we expect that there are other factors present that also activate Akt, and DIM may also inhibit those compounds or their downstream effectors. Under such conditions, we expect that a constitutively activate c-Met would only partially reverse DIM's effects on Akt activation.

Determine how DIM promotes degradation of c-Met

We have shown that DIM induces degradation of c-Met upstream of the endocytosis step, but that DIM decreases phosphorylation of c-Met at Y1003. To determine a more specific mechanism for promotion of c-Met degradation by DIM, we can use co-immunoprecipitation

experiments to determine if DIM is increasing Cbl recruitment to c-Met or if DIM is increasing ubiquitination of c-Met. We can also assess the expression and activity of Cbl or Hrs.

Determine if c-Met degradation and c-Met inactivation are related

It is possible that DIM's effects on c-Met degradation and c-Met activation are related, since both events involve phosphorylation of tyrosine residues. We have ruled out the involvement of phosphatases in DIM's effects since neither sodium orthovanadate nor okadaic acid reverse DIM's effects on c-Met phosphorylation at Y1234/1235. More intensive studies on the kinetics of inhibition of c-Met tyrosine phosphorylation will be helpful to determine if one phosphorylation is blocked before the other, since, for example, inhibition of Y1234/1235 phosphorylation may prevent recruitment of various scaffolding or signaling proteins necessary for the internalization and degradation of c-Met.

It would also be interesting to determine if DIM is inhibiting any step upstream of c-Met phosphorylation. Some possibilities are that DIM prevents HGF binding from c-Met or that DIM inhibits c-Met dimerization.

Determine how DIM decreases c-Met phosphorylation

While we have shown that a calcineurin inhibitor, CsA, reverses c-Met inhibition by DIM, we do not know a mechanism for this. We will need to rule out any non-specific activities of CsA by knocking out the regulatory subunit of calcineurin (*PPP3R1*) by shRNA to see if DIM inhibits c-Met without an active calcineurin. We have determined that calcineurin in lysates of cells treated with DIM does not have increased activity compared to that in lysates of DMSO-treated cells. However, we are still interested in whether or not DIM activates calcineurin in live intact cells. We can test this by analyzing levels of phosphorylated NFAT, a calcineurin substrate, by Western blotting. If DIM activates calcineurin, we expect to see decreased phosphorylation of NFAT with DIM treatment.

Determine global effects on gene transcription of p38 activation by DIM

We have demonstrated that DIM activates p38, and blocking p38 activation reverses many of DIM's effects on gene expression, particularly on up regulated genes. To expand on the findings in the relatively few genes tested, we could conduct an additional microarray experiment to determine the gene expression profiles of MDA-MB-231 cells treated with or without DIM and with or without the p38 inhibitor SB202190. Such an experiment will give us a better picture of the overall number of genes that DIM regulates by activating p38. Motif finding analysis and chromatin immunoprecipitation experiments can also help us to identify potential transcription factors, co-activators, or co-repressors that are modulated by p38 as a result of DIM treatment.

We also showed that DIM induces apoptosis, determined by detection of cleaved PARP, by activation of p38. Because p38 activation is responsible for many changes in gene expression and apoptosis induction by DIM, it would be interesting to conduct gene expression experiments

at later time points and gene knock down experiments to confirm the roles of individual genes in DIM's pro-apoptotic activities.

Follow up on interesting DIM-regulated genes identified by microarray analysis

The gene expression profile experiment identified several interesting DIM-regulated genes that are worthy of further study. Two of the most interesting are *IL24* and *VDR*. IL-24 is a pro-apoptotic interleukin that selectively kills cancer cells in a paracrine fashion without harming normal cells. Throughout the course of this study, we have attempted follow-up experiments on *IL24* and used it as a model gene for studying mechanisms of regulation by DIM. We have determined that *IL24* is strongly induced by DIM after a short time (2-4 hours) and this induction is reversed by pre-treatment of cells with antioxidants or a p38 inhibitor. However, despite the robust results from QPCR analysis, we were unable to detect IL-24 protein at any time point with any antibody via Western blotting or ELISA. This could be due to lack of antibodies to endogenous IL-24, as all commercially available antibodies detect recombinant IL-24. Or, we could be observing an IL-24 protein translational block induced by ROS [145]. Future experiments should focus on detection of IL-24 protein or confirmation of the translational block so that the relevance of *IL24* induction by DIM in breast cancer cells can be uncovered.

VDR is also an important gene for further study. While we confirmed by QPCR that *VDR* is activated by DIM, the degree of activation was highly variable from experiment to experiment. We need to confirm that DIM is activating expression of the VDR protein, and it will be very interesting to determine whether DIM activates transcription of VDR/RXR-activated genes by using reporter assays and QPCR. These results would be helpful for determining if DIM's anti-breast cancer effects and induction of *VDR* are related.

ACKNOWLEDGMENTS

Thank you to Len Bjeldanes for being my mentor and for guidance, training, and patience regarding my research and my career development.

Thank you to Wally Wang and Gary Firestone for serving on my dissertation committee and for your helpful advice regarding my research and my career.

Thank you to Joe Napoli, Steve Martin, Chris Vulpe, Bob Ryan, and Barry Shane for serving on my oral qualifying exam and guidance committees. The exam was one of the best learning experiences I have ever had.

Thank you to all past and present members of the Bjeldanes lab, including Johann Sohn, Theresa Stueve, Narayan Jeya Parthasarathy, Omar Vivar, and Jacques Riby, for your training, help, and support, and for making the leaky basement an enjoyable place to work.

Thank you to the undergraduate students who have helped with these projects by contributing data, assistance, and ideas, including Jennifer Chen, Leanne Almario, Dawn Yu, Rudy Silva, Marisela Tan, Kristin Lee, and Andy Chan.

Thank you to all faculty members, especially Dale Leitman, and to the post-docs, graduate students, and support staff in NST for your helpful feedback and suggestions regarding my research.

Thank you to Wally Wang, Dale Leitman, Jacques Riby, Emma Shtivelman, Denise Schichnes, Shyam Sundar, Lauren Shipp, Chandi Griffin, Xiaoyue Zhao, Nora Gray, Lonnele Ball, Omar Vivar, Theresa Stueve, and Crystal Marconett for training me in the laboratory techniques necessary to complete this dissertation.

Thank you to the California Breast Cancer Research program for financial support.

Thank you to Keith Martin, Leeanne Young Baroni, and Dane Winner for introducing me to research, training me in many techniques, and preparing me for graduate school.

Thank you to my supportive friends in graduate school, especially those of us who started together, including Marta Soden, Chuck Krois, and Max Ruby. We did it!

Thank you to my parents and family for your love and support throughout graduate school.

Thank you to my husband Tony for everything. I dedicate my dissertation to you.

REFERENCES

1. Doll R, and Peto R (1981). The causes of cancer : quantitative estimates of avoidable risks of cancer in the United States today, (Oxford ; New York: Oxford University Press).

2. WCRF/AICR (1997). Food, Nutrition, Physical Activity and the Prevention of Cancer: a Global Perspective. In, (Washington, DC).

3. Negri E, La Vecchia C, Franceschi S, D'Avanzo B, and Parazzini F (1991) Vegetable and fruit consumption and cancer risk. Int J Cancer *48*: 350-354.

4. Greenwald P (2004) Clinical trials in cancer prevention: current results and perspectives for the future. J Nutr *134*: 3507S-3512S.

5. Steinmetz KA, and Potter JD (1991) Vegetables, fruit, and cancer. II. Mechanisms. Cancer Causes Control *2*: 427-442.

6. Steinmetz KA, and Potter JD (1991) Vegetables, fruit, and cancer. I. Epidemiology. Cancer Causes Control *2*: 325-357.

7. Kristal AR, and Lampe JW (2002) Brassica vegetables and prostate cancer risk: a review of the epidemiological evidence. Nutr Cancer *42*: 1-9.

8. Verhoeven DT, Goldbohm RA, van Poppel G, Verhagen H, and van den Brandt PA (1996) Epidemiological studies on brassica vegetables and cancer risk. Cancer Epidemiol Biomarkers Prev *5*: 733-748.

9. Higdon JV, Delage B, Williams DE, and Dashwood RH (2007) Cruciferous vegetables and human cancer risk: epidemiologic evidence and mechanistic basis. Pharmacol Res *55*: 224-236.

10. Kim YS, and Milner JA (2005) Targets for indole-3-carbinol in cancer prevention. J Nutr Biochem *16*: 65-73.

11. Brew CT, Aronchik I, Hsu JC, Sheen JH, Dickson RB, Bjeldanes LF, and Firestone GL (2006) Indole-3-carbinol activates the ATM signaling pathway independent of DNA damage to stabilize p53 and induce G1 arrest of human mammary epithelial cells. Int J Cancer *118*: 857-868.

12. Hsu JC, Dev A, Wing A, Brew CT, Bjeldanes LF, and Firestone GL (2006) Indole-3-carbinol mediated cell cycle arrest of LNCaP human prostate cancer cells requires the induced production of activated p53 tumor suppressor protein. Biochemical pharmacology *72*: 1714-1723.

13. Nguyen HH, Aronchik I, Brar GA, Nguyen DH, Bjeldanes LF, and Firestone GL (2008) The dietary phytochemical indole-3-carbinol is a natural elastase enzymatic inhibitor that disrupts cyclin E protein processing. Proceedings of the National Academy of Sciences of the United States of America *105*: 19750-19755.

14. Raj MH, Abd Elmageed ZY, Zhou J, Gaur RL, Nguyen L, Azam GA, Braley P, Rao PN, Fathi IM, and Ouhtit A (2008) Synergistic action of dietary phyto-antioxidants on survival and proliferation of ovarian cancer cells. Gynecol Oncol *110*: 432-438.

15. Chen DZ, Qi M, Auborn KJ, and Carter TH (2001) Indole-3-carbinol and diindolylmethane induce apoptosis of human cervical cancer cells and in murine HPV16-transgenic preneoplastic cervical epithelium. J Nutr *131*: 3294-3302.

16. Grose KR, and Bjeldanes LF (1992) Oligomerization of indole-3-carbinol in aqueous acid. Chem Res Toxicol *5*: 188-193.

17. Chen I, McDougal A, Wang F, and Safe S (1998) Aryl hydrocarbon receptor-mediated antiestrogenic and antitumorigenic activity of diindolylmethane. Carcinogenesis *19*: 1631-1639.

18. Chang X, Tou JC, Hong C, Kim HA, Riby JE, Firestone GL, and Bjeldanes LF (2005) 3,3'-Diindolylmethane inhibits angiogenesis and the growth of transplantable human breast carcinoma in athymic mice. Carcinogenesis *26*: 771-778.

19. Hong C, Firestone GL, and Bjeldanes LF (2002) Bcl-2 family-mediated apoptotic effects of 3,3'-diindolylmethane (DIM) in human breast cancer cells. Biochemical pharmacology *63*: 1085-1097.

20. Hong C, Kim HA, Firestone GL, and Bjeldanes LF (2002) 3,3'-Diindolylmethane (DIM) induces a G(1) cell cycle arrest in human breast cancer cells that is accompanied by Sp1-mediated activation of p21(WAF1/CIP1) expression. Carcinogenesis *23*: 1297-1305.

21. Bell MC, Crowley-Nowick P, Bradlow HL, Sepkovic DW, Schmidt-Grimminger D, Howell P, Mayeaux EJ, Tucker A, Turbat-Herrera EA, and Mathis JM (2000) Placebo-controlled trial of indole-3-carbinol in the treatment of CIN. Gynecol Oncol *78*: 123-129.

22. Wiatrak BJ (2003) Overview of recurrent respiratory papillomatosis. Curr Opin Otolaryngol Head Neck Surg *11*: 433-441.

23. Auborn KJ (2002) Therapy for recurrent respiratory papillomatosis. Antivir Ther *7*: 1-9.

24. ClinicalTrials.gov. In.

25. Anderton MJ, Manson MM, Verschoyle R, Gescher A, Steward WP, Williams ML, and Mager DE (2004) Physiological modeling of formulated and crystalline 3,3'-diindolylmethane pharmacokinetics following oral administration in mice. Drug Metab Dispos *32*: 632-638.

26. Howells LM, Moiseeva EP, Neal CP, Foreman BE, Andreadi CK, Sun YY, Hudson A, and Manson MM (2007) Predicting the physiological relevance of in vitro cancer preventive activities of phytochemicals. Acta Pharmacologica Sinica *28*: 1274-1304.

27. Gong Y, Sohn H, Xue L, Firestone GL, and Bjeldanes LF (2006) 3,3'-Diindolylmethane is a novel mitochondrial H(+)-ATP synthase inhibitor that can induce p21(Cip1/Waf1) expression by induction of oxidative stress in human breast cancer cells. Cancer research *66*: 4880-4887.

28. Xue L, Firestone GL, and Bjeldanes LF (2005) DIM stimulates IFNgamma gene expression in human breast cancer cells via the specific activation of JNK and p38 pathways. Oncogene *24*: 2343-2353.

29. Xue L, Pestka JJ, Li M, Firestone GL, and Bjeldanes LF (2008) 3,3'-Diindolylmethane stimulates murine immune function in vitro and in vivo. J Nutr Biochem *19*: 336-344.

30. Roberts PJ, and Der CJ (2007) Targeting the Raf-MEK-ERK mitogen-activated protein kinase cascade for the treatment of cancer. Oncogene *26*: 3291-3310.

31. Madhusudan S, and Ganesan TS (2007) Tyrosine kinase inhibitors and cancer therapy. Recent Results Cancer Res *172*: 25-44.

32. Chang L, and Karin M (2001) Mammalian MAP kinase signalling cascades. Nature *410*: 37-40.

33. Garrington TP, and Johnson GL (1999) Organization and regulation of mitogen-activated protein kinase signaling pathways. Curr Opin Cell Biol *11*: 211-218.

34. Widmann C, Gibson S, Jarpe MB, and Johnson GL (1999) Mitogen-activated protein kinase: conservation of a three-kinase module from yeast to human. Physiol Rev *79*: 143-180.

35. Wagner EF, and Nebreda AR (2009) Signal integration by JNK and p38 MAPK pathways in cancer development. Nat Rev Cancer *9*: 537-549.

36. Ono K, and Han J (2000) The p38 signal transduction pathway: activation and function. Cell Signal *12*: 1-13.

37. Cuenda A, and Rousseau S (2007) p38 MAP-kinases pathway regulation, function and role in human diseases. Biochim Biophys Acta *1773*: 1358-1375.

38. Bode AM, and Dong Z (2007) The functional contrariety of JNK. Molecular carcinogenesis *46*: 591-598.

39. Eferl R, and Wagner EF (2003) AP-1: a double-edged sword in tumorigenesis. Nat Rev Cancer *3*: 859-868.

40. Sun S, Han J, Ralph WM, Jr., Chandrasekaran A, Liu K, Auborn KJ, and Carter TH (2004) Endoplasmic reticulum stress as a correlate of cytotoxicity in human tumor cells exposed to diindolylmethane in vitro. Cell Stress Chaperones *9*: 76-87.

41. Vivar OI, Lin CL, Firestone GL, and Bjeldanes LF (2009) 3,3'-Diindolylmethane induces a G(1) arrest in human prostate cancer cells irrespective of androgen receptor and p53 status. Biochemical pharmacology *78*: 469-476.

42. Khwaja FS, Wynne S, Posey I, and Djakiew D (2009) 3,3'-diindolylmethane induction of p75NTR-dependent cell death via the p38 mitogen-activated protein kinase pathway in prostate cancer cells. Cancer Prev Res (Phila Pa) *2*: 566-571.

43. Rahimi M, Huang KL, and Tang CK (2010) 3,3'-Diindolylmethane (DIM) inhibits the growth and invasion of drug-resistant human cancer cells expressing EGFR mutants. Cancer Lett.

44. Zhang C, Kawauchi J, Adachi MT, Hashimoto Y, Oshiro S, Aso T, and Kitajima S (2001) Activation of JNK and transcriptional repressor ATF3/LRF1 through the IRE1/TRAF2 pathway is implicated in human vascular endothelial cell death by homocysteine. Biochem Biophys Res Commun *289*: 718-724.

45. Urano F, Wang X, Bertolotti A, Zhang Y, Chung P, Harding HP, and Ron D (2000) Coupling of stress in the ER to activation of JNK protein kinases by transmembrane protein kinase IRE1. Science (New York, NY *287*: 664-666.

46. Carter TH, Liu K, Ralph W, Jr., Chen D, Qi M, Fan S, Yuan F, Rosen EM, and Auborn KJ (2002) Diindolylmethane alters gene expression in human keratinocytes in vitro. J Nutr *132*: 3314-3324.

47. Li Y, Li X, and Sarkar FH (2003) Gene expression profiles of I3C- and DIM-treated PC3 human prostate cancer cells determined by cDNA microarray analysis. J Nutr *133*: 1011-1019.

48. Rahman KW, Li Y, Wang Z, Sarkar SH, and Sarkar FH (2006) Gene expression profiling revealed survivin as a target of 3,3'-diindolylmethane-induced cell growth inhibition and apoptosis in breast cancer cells. Cancer research *66*: 4952-4960.

49. Hynes NE, and Lane HA (2005) ERBB receptors and cancer: the complexity of targeted inhibitors. Nat Rev Cancer *5*: 341-354.

50. Sebolt-Leopold JS, Dudley DT, Herrera R, Van Becelaere K, Wiland A, Gowan RC, Tecle H, Barrett SD, Bridges A, Przybranowski S*, et al.* (1999) Blockade of the MAP kinase pathway suppresses growth of colon tumors in vivo. Nature medicine *5*: 810-816.

51. Tsai J, Lee JT, Wang W, Zhang J, Cho H, Mamo S, Bremer R, Gillette S, Kong J, Haass NK*, et al.* (2008) Discovery of a selective inhibitor of oncogenic B-Raf kinase with potent antimelanoma activity. Proceedings of the National Academy of Sciences of the United States of America *105*: 3041-3046.

52. Garnett MJ, and Marais R (2004) Guilty as charged: B-RAF is a human oncogene. Cancer cell *6*: 313-319.

53. Cox AD, and Der CJ (2002) Ras family signaling: therapeutic targeting. Cancer Biol Ther *1*: 599-606.

54. McGuire KP, Ngoubilly N, Neavyn M, and Lanza-Jacoby S (2006) 3,3'-diindolylmethane and paclitaxel act synergistically to promote apoptosis in HER2/Neu human breast cancer cells. The Journal of surgical research *132*: 208-213.

55. Chen Y, Xu J, Jhala N, Pawar P, Zhu ZB, Ma L, Byon CH, and McDonald JM (2006) Fas-mediated apoptosis in cholangiocarcinoma cells is enhanced by 3,3'-diindolylmethane through inhibition of AKT signaling and FLICE-like inhibitory protein. Am J Pathol *169*: 1833-1842.

56. Leong H, Riby JE, Firestone GL, and Bjeldanes LF (2004) Potent ligand-independent estrogen receptor activation by 3,3'-diindolylmethane is mediated by cross talk between the protein kinase A and mitogen-activated protein kinase signaling pathways. Mol Endocrinol *18*: 291-302.

57. Kunimasa K, Kobayashi T, Kaji K, and Ohta T (2010) Antiangiogenic effects of indole-3-carbinol and 3,3'-diindolylmethane are associated with their differential regulation of ERK1/2 and Akt in tube-forming HUVEC. J Nutr *140*: 1-6.

58. Chang X, Firestone GL, and Bjeldanes LF (2006) Inhibition of growth factor-induced Ras signaling in vascular endothelial cells and angiogenesis by 3,3'-diindolylmethane. Carcinogenesis *27*: 541-550.

59. Alessi DR, James SR, Downes CP, Holmes AB, Gaffney PR, Reese CB, and Cohen P (1997) Characterization of a 3-phosphoinositide-dependent protein kinase which phosphorylates and activates protein kinase Balpha. Curr Biol *7*: 261-269.

60. Hresko RC, and Mueckler M (2005) mTOR.RICTOR is the Ser473 kinase for Akt/protein kinase B in 3T3-L1 adipocytes. The Journal of biological chemistry *280*: 40406-40416.

61. Sarbassov DD, Guertin DA, Ali SM, and Sabatini DM (2005) Phosphorylation and regulation of Akt/PKB by the rictor-mTOR complex. Science (New York, NY *307*: 1098-1101.

62. Deng J, Xia W, Miller SA, Wen Y, Wang HY, and Hung MC (2004) Crossregulation of NF-kappaB by the APC/GSK-3beta/beta-catenin pathway. Molecular carcinogenesis *39*: 139-146.

63. Yost C, Torres M, Miller JR, Huang E, Kimelman D, and Moon RT (1996) The axis-inducing activity, stability, and subcellular distribution of beta-catenin is regulated in Xenopus embryos by glycogen synthase kinase 3. Genes Dev *10*: 1443-1454.

64. Kikuchi A (1999) Roles of Axin in the Wnt signalling pathway. Cell Signal *11*: 777-788.

65. Wen Y, Hu MC, Makino K, Spohn B, Bartholomeusz G, Yan DH, and Hung MC (2000) HER-2/neu promotes androgen-independent survival and growth of prostate cancer cells through the Akt pathway. Cancer research *60*: 6841-6845.

66. Kops GJ, and Burgering BM (2000) Forkhead transcription factors are targets of signalling by the proto-oncogene PKB (C-AKT). J Anat *197 Pt 4*: 571-574.

67. Brunet A, Bonni A, Zigmond MJ, Lin MZ, Juo P, Hu LS, Anderson MJ, Arden KC, Blenis J, and Greenberg ME (1999) Akt promotes cell survival by phosphorylating and inhibiting a Forkhead transcription factor. Cell *96*: 857-868.

68. Fingar DC, Richardson CJ, Tee AR, Cheatham L, Tsou C, and Blenis J (2004) mTOR controls cell cycle progression through its cell growth effectors S6K1 and 4E-BP1/eukaryotic translation initiation factor 4E. Molecular and cellular biology *24*: 200-216.

69. Kane LP, Shapiro VS, Stokoe D, and Weiss A (1999) Induction of NF-kappaB by the Akt/PKB kinase. Curr Biol *9*: 601-604.

70. Aggarwal BB (2004) Nuclear factor-kappaB: the enemy within. Cancer cell *6*: 203-208.

71. Bhuiyan MM, Li Y, Banerjee S, Ahmed F, Wang Z, Ali S, and Sarkar FH (2006) Down-regulation of androgen receptor by 3,3'-diindolylmethane contributes to inhibition of cell proliferation and induction of apoptosis in both hormone-sensitive LNCaP and insensitive C4-2B prostate cancer cells. Cancer research *66*: 10064-10072.

72. Li Y, Wang Z, Kong D, Murthy S, Dou QP, Sheng S, Reddy GP, and Sarkar FH (2007) Regulation of FOXO3a/beta-catenin/GSK-3beta signaling by 3,3'-diindolylmethane contributes to inhibition of cell proliferation and induction of apoptosis in prostate cancer cells. The Journal of biological chemistry *282*: 21542-21550.

73. Kong D, Banerjee S, Huang W, Li Y, Wang Z, Kim HR, and Sarkar FH (2008) Mammalian target of rapamycin repression by 3,3'-diindolylmethane inhibits invasion and angiogenesis in platelet-derived growth factor-D-overexpressing PC3 cells. Cancer research *68*: 1927-1934.

74. Garikapaty VP, Ashok BT, Tadi K, Mittelman A, and Tiwari RK (2006) 3,3'-Diindolylmethane downregulates pro-survival pathway in hormone independent prostate cancer. Biochem Biophys Res Commun *340*: 718-725.

75. Zhang L, Lee KC, Bhojani MS, Khan AP, Shilman A, Holland EC, Ross BD, and Rehemtulla A (2007) Molecular imaging of Akt kinase activity. Nat Med *13*: 1114-1119.

76. Rahman KW, and Sarkar FH (2005) Inhibition of nuclear translocation of nuclear factor-{kappa}B contributes to 3,3'-diindolylmethane-induced apoptosis in breast cancer cells. Cancer research *65*: 364-371.

77. Rahman KM, Ali S, Aboukameel A, Sarkar SH, Wang Z, Philip PA, Sakr WA, and Raz A (2007) Inactivation of NF-kappaB by 3,3'-diindolylmethane contributes to increased apoptosis induced by chemotherapeutic agent in breast cancer cells. Mol Cancer Ther *6*: 2757-2765.

78. Heldin CH, Ostman A, and Ronnstrand L (1998) Signal transduction via platelet-derived growth factor receptors. Biochim Biophys Acta *1378*: F79-113.

79. Greenfield C, Hiles I, Waterfield MD, Federwisch M, Wollmer A, Blundell TL, and McDonald N (1989) Epidermal growth factor binding induces a conformational change in the external domain of its receptor. EMBO J *8*: 4115-4123.

80. Heldin CH (1996) Protein tyrosine kinase receptors. Cancer Surv *27*: 7-24.

81. Heldin CH (1995) Dimerization of cell surface receptors in signal transduction. Cell *80*: 213-223.

82. Robinson DR, Wu YM, and Lin SF (2000) The protein tyrosine kinase family of the human genome. Oncogene *19*: 5548-5557.

83. Zwick E, Bange J, and Ullrich A (2001) Receptor tyrosine kinase signalling as a target for cancer intervention strategies. Endocr Relat Cancer *8*: 161-173.

84. Kamath S, and Buolamwini JK (2006) Targeting EGFR and HER-2 receptor tyrosine kinases for cancer drug discovery and development. Med Res Rev *26*: 569-594.

85. Migliore C, and Giordano S (2008) Molecular cancer therapy: can our expectation be MET? Eur J Cancer *44*: 641-651.

86. Batra SK, Castelino-Prabhu S, Wikstrand CJ, Zhu X, Humphrey PA, Friedman HS, and Bigner DD (1995) Epidermal growth factor ligand-independent, unregulated, cell-transforming potential of a naturally occurring human mutant EGFRvIII gene. Cell Growth Differ *6*: 1251-1259.

87. Huang HS, Nagane M, Klingbeil CK, Lin H, Nishikawa R, Ji XD, Huang CM, Gill GN, Wiley HS, and Cavenee WK (1997) The enhanced tumorigenic activity of a mutant epidermal growth factor receptor common in human cancers is mediated by threshold levels of constitutive tyrosine phosphorylation and unattenuated signaling. The Journal of biological chemistry *272*: 2927-2935.

88. Chang YC, Riby J, Chang GH, Peng BC, Firestone G, and Bjeldanes LF (1999) Cytostatic and antiestrogenic effects of 2-(indol-3-ylmethyl)-3,3'-diindolylmethane, a major in vivo product of dietary indole-3-carbinol. Biochemical pharmacology *58*: 825-834.

89. Montagut C, and Settleman J (2009) Targeting the RAF-MEK-ERK pathway in cancer therapy. Cancer Lett *283*: 125-134.

90. Fresno Vara JA, Casado E, de Castro J, Cejas P, Belda-Iniesta C, and Gonzalez-Baron M (2004) PI3K/Akt signalling pathway and cancer. Cancer treatment reviews *30*: 193-204.

91. Luo J, Manning BD, and Cantley LC (2003) Targeting the PI3K-Akt pathway in human cancer: rationale and promise. Cancer cell *4*: 257-262.

92. Hubbard SR, and Till JH (2000) Protein tyrosine kinase structure and function. Annu Rev Biochem *69*: 373-398.

93. Morgensztern D, and McLeod HL (2005) PI3K/Akt/mTOR pathway as a target for cancer therapy. Anticancer Drugs *16*: 797-803.

94. Fan S, Ma YX, Wang JA, Yuan RQ, Meng Q, Cao Y, Laterra JJ, Goldberg ID, and Rosen EM (2000) The cytokine hepatocyte growth factor/scatter factor inhibits apoptosis and enhances DNA repair by a common mechanism involving signaling through phosphatidyl inositol 3' kinase. Oncogene *19*: 2212-2223.

95. Wang Z, Yu BW, Rahman KM, Ahmad F, and Sarkar FH (2008) Induction of growth arrest and apoptosis in human breast cancer cells by 3,3-diindolylmethane is associated with induction and nuclear localization of p27kip. Mol Cancer Ther *7*: 341-349.

96. King FW, Fong S, Griffin C, Shoemaker M, Staub R, Zhang YL, Cohen I, and Shtivelman E (2009) Timosaponin AIII is preferentially cytotoxic to tumor cells through inhibition of mTOR and induction of ER stress. PLoS One *4*: e7283.

97. Jackson JG, Kreisberg JI, Koterba AP, Yee D, and Brattain MG (2000) Phosphorylation and nuclear exclusion of the forkhead transcription factor FKHR after epidermal growth factor treatment in human breast cancer cells. Oncogene *19*: 4574-4581.

98. Bartucci M, Morelli C, Mauro L, Ando S, and Surmacz E (2001) Differential insulin-like growth factor I receptor signaling and function in estrogen receptor (ER)-positive MCF-7 and ER-negative MDA-MB-231 breast cancer cells. Cancer Res *61*: 6747-6754.

99. Lee WJ, Chen WK, Wang CJ, Lin WL, and Tseng TH (2008) Apigenin inhibits HGF-promoted invasive growth and metastasis involving blocking PI3K/Akt pathway and beta 4 integrin function in MDA-MB-231 breast cancer cells. Toxicol Appl Pharmacol *226*: 178-191.

100. Xue C, Wyckoff J, Liang F, Sidani M, Violini S, Tsai KL, Zhang ZY, Sahai E, Condeelis J, and Segall JE (2006) Epidermal growth factor receptor overexpression results in increased tumor cell motility in vivo coordinately with enhanced intravasation and metastasis. Cancer Res *66*: 192-197.

101. Sachdev D, and Yee D (2007) Disrupting insulin-like growth factor signaling as a potential cancer therapy. Mol Cancer Ther *6*: 1-12.

102. Yamashita J, Ogawa M, Yamashita S, Nomura K, Kuramoto M, Saishoji T, and Shin S (1994) Immunoreactive hepatocyte growth factor is a strong and independent predictor of recurrence and survival in human breast cancer. Cancer Res *54*: 1630-1633.

103. Beviglia L, Matsumoto K, Lin CS, Ziober BL, and Kramer RH (1997) Expression of the c-Met/HGF receptor in human breast carcinoma: correlation with tumor progression. Int J Cancer *74*: 301-309.

104. Cross DA, Alessi DR, Cohen P, Andjelkovich M, and Hemmings BA (1995) Inhibition of glycogen synthase kinase-3 by insulin mediated by protein kinase B. Nature *378*: 785-789.

105. Li DM, and Sun H (1998) PTEN/MMAC1/TEP1 suppresses the tumorigenicity and induces G1 cell cycle arrest in human glioblastoma cells. Proceedings of the National Academy of Sciences of the United States of America *95*: 15406-15411.

106. Datta SR, Dudek H, Tao X, Masters S, Fu H, Gotoh Y, and Greenberg ME (1997) Akt phosphorylation of BAD couples survival signals to the cell-intrinsic death machinery. Cell *91*: 231-241.

107. Koh DW, Dawson TM, and Dawson VL (2005) Mediation of cell death by poly(ADP-ribose) polymerase-1. Pharmacol Res *52*: 5-14.

108. Jiang BH, and Liu LZ (2009) PI3K/PTEN signaling in angiogenesis and tumorigenesis. Adv Cancer Res *102*: 19-65.

109. Sheng S, Qiao M, and Pardee AB (2009) Metastasis and AKT activation. J Cell Physiol *218*: 451-454.

110. Li SY, Rong M, Grieu F, and Iacopetta B (2006) PIK3CA mutations in breast cancer are associated with poor outcome. Breast Cancer Res Treat *96*: 91-95.

111. Clark AS, West K, Streicher S, and Dennis PA (2002) Constitutive and inducible Akt activity promotes resistance to chemotherapy, trastuzumab, or tamoxifen in breast cancer cells. Mol Cancer Ther *1*: 707-717.

112. Knuefermann C, Lu Y, Liu B, Jin W, Liang K, Wu L, Schmidt M, Mills GB, Mendelsohn J, and Fan Z (2003) HER2/PI-3K/Akt activation leads to a multidrug resistance in human breast adenocarcinoma cells. Oncogene *22*: 3205-3212.

113. Adams LS, Phung S, Yee N, Seeram NP, Li L, and Chen S (2010) Blueberry phytochemicals inhibit growth and metastatic potential of MDA-MB-231 breast cancer cells through modulation of the phosphatidylinositol 3-kinase pathway. Cancer research *70*: 3594-3605.

114. Bigelow RL, and Cardelli JA (2006) The green tea catechins, (-)-Epigallocatechin-3-gallate (EGCG) and (-)-Epicatechin-3-gallate (ECG), inhibit HGF/Met signaling in immortalized and tumorigenic breast epithelial cells. Oncogene *25*: 1922-1930.

115. Gong L, Li Y, Nedeljkovic-Kurepa A, and Sarkar FH (2003) Inactivation of NF-kappaB by genistein is mediated via Akt signaling pathway in breast cancer cells. Oncogene *22*: 4702-4709.

116. Kim HI, Huang H, Cheepala S, Huang S, and Chung J (2008) Curcumin inhibition of integrin (alpha6beta4)-dependent breast cancer cell motility and invasion. Cancer Prev Res (Phila Pa) *1*: 385-391.

117. Squires MS, Hudson EA, Howells L, Sale S, Houghton CE, Jones JL, Fox LH, Dickens M, Prigent SA, and Manson MM (2003) Relevance of mitogen activated protein kinase (MAPK) and phosphotidylinositol-3-kinase/protein kinase B (PI3K/PKB) pathways to induction of apoptosis by curcumin in breast cells. Biochemical pharmacology *65*: 361-376.

118. Longati P, Bardelli A, Ponzetto C, Naldini L, and Comoglio PM (1994) Tyrosines1234-1235 are critical for activation of the tyrosine kinase encoded by the MET proto-oncogene (HGF receptor). Oncogene *9*: 49-57.

119. Birchmeier C, Birchmeier W, Gherardi E, and Vande Woude GF (2003) Met, metastasis, motility and more. Nat Rev Mol Cell Biol *4*: 915-925.

120. Peschard P, Fournier TM, Lamorte L, Naujokas MA, Band H, Langdon WY, and Park M (2001) Mutation of the c-Cbl TKB domain binding site on the Met receptor tyrosine kinase converts it into a transforming protein. Mol Cell *8*: 995-1004.

121. Hammond DE, Carter S, McCullough J, Urbe S, Vande Woude G, and Clague MJ (2003) Endosomal dynamics of Met determine signaling output. Mol Biol Cell *14*: 1346-1354.

122. Abella JV, Peschard P, Naujokas MA, Lin T, Saucier C, Urbe S, and Park M (2005) Met/Hepatocyte growth factor receptor ubiquitination suppresses transformation and is required for Hrs phosphorylation. Molecular and cellular biology *25*: 9632-9645.

123. Gallego MI, Bierie B, and Hennighausen L (2003) Targeted expression of HGF/SF in mouse mammary epithelium leads to metastatic adenosquamous carcinomas through the activation of multiple signal transduction pathways. Oncogene *22*: 8498-8508.

124. Comoglio PM, and Boccaccio C (2001) Scatter factors and invasive growth. Semin Cancer Biol *11*: 153-165.

125. Rong S, Segal S, Anver M, Resau JH, and Vande Woude GF (1994) Invasiveness and metastasis of NIH 3T3 cells induced by Met-hepatocyte growth factor/scatter factor autocrine stimulation. Proc Natl Acad Sci U S A *91*: 4731-4735.

126. Abounader R, Lal B, Luddy C, Koe G, Davidson B, Rosen EM, and Laterra J (2002) In vivo targeting of SF/HGF and c-met expression via U1snRNA/ribozymes inhibits glioma growth and angiogenesis and promotes apoptosis. FASEB J *16*: 108-110.

127. Ghoussoub RA, Dillon DA, D'Aquila T, Rimm EB, Fearon ER, and Rimm DL (1998) Expression of c-met is a strong independent prognostic factor in breast carcinoma. Cancer *82*: 1513-1520.

128. Lindemann K, Resau J, Nahrig J, Kort E, Leeser B, Annecke K, Welk A, Schafer J, Vande Woude GF, Lengyel E, and Harbeck N (2007) Differential expression of c-Met, its ligand HGF/SF and HER2/neu in DCIS and adjacent normal breast tissue. Histopathology *51*: 54-62.

129. Stellrecht CM, and Gandhi V (2009) MET receptor tyrosine kinase as a therapeutic anticancer target. Cancer Lett *280*: 1-14.

130. Eder JP, Vande Woude GF, Boerner SA, and LoRusso PM (2009) Novel therapeutic inhibitors of the c-Met signaling pathway in cancer. Clin Cancer Res *15*: 2207-2214.

131. Khan N, Afaq F, Kweon MH, Kim K, and Mukhtar H (2007) Oral consumption of pomegranate fruit extract inhibits growth and progression of primary lung tumors in mice. Cancer Res *67*: 3475-3482.

132. Labbe D, Provencal M, Lamy S, Boivin D, Gingras D, and Beliveau R (2009) The flavonols quercetin, kaempferol, and myricetin inhibit hepatocyte growth factor-induced medulloblastoma cell migration. J Nutr *139*: 646-652.

133. Wang S, Liu Q, Zhang Y, Liu K, Yu P, Luan J, Duan H, Lu Z, Wang F, Wu E*, et al.* (2009) Suppression of growth, migration and invasion of highly-metastatic human breast cancer cells by berbamine and its molecular mechanisms of action. Mol Cancer *8*: 81.

134. Gandino L, Munaron L, Naldini L, Ferracini R, Magni M, and Comoglio PM (1991) Intracellular calcium regulates the tyrosine kinase receptor encoded by the MET oncogene. J Biol Chem *266*: 16098-16104.

135. Du P, Kibbe WA, and Lin SM (2008) lumi: a pipeline for processing Illumina microarray. Bioinformatics *24*: 1547-1548.

136. Smyth GK (2005). limma: Linear Models for Microarray Data, (New York: Springer).

137. Paruthiyil S, Cvoro A, Zhao X, Wu Z, Sui Y, Staub RE, Baggett S, Herber CB, Griffin C, Tagliaferri M*, et al.* (2009) Drug and cell type-specific regulation of genes with different classes of estrogen receptor beta-selective agonists. PLoS One *4*: e6271.

138. Sauane M, Gopalkrishnan RV, Sarkar D, Su ZZ, Lebedeva IV, Dent P, Pestka S, and Fisher PB (2003) MDA-7/IL-24: novel cancer growth suppressing and apoptosis inducing cytokine. Cytokine Growth Factor Rev *14*: 35-51.

139. Gissel T, Rejnmark L, Mosekilde L, and Vestergaard P (2008) Intake of vitamin D and risk of breast cancer--a meta-analysis. J Steroid Biochem Mol Biol *111*: 195-199.

140. Moreno J, Krishnan AV, and Feldman D (2005) Molecular mechanisms mediating the anti-proliferative effects of Vitamin D in prostate cancer. J Steroid Biochem Mol Biol *97*: 31-36.

141. Holt PR, Arber N, Halmos B, Forde K, Kissileff H, McGlynn KA, Moss SF, Kurihara N, Fan K, Yang K, and Lipkin M (2002) Colonic epithelial cell proliferation decreases with increasing levels of serum 25-hydroxy vitamin D. Cancer Epidemiol Biomarkers Prev *11*: 113-119.

142. Christakos S, Dhawan P, Benn B, Porta A, Hediger M, Oh GT, Jeung EB, Zhong Y, Ajibade D, Dhawan K, and Joshi S (2007) Vitamin D: molecular mechanism of action. Ann N Y Acad Sci *1116*: 340-348.

143. Park D, Lapteva N, Seethammagari M, Slawin KM, and Spencer DM (2006) An essential role for Akt1 in dendritic cell function and tumor immunotherapy. Nature biotechnology *24*: 1581-1590.

144. Spencer DM (1996) Creating conditional mutations in mammals. Trends Genet *12*: 181-187.

145. Lebedeva IV, Su ZZ, Vozhilla N, Chatman L, Sarkar D, Dent P, Athar M, and Fisher PB (2008) Mechanism of in vitro pancreatic cancer cell growth inhibition by melanoma differentiation-associated gene-7/interleukin-24 and perillyl alcohol. Cancer research *68*: 7439-7447.